The role of Muscleblind-Like proteins in Myotonic Dystrophy

Sukrat Arya; MRes, BSc (Hons)

School of Life Sciences

The University of Nottingham

Thesis submitted to the University of Nottingham for the degree of Doctor of Philosophy (Genetics)

July, 2014

Supervisor

Professor JD Brook

Table of Contents

List of Abbreviations:

AONs	Antisense oligonucleotides
BCP	Bromochloropropane
BSA	Bovine serum albumin
CDM	Congenital Myotonic Dystrophy
CELF	CUG-BP- and ETR-3-like factor
CLC 1	Chloride channel 1
CUG-BP1	CUG binding protein
DEPC	Diethylpyrocarbonate
DM	Myotonic dystrophy (DM)
DMEM	Dulbecco's Modified Eagles Medium
DMPK	Dystrophica Myotonia protein kinase
DMSO	Dimethyl sulfoxide
DMWD	Dystrophia myotonic-containing WD repeat motif
EDTA	Ethylenediaminetetraacetic acid
FCGRT	IgG receptor FcRn large subunit p51
FISH	Fluorescent in situ hybridization
FSH	Follicle stimulating hormone
GIPR	Gastric inhibitory polypeptide receptor
HSALR	Human skeletal actin
IMOX	Imidazolo-oxindole

INSR/IR	Insulin receptor
LDS	Lithium dodecyl sulfate
Mbl	Muscleblind protein
MBNL	Muscleblind-like protein
MTMR1	Myotubularin-related protein 1
MyoD	Myogenic differentiation
NCBI	National Centre for Biotechnology Information
NFTs	Neurofibrillary Tangels
PBS	Phosphate buffer saline
PEV	Position effect variegation
PMSF	Phenylmethylsulfonyl fluoride
PROMM	Proximal Myotonic Myopathy
PVDF	Polyvinylidene fluoride
RIPA buffer	Radioimmunoprecipitation assay buffer
RT-PCR	Reverse Transcriptase Polymerase Chain Reaction
RyR1	Ryanodine receptor 1
SCR	Scrambled
SERCA	Sarcoplasmic/endoplasmic reticulum Ca2ATPase
siRNA	Small interfering RNA
SO	Sine Oculis
TBS-T	Tris Buffered saline
TNNT2	Troponin T type
TNRs	Trinucleotide repeats

TZF	Tandem zinc finger
UREDs	Unstable repeat expansion disorders
UTR	Untranslated region
ZNF9	Zinc finger 9

List of Figures

Figure

List of Tables

Table

Acknowledgement

Completing a PhD is not less than completing a marathon event, and I would not have been able to complete this journey on time without the help and support of many people over the past 4 years. First of all, I am extremely grateful to my supervisor David Brook, for his ongoing support and guidance throughout the duration of my PhD. I thank you for your helpful comments and suggestions

I would like to thank all members of David's lab, especially Javier Grandos Riveron and Tushar Ghosh for sharing their practical experience and for their assistance during my time in the lab. I want to thank Ami and Sarah for their help and for their lovely company during coffee breaks. I am surely going to miss our random chats!

I will forever be thankful to my wife, Bhumika Sood, without her love and support I would not have been able to complete this thesis on time.

I especially thank my Dad and Mom. They sacrificed their own comfort for my sister and myself and have always blessed us with love and care. I love them so much, and I would not have made it this far without them.

I dedicate this thesis to

my Dad, my Mom, my Wife, my Sister

for their constant support and unconditional love.

I am lucky to have you all in my life

Abstract

Myotonic dystrophy (DM) is a progressive multisystemic genetic disorder which is inherited as an autosomal dominant trait. There are two subtypes of the disorder, DM type 1 and DM type 2. DM type1 is caused by an expansion of a CTG repeat located in the 3' untranslated region of the DMPK gene on chromosome 19q13.3, whereas DM type 2 is caused by a CCTG expansion in intron 1 of ZNF9 gene located on chromosome 3q. The mutant RNAs containing the expanded CTG/CCTG repeats alters the activity of various alternative splicing factors like Muscleblind-like (MBNL) proteins, which are sequestered in the ribonuclear foci in nucleus by the expanded mutant transcripts resulting in a number of splicing defects observed in DM patients.

In first part of my thesis, I have assessed the nuclear and cytosolic distribution of MBNL proteins in both normal and DM cells. In both DM1 and DM2 cells the amount of nuclear MBNL1 was found to be at least 50% greater than seen in normal cells. In addition to this, I studied the distribution of MBNL1 protein in nuclear and cytosolic fractions of DM cells before and after treatment with compounds chromomycin A3, gemcitabine, IMOX, RO 31-8220 and hypericin which were highlighted in the primary screen. Treatment with the compounds produced a significant reduction in the proportion of nuclear MBNL1 compared to DMSO treated cells in DM fibroblast and myoblasts.

In second part of this thesis I have examined the effect of MBNL1/2 down regulation on both RNA and MBNL1 foci in DM cells. MBNL1 and MBNL2 double knockdown resulted in a 40% increase of nuclear RNA foci than observed in scrambled siRNA treated cells, though a significant reduction was observed in case of MBNL (protein) foci. Also, MBNL 1 and MBNL2 down regulation did not result in the release of mutant transcript from the nucleus to the cytoplasm in KB-Telo MyoD (DM) cells as seen in *BpmI* restriction polymorphism assay. However, it had a degradative effect on the mutant DMPK transcript.

Chapter 1: Introduction

1.1 History of Myotonic Dystrophy

Myotonic dystrophy (DM) is described as the most variable of all human disorders (Harper, 2001). It is an autosomal dominant inherited disorder of muscle weakness and wasting. DM is also recognized by other previously used terms such as 'myotonia dystrophica', 'dystrophica myotonia', and 'myotonia atrophica'. However, the term 'Myotonic Dystrophy' is the most widely used. In some continental European countries it is still known as 'Steinert's disease', in honour of the doctor who first described Myotonic Dystrophy as an independent disorder. Myotonia refers to certain neuromuscular disorders characterized by delayed relaxation of skeletal muscles (Gutmann and Phillips, 1991), whereas dystrophy is a name given to muscle disorders in which muscles shows degeneration of tissue. Myotonic dystrophy combines these two features, thus its name. The history of myotonia dates back to the 1870's not with the DM but with the description of 'myotonia congenita' by Dr. Julius Thomsen. The Danish physician observed an autosomal dominant inheritance pattern in himself and his family members. Myotonia congenita is therefore also known as 'Thomsen's myotonia congentia'. However the terms myotonia congentia and congenital muscular dystrophy should not be confused with congenital Myotonic dystrophy, which is an early childhood form of DM (Harper, 2001). Table 1.1 gives some of the historical landmarks in the recognition and breakthroughs of Myotonic Dystrophy. Two research groups, Steinert and Batten-Gibb, independently described DM as a disease for the first

time in the year 1909. J.G Greenfield in 1911 documented cataract as a characteristic symptom of DM after he observed a high occurrence of cataracts in a large family affected by DM. (Harper, 2001). In 1912, DM was classed as a multi systemic disorder rather than just a muscular one by Curschmann. In the year 1960, Vanier recognized the congenital form of myotonic dystrophy, where he identified the patients problems as dating from birth (Vanier, 1960). In 1971, the genetic linkage was confirmed between myotonic dystrophy and two proteins polymorphisms (Lutheran and ABH secretor loci) by Renwick and Harper (Harper et al., 1972; Renwick et al., 1971). In 1992, after the identification of unstable DNA sequence in Myotonic dystrophy, the mutation that caused DM (type 1) was then confirmed as a trinucleotide (CTG) repeat expansion in a protein kinase gene (Brook et al., 1992; Fu et al., 1992; Mahadevan et al., 1992). Later in the year 1994, another form of myotonic dystrophy was recognized as DM type 2 (Ricker et al., 1994). Expanded CCTG repeats in intron 1 of the ZNF9 gene caused DM2 (Liquori et al., 2001).

DM is an autosomal dominant inherited disorder which affects the muscles and other organ systems. There is a one in two chance (50%) that the affected individual's offspring would inherit the disease. DM is the most prevalent form of muscular dystrophy in adults, which is characterised by progressive muscle wasting and weakness predominantly occurring in hands, lower legs, face and neck. Involuntary delayed relaxation or prolonged contraction of skeletal muscles, cataracts, heart conduction abnormalities and specific sets of endocrine changes are some of the other common symptoms of DM. (Harper, 2001).

Table1.1	Myotonic dystrophy – historical landmarks
1909	First definitive description of myotonic dystrophy
1911	Cataract associated with myotonic dystrophy
1916	Detailed histopathology of muscle changes
1947	First full family and genetic studies
1960	Congenital form of myotonic dystrophy first recognized
1971	Mapping of myotonic dystrophy gene
1992	Isolation of myotonic dystrophy protein kinase gene and identification of trinucleotide repeat mutation
1994	Recognition of type 2 myotonic dystrophy
2000	Mouse used as first experimental model for DM
2001	Gene for type 2 myotonic dystrophy identified

Table 1.1 Historical milestones of myotonic dystrophy.

The severity and the symptoms of the disorder can vary widely from patient to patient. The effects can be fairly different even among affected individuals of the same family.

Myotonic dystrophy affects about 1 in 8000 people worldwide (Harper, 2001). The occurrence of the two forms varies greatly among different geographic and ethnic groups. In majority of populations, DM1 is more common than DM2. However, it has been reported that among German and Finland populations, DM2 may be as prevalent as DM1. (Machuca-Tzili et al., 2005).

1.2 Comparison of clinical features of DM type 1 and DM type2

1.2.1 Muscular dysfunction

DM affects majority of the body systems. Although primarily characterized by skeletal muscle weakness, muscle wasting predominantly in lower legs, hands, neck and face. Mostly patients with DM1 and DM2 have clinically recognisable muscle involvement at the time of diagnosis and often come to medical attention with muscle dysfunction complaints like myotonia (figure 1.3), muscle weakness or pain (Day et al., 1999; Moxley, 1996; Ricker, 1999) (Harper, 2001).

There are many similarities and differences in muscle features of DM1 and DM2. Distal muscle weakness is a predominant symptom in individuals with DM1, whereas patients with DM2 show more of proximal muscle weakness. DM1 patients show severe muscle atrophy but in DM2 muscle weakness tends to be milder and progresses slowly. Ptosis, facial and sternomastoid weakness are some of the distinct features present in DM1 (figure 1.2) but absent or inconspicuous in DM2 (Harper, 2001) (Table 1.2).

Myotonia, the hallmark of myotonic dystrophy is involuntary muscle contraction and delayed relaxation caused by muscle hyperexcitabilty. Myotonia is present in almost all symptomatic adult patients and is frequently found in presymptomatic individuals having DM1. Individuals with DM2 show mild myotonia which rarely causes severe symptoms.

Patients with myotonic dystrophy show dysphagia and constipation because of smooth muscle involvement, though there is a substantial variability between different patients.

Table 1.2	DM1	DM2
Facial weakness	++	±
Ptosis	++	±
Jaw muscles	++	±
Sternomastoids	++	±
Shoulder girdle	±	++
Pelvic girdle	±	++
Proxmimal limb muscles	+	++
Distal limb muscles	++	+
Myotonia	++	+
Pseudohypertrophy	±	-

++, Prominent feature; +, may occur; ±, inconsistent or late feature; -, absent.

Table 1.2 Muscle involvements in DM1 and DM2 (modified from Harper, 2001).

1.2.2 Multisystemic features

DM also affects various other organs of the body such as the eye, heart and the endocrine system. There has been evidence of series of ocular abnormalities like cataract, retinal degeneration, ptosis, corneal lesions and extraocular myotonia. Cataract was first described as an integral feature of myotonic dystrophy by Greenfield in 1911. Slit lamp examination in nearly all affected DM1 and DM2 individuals showed posterior subcapsular cataracts, with distinctive red and green iridescent opacities. Individuals with cataracts may require lens removal as early as early as second decade of life (Day et al., 2003). Griffith in 1911, observed cardiac involvement in DM for the first time. DM shows cardiac conduction defects of varying degrees of severity. Cardiac involvement leads to conduction abnormalities like arrhythmias, which seems to occur in DM2 as prominently as in DM1 (Colleran et al., 1997; Nguyen et al., 1988; Philips et al., 1998), but there is no correlation with repeat length or severity of skeletal muscle involvement (Lazarus et al., 1999). However it been documented that the cardiac involvement in patients with DM2 appears to be more mild than in DM1 (Meola et al., 2002).

Endocrine abnormalities occur in DM2 individuals in form of impaired glucose tolerance (Day et al., 2003; Savkur et al., 2004). Testicular failure problems resulting to infertility are also common in both DM1 and DM2, with associated hypotestosteronemia, elevated FSH levels. Patients with DM1 and DM2 have a weaker immune system with low levels of both IgG and IgM. (Hypogammaglobulinemia) (Harper, 2001).

1.2.3 Congenital DM

The presence of large CTG trinucleotide repeats (usually> 2000) results in an early onset and a more severe disorder called Congenital Myotonic Dystrophy (CDM). The occurrence of CDM is estimated to be one per 3500 to 16,000 individuals (Wesstrom et al., 1986), though no published population-based incidence data exist. DM1 leads to a severe congenital condition but the same has not been observed in case of DM2. Previous data has reported that largest germline expansions happen at the time of maternal transmission (maternal bias transmission), although transmission of congenital DM by the father has been reported (Zeesman et al., 2002). It has also been reported that the length of CTG repeats could even increase somatically in patients affected with DM (Martorell et al., 1998). The symptoms for congenital myotonic dystrophy includes severe generalized muscle weakness, club feet, hypotonia and tented or 'fish'-shaped upper lip. Mortality in affected infants from respiratory failure is common.

1.2.4 CNS involvement

Individuals with DM1 and DM2 show central nervous system abnormalities such as cognitive difficulties, psychological dysfunctions, abnormal behaviour trait, increased day time sleepiness and neuropsychological alterations. These changes have been associated with abnormalities in Tau–associated neurofibrillary tangles observed in brain neurons (Leroy et al., 2006; Oyamada et al., 2006). However, mental retardation has only been reported in DM1 and is not recognized in DM2 (Day et al., 2003; Meola et al., 2002). Patients with CNS abnormalities showed prominent white matter changes on MRI scanning

and reduced cerebral blood flow in the temporal and the frontal region which were evident during PET scan (Hund et al., 1997; Meola et al., 1999).

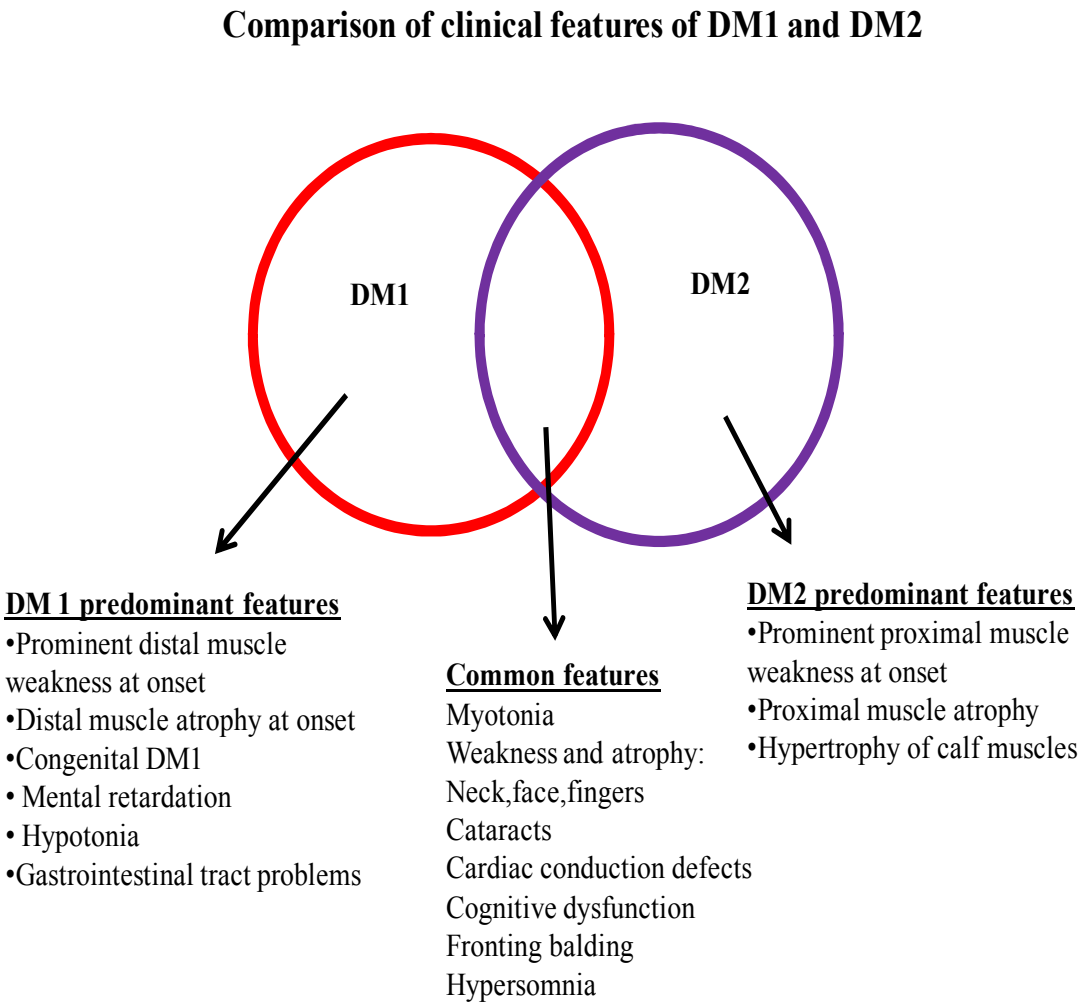

Figure 1. 1 Clinical traits of DM1 and DM2 (taken from Cho and Tapscott, 2007).

Figure 1.2 Characteristic features of myotonic dystrophy patients. Weakness in the jaw and in facial muscles is predominant in DM patients. (Hallmark of DM) (Harper, 2001).

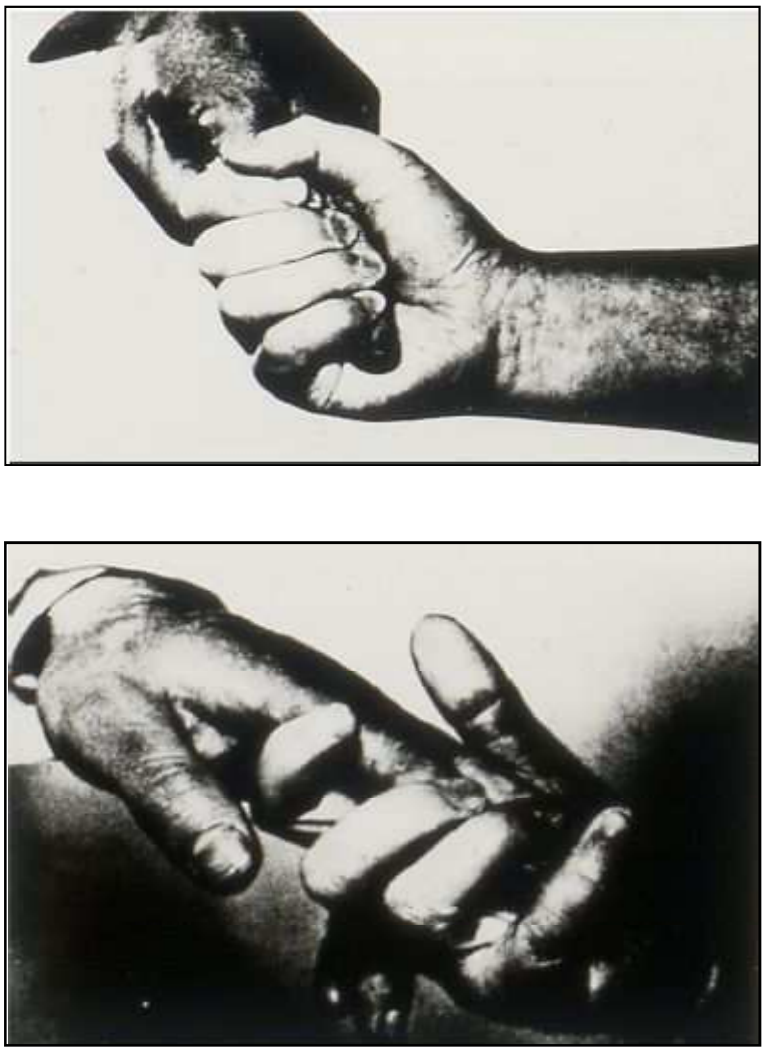

Figure 1.3 Grip Myotonia in a myotonic dystrophy patient (taken from Harper, 2001). Patients with DM have difficulty releasing their grip on objects (Harper, 2001).

1.3 Genetic basis of myotonic dystrophy

1.3.1 The genetic basis of DM type 1

Myotonic dystrophy type 1 is a progressive multi-systemic disorder characterized by myotonia, skeletal muscle weakness, wasting and pain. In 1992, the genetic mutation responsible for DM1 was identified as CTG repeat expansion in exon 15 in the 3′- untranslated region of the *DMPK* gene (Brook et al., 1992; Fu et al., 1992; Mahadevan et al., 1992). The DMPK gene is located on chromosome 19q13.3. Previous data has reported that largest germline expansions happen at the time of maternal transmission., although transmission of congenital DM by the father has been reported (Zeesman et al., 2002) but the length of CTG repeats could even increase somatically in people affected with DM. (Martorell et al., 1998). The children of affected individuals with gene mutation or with premutations inherit longer repeats than their parents, the phenomenon known as anticipation (Figure 1.4). The disease severity is directly proportional to the size of the CTG repeat expansion in the person. Patients with more than 50 CTG repeats have mild adult-onset DM, whereas patients with more than 100 to ~1000 repeats have the classical adult-onset DM. Greater than 2000 or 3000 repeats generally results in the severe congenital form of the DM. Table 1.3 shows the correlation of phenotype and CTG repeats in myotonic dystrophy.

Phenotype	Clinical features	CTG repeat size[1,2]	Age of onset
Premutation	None	35 to 49	Not applicable
Mild	Cataract Mild myotonia	50 to 150	20 to 70 years
Classical	Muscle weakness Myotonia Cataracts Cardiac conduction defects Others	~150 to ~1000	10 to 30 years
Congenital	Respiratory abnormalities Mental retardation	➢ 2000	Birth to 10 years

1. CTG repeat sizes are known to overlap between phenotypes.

2. Normal CTG repeat size is between 5 to 34 repeats.

Table 1.3 Link between phenotype and CTG repeat size in DM1 patients (de Die-Smulders et al., 1998; Mathieu et al., 1999).

Figure 1.4 DM and Anticipation. The image shows a congenitally affected child with his mother (on right) and grandmother (on left). Features like open-mouthed appearance can be seen clearly in the child whereas the mildly affected mother shows reduced facial expression (taken from Harper, 2001).

1.3.2 The genetic basis of DM2

DM2 is caused by a CCTG repeat expansion in intron 1 of the Zinc finger 9 (*ZNF9)* gene on chromosome 3q21.3 (Liquori et al., 2001). The number of the expanded repeats in case of DM2 can range between 75 to 11000 repeats. However, the normal repeat length is approximately less than 30 CTG repeats in a normal individual (Liquori et al., 2003). DM2 shows a milder pattern than DM1 but shows more of proximal muscle involvement than distal muscle involvement. DM1 can lead to a severe congenital condition but the same has not been observed in DM2.

1.4 Genetic instability of repeat expansions in DM and UREDs

Several human disorders are now known to be caused by expansion of unstable repeat sequences, including fragile X syndrome, myotonic dystrophy, Huntington disease, myotonic dystrophy, spinocerebellar ataxia type 1 and Friedreich ataxia. All these disorders are covered under a set of genetic disorders named UREDs (unstable repeat expansion disorders). Mutations in myotonic dystrophy and fragile X syndrome are due to continuous intergenerational expansion of trinucleotide repeats. So far more than 30 UREDs have been identified. Most of these disorders are caused by trinucleotide repeats (TNRs) but it also includes tetranucleotides (Liquori et al., 2001) (myotonic dystrophy type 2), pentanucleotides (Matsuura et al., 2000) (spinocerebellar ataxia 10, SCA10). These UREDs can be grouped under five

major classes according to the location of the repeat expansion in different regions of their genes:

1. In the coding region of their gene (results in altered protein function) as in case of glutamine-encoding repeats in polyglutamine and polyalalanine disorders.
2. Expansions in the 5′-untranslated regions (5′-UTRs) e.g. spinocerebellar ataxia and fragile X syndrome.
3. In 3′-untranslated regions (3′-UTRs) as observed in DM1 and Huntington's disease.
4. In intron regions, as observed in DM 2.
5. Repeat expansions in the promoter regions, as observed in progressive myoclonic epilepsy 1.

The normal alleles of the genes associated with UREDs, generally contain stable repeats with either small expanded repeats or long stretches with stable interruptions (as found observed in fragile X syndrome, which has AGG inserts in $(CCG)_n$ runs in the gene). As the repeat expansions reach a critical threshold limit, the repeats become highly unstable and lead to particular diseases (Parniewski and Staczek, 2002). Certain factors like unusual secondary structures within trinucleotide repeats, DNA-repair models or DNA replication models might result in this genetic instability but the exact mechanisms of CTG repeat expansion is still unclear (Harper, 2001).

1.5 Proposed Molecular Models for Pathogenesis of DM

Three molecular models have been suggested to explain how repeat expansions in noncoding regions at two different loci cause DM and the mechanism of DM pathogenesis. The first two models, haploinsufficency of DMPK model and altered chromatin structure model does not account for all the clinical features or symptoms seen in DM1 and DM2. However, the RNA dominance mutant model is considered as the most accepted and probable model which explains the DM pathogenesis.

1.5.1 Haploinsufficiency of DMPK model

Most dominant disorders are caused by the expression of a malformed protein with an altered function. So it was not clear how the trinucleotide repeat expansion which did not affect the protein coding portion of a gene in DM1 resulted in the multisystemic clinical features of the disease (Tapscott, 2000). It was initially thought that the expanded CTG repeat in the 3′-UTR of the *DMPK* gene altered the level of DMPK expression and its protein level which might be responsible for the multisystemic clinical features of the disease. In order to test this hypothesis several groups attempted to quantify the expression of the *DMPK* RNA from DM tissues and fibroblast cell lines, which all generated inconsistent and confusing results. Fu *et al. (*1993) used RT-PCR of the total RNA extracted from muscle and showed that the *DMPK* expression level from the expanded allele was reduced. Two other groups also reported the absence of mutant *DMPK* transcripts and reduction in *DMPK* expression

level from the normal allele in their studies (Carango et al., 1993; Hofmann-Radvanyi et al., 1993). However, Mahadevan *et al.* showed an increase in the *DMPK* RNA from DM sources because of increased mRNA stability (Mahadevan et al., 1993). However more recent reports agreed that the DMPK mRNA levels were reduced.

In 1996, two groups independently generated *DMPK* knockout mice in order to better assess the role of *DMPK* in DM pathogenesis and to ascertain if some or all of the symptoms of DM are caused due to reduced levels of DMPK. The first mouse generated by Reddy *et al.* (1996) had a targeted disruption of the mouse *dmpk* gene. They reported that the homozygous loss of DMPK in mice resulted in late-onset progressive myopathy that shares some clinical features with DM. The mice also showed structural abnormalities of skeletal muscle fibres and weakness. The heterozygous knockout mice generated showed only a mild phenotype. (Reddy et al., 1996). None of the two mouse models showed any sign of myotonia, hallmark feature of DM. Jansen *et al*. (1996) generated a *DMPK* knockout mouse in which endogenous DMPK was disrupted. The mouse showed only mild symptoms and no progressive symptoms were noted.

Jansen *et al.* (1996) also generated mice which overexpressed the normal human DMPK transgene. The mice showed cardiac abnormalities but no skeletal muscle phenotype. When considered together, all these data from mouse models suggested that DMPK haploinsufficiency alone does not explain the mutisystemic clinical features of DM. Also there has been no evidence for DM1 caused by point mutation in the DMPK gene. Additionally, DM2 is caused by a repeat expansion in another locus (*ZNF9*), which again cannot be described by the haploinsufficiency of *DMPK* gene which is on another locus.

1.5.2 Chromatin structure model

According to this model the CTG repeat expansion mutation alters the chromatin structure and affects the expression of DMPK and multiple other genes in the neighbourhood. It has been known that the repetitive elements in the genome like the ones at the heterochromatin of telomeres and centromeres can suppress the expansion of adjacent genes. For example, it was reported that the genes located adjacent to regions in heterochromatin had an increased chance of being suppressed in Drosophila, which sometimes resulted in variegation known as position effect variegation (PEV). So it was reasonable to believe that the CTG expansion might alter the expression of several other adjacent genes. Support for this model first came from Wang *et al.* (1994), who showed that strong nucleosome positioning signals were created by CTG repeats which potentially altered the local chromatin structure (Wang et al., 1994). Work from Otten and Tapscott (1995) showed that the repeat expansion led to the formation of condensed chromatin structure which may affect transcription due to limited access of transcription factors or by abnormal RNA polymerase processing(Otten and Tapscott, 1995). Several other genes have been mapped around the DMPK gene. These includes the *SIX5* (formerly *DMAHP*), *DMWD* (Dystrophia myotonic-containing WD repeat motif), *GIPR* (human gastric inhibitory polypeptide receptor gene), *FCGRT* (4Mb from the CTG expansion), *Symplekin* and 20-*D7* (Alwazzan et al., 1998; Boucher et al., 1995; Shaw et al., 1993).

The repeat expansion overlaps not only the 3′ end of DMPK, but with the 5′ end of promoter region of the immediately downstream gene *SIX5*. *SIX5* (formerly *DMAHP*) belongs to the family of *Six* family of genes and bear a

strong resemblance to the Drosophila homeodomain-containing protein gene *sine oculis* (SO) that is responsible for eye development and to family of mouse genes that are implicated in distal muscle development (Winchester et al., 1999). Cataracts and distal muscle weakness are common symptoms in DM1, so haploinsufficiency of SIX5 was suggested as possible cause for the formation of cataracts observed in DM1 patients. Several studies have shown that there was a remarkable reduction in *SIX5* gene expression in the DM1 patients compared to normal controls (Alwazzan et al., 1999; Klesert et al., 1997; Thornton et al., 1997).

SIX5 knockout mice models were created independently by two research groups (Klesert et al., 2000; Sarkar et al., 2000). Both the mice models developed ocular cataracts. This suggested that reduced *SIX5* expression contributes to cataract phenotype, and was convincing data to account for the function of adjacent genes in DM pathogenesis. However, the cataracts observed in *SIX5* knockout mouse didn't have characteristic iridescent opacities observed in DM patients.

DMWD gene which is located immediately upstream of DMPK gene is shown to be expressed strongly in the brain and testis. Alwazzan and colleagues (1999) reported there was 20-50% reduction in the level of RNA from the DM-linked allele of *DMWD* in the cytoplasmic fraction but there was no reduction in the nuclear fraction. It was suggested that haploinsufficiency of *DMWD* may be responsible for mental retardation and testicular symptoms seen in DM1 patients and may contribute to DM1 pathogenesis.

However, the DM2 locus (ZNF9 and neighbouring genes) is on an entirely different chromosome therefore the genomic arrangement neighbouring the repeat is entirely different from DM1; thus the chromatin structure model is not able to explain the phenotypes observed in both DM1 and DM2.

1.5.3 RNA dominance mutant model

The demonstration that the haploinsufficiency of DMPK and other neighbouring genes does not fully explain the multisystemic clinical features of DM leads to the possibility of a RNA dominant gain-of-function model. This model suggests that CUG/CCUG repeats exert a toxic effect that disrupts splicing and other possible functions. Support for this model first came from Taneja *et al.* (1995). They used the fibroblasts and muscle biopsies from myotonic dystrophy patients and normal controls to detect the localization of *DMPK* transcripts using oligonucleotides probe (10 repeats of CAG) labelled with a fluorochrome. The expanded transcripts were seen to accumulate in the nucleus as bright foci in fibroblasts and muscle biopsies from DM patients but not in normal controls (Davis et al., 1997; Taneja et al., 1995).

Davis *et al.* (1997) also showed that the mutant transcripts formed stable clusters that were tightly linked to the nuclear matrix. They used northern blotting and *In situ* hybridisation to analyse the *DMPK* transcripts in differentiated cultured myoblasts. In 1997 Hamshere *et al.* used allele specific RT-PCR to analyse sub-cellular fractionation (RNA from cytoplasmic and nuclear fractions) from DM fibroblast cells. They reported the nuclear retention of the transcripts from the expanded DMPK alleles and their absence from the

cytoplasm of the DM cells. Further analysis also suggested that the nuclear retention of transcripts from the expanded DMPK alleles occurs above a critical threshold frequency between 80 and 400 CTGs (Hamshere et al., 1997).

In 1999, Amack and colleagues showed that mutant DMPK 3′-UTR mRNA along with CUG (200) inhibited myogenic differentiation in C2C12 mouse myoblasts model system by reducing the levels of MyoD. They also demonstrated that the expression of 57 CTGs in mutant DMPK 3′-UTR alone was able to form foci (ribonuclear spots) (Amack et al., 1999).

Evidence that there is a common underlying pathogenic RNA mechanism between DM1 and DM2 came from the studies of Liquori *et al.* (2001). They used *in situ* hybridisation to demonstrate that CCUG-containing RNA can also form foci in DM2 muscle. These studies gave further evidence that RNA gain-of-function played an important role in DM pathogenesis.

The direct support for the pathogenic effect of the repeat expansion was reported in a mouse model developed by Mankodi *et al.* (2000). They generated transgenic mice by inserting (CTG_{250}) repeat expansion into the 3′ end of the human skeletal actin gene (HSA^{LR}), a transcript unrelated to the DM1 and DM2 loci. The mouse showed myotonia and myopathic features characteristic of DM. The mouse model also showed MBNL1 sequestration and mis-splicing of multiple other transcripts like Clcn1, Mbnl1, Ldb3/Cypher and Serca1 (Mankodi et al., 2000).

Seznec *et al.* (2001) also developed a mouse model which expressed 300 CTG repeats in the context of the human DM1 locus (>45Kb). This mouse showed ribonuclear foci in various tissues like skeletal muscle and heart. It displayed

myotonia, progressive muscle weakness and muscle histopathology consistent with that seen in DM1 patients. It also showed abnormal distribution of tau protein isoforms as seen in DM patients (Seznec et al., 2001).

In 2006, Mahadevan and colleagues used an inducible mouse model to demonstrate the reversible nature of RNA toxicity. They used the tetracycline (Tet) inducible system to generate mice with the wild type $(CTG)_5$ DMPK 3′ UTR and the mutant $(CTG)_{200}$ DMPK 3′ UTR. Transgene expression in mutant $(CTG)_{200}$ DMPK 3′ UTR resulted in foci formation and MBNL1 protein sequestration but no RNA foci or MBNL sequestration was seen in the case of wild type $(CTG)_5$ DMPK 3′ UTR. The mouse with the short repeat $(CTG)_5$ developed profound myotonia and cardiac conduction abnormalities which is not analogous to symptoms seen in unaffected human individuals or humans carrying 5 CTGs repeats. So this limits its application in therapeutic assays.

The experimental studies mentioned above suggested that repeat expansion (CTG/CCTG) in mutant RNA leads to toxic gain-of function but the reason transcripts with expanded CUG/CCUG repeats caused the multiple features of DM came from the hypothesis of protein sequestration (Timchenko et al., 1996). Various studies have reported that expanded CUG and CCUG-containing transcripts in DM1 and DM2 respectively sequester certain RNA-binding proteins into nuclear foci (Michalowski et al., 1999). RNA-binding proteins play a vital role in post-transcriptional control of RNAs, such as RNA metabolism, nucleocytoplasmic transport, splicing, polyadenylation and translation. Sequestration and depletion of these transcription factors from their active sites, prevents these proteins from performing their normal cellular functions. Two families of proteins have been identified which cause the RNA

transdominant effect. The first one is the CUG-BP1 (CUG binding protein) , it belongs to a family of RNA binding protein known as CELF (CUG-BP- and ETR-3-like factor) family of RNA processing factors, which is responsible for alternative splicing of different transcripts (Ladd et al., 2001).The second is the Muscleblind-like proteins (further discussed in section-1.7.2). Disrupted function of RNA-binding proteins such as CUG-BP1, MBNL and hnRNPs leads to a number of splicing defects observed in DM patients which results in the occurrence of disease symptoms.

1.6 Spliceopathy/ Aberrant Alternative Splicing in DM

1.6.1 Alternative splicing

RNA splicing is a regulated post-transcriptional process that occurs prior to the translation of the mRNA. In this process the coding regions or exons are either retained or excluded to generate different sets of mRNAs, which further result in several protein isoforms from a single gene. Alternative splicing has an effect on most of genes in the human genome; therefore misregulation of RNA splicing has been linked with many human disorders (Cooper et al., 2009; Wang and Cooper, 2007). It has been reported that the expanded CTG/CCTG repeats sequester various RNA binding proteins, which are crucial for normal alternative splicing. Thus the depletion or sequestration leads to aberrant alternative splicing of many other gene transcripts related to DM which then causes the multisystemic features of the disease (Mankodi et al., 2002). Misregulation of splicing has been reported in DM patients' cells in many gene

transcripts like chloride channel 1, insulin receptor, cardiac troponin T. Some of the typical splicing alterations are discussed below:

1.6.1.1 Chloride channel 1 (*Clc1*)

Clc1 is a voltage-gate chloride channel encoded by the CLCN1 gene (also named CLC1). The CLCN1 gene belongs to a family of genes called CLCN (chloride channels, voltage-sensitive). These channels are responsible for transporting negatively charged chlorine atoms (chloride ions) across cell membranes. They play a key role in stabilizing the resting membrane potential and help in regulating electrical excitability in skeletal muscle (Dutzler et al., 2002). More than 60 CLCN1 mutations have been identified in people with myotonia congenita (MC). Most of these mutations have been associated with the recessive form of MC (Becker disease) and with the dominant form (Thomsen disease) (Grunnet et al., 2003; Sasaki et al., 1999; Sasaki et al., 2001).

A predominant and a classic feature of both DM1 and DM2 is myotonia, which is caused by involuntary repetitive firing of action potentials that delays skeletal muscle relaxation following voluntary muscle contraction (Harper, 2001). Mankodi and colleagues (2000, 2002) used skeletal muscle from a transgenic mouse to show that expression of expanded CUG repeats reduces the transmembrane chloride conductance to levels thought to be enough to cause myotonia in DM patients (Mankodi et al., 2002). It has been demonstrated that loss of CLCN1 mRNA and protein observed in DM1 muscle samples was due to aberrant splicing of CLCN-1, the main chloride channel in

muscle. Misplicing of CLCN1 involves retention of intron 2, which contains a premature stop codon, or inclusion of two novel exons between exon 6 and exon 7 (Charlet et al., 2002). Charlet and colleagues (2002) showed that CUG-BP is elevated in DM1 striated muscle and binds to the CLCN1 pre-mRNA, and overexpression of CUG-BP in transfected cells (normal cells) reproduces the aberrant pattern of CLCN1 splicing, similar to that observed in DM1 skeletal muscle.

Similar splicing alterations were observed in muscle tissue from DM1 and DM2 patients, suggesting a common pathogenic mechanism for both types of disease (Charlet et al., 2002; Mankodi et al., 2002).

1.6.1.2 Insulin receptor (*IR*)

The *IR* is a heterotetramer structure made up of two α-subunits and two β-subunits, encoded by a single gene *INSR*. Binding of insulin to the extracellular α-subunit, leads to autophosphorylation of the intracellular β- subunit. There are two isoforms of insulin receptor because of alternative splicing of the 36 nucleotides exon 11 of the α-subunit: Isoform IR-A (lacking exon 11) and isoforms IR-B (including exon 11). Expression of these two isoforms is tissue-specific (Moller et al., 1989; Seino and Bell, 1989). The isoforms lacking exon 11 (IR-A) has higher affinity for insulin than the isoforms including exon 11 (IR-B). Isoform IR-B is predominantly expressed in adipose tissue, liver and skeletal muscle, all of them responsible for glucose homeostasis (Moller et al., 1989; Mosthaf et al., 1990).

A common clinical feature in both DM1 and DM2 patients is insulin resistance. Insulin resistance is a condition in which cells fail to respond to the normal actions of the hormone insulin. It has already been shown that the reduced insulin response in skeletal muscle predisposes DM patients to diabetes. Savkur and colleagues (2001) demonstrated that alternative splicing of the insulin receptor (IR) pre-mRNA is aberrantly regulated in DM1 skeletal muscle cultures (Savkur et al., 2001), which resulted in inappropriate expression of the IR-A isoform (lacking exon 11) in skeletal muscle. They also showed that there was an increase in steady state levels of CUG-BP in skeletal muscle of DM1 patients and overexpression of CUG-BP also induces a switch in the splice form, towards IR-A in normal cultured cells. This strongly suggested that CUG-BP mediates this alternative splicing switch by binding to an intronic element upstream of the alternatively spliced exon 11. Thus, increase in CUG-BP levels was considered as the primary determinant for the misregulation of Insulin receptor (IR) (Savkur et al., 2001).

In addition to this, it has been found that the same insulin receptor splicing alterations occur in muscle biopsies from patients from DM2 (Savkur et al., 2004).

1.6.1.3 Cardiac Troponin T (*cTNT*)

In humans, the protein Troponin T type 2 (cardiac) or TNNT2, is encoded by the TNNT2 gene. Cardiac troponin T is a thin filament contractile protein. It is the tropomyosin-binding subunit of the troponin complex, which is located on the thin filament of striated muscles and regulates muscle contraction. Mutations in this gene in humans are responsible for causing familial hypertrophic cardiomyopathy, and can also cause dilated cardiomyopathy (Kamisago et al., 2000; Seidman and Seidman, 2001). Transcripts for TNNT2 undergo alternative splicing of 15-bp (exon 4) and 30-bp (exon 5) mini-exons which results into multiple tissue-specific isoforms. Exon 5 is included in transcripts produced during the early development of heart and skeletal muscle, but not in adult heart.

In 1998, Phillips and colleagues analysed cardiac tissues from DM1 patients and demonstrated that there was a shift to the embryonic isoforms by preferential inclusion of exon 5 in the adult tissues (Philips et al., 1998). This aberrant splicing pattern was due to the binding of CUG-BP to the human cardiac troponin T (cTNT) pre-mRNA, resulting in a transdominant effect and suggesting a role in the regulation of its alternative splicing. To confirm this, transgenic mice overexpressing CUG-BP1 in heart and skeletal muscle, two tissues affected in DM, was generated. The mice showed disrupted splicing for cTNT, CLCN1 and Mtmr1 (Ho et al., 2005a). Cardiac Troponin T was the first pre-mRNA shown to be aberrantly spliced in DM1 (Philips et al., 1998).

1.6.1.4 *Tau*

Tau proteins play an important role in stabilizing microtubules. They are abundant in neurons of the CNS but are also expressed at very low level in CNS astrocytes and oligodendrocytes (Shin et al., 1991). Tau protein assists with the formation and stabilization of microtubules by binding to them. But when Tau proteins become hyperphosphorylated, it is unable to bind and leads to the disintegration of microtubules. The unbound tau clumps together to form a complex known as Neurofibrillary Tangels (NFTs), which then interfere with various other normal intracellular functions. NFTs presence is found in several neurodegenerative diseases like Alzheimer's disease, frontotemporal dementia with Parkinsonism linked to chromosome 17 and other conditions known collectively as tauopathies. Six tau isoforms have been identified in human central nervous system. These isoforms are a result of alternative splicing in exons 2, 3 and 10 of the *tau* gene. A specific set of tau isoforms are aggregated in the neocortex and subcortical nuclei in DM1 patients as reported by different research groups (Kiuchi et al., 1991; Mitake et al., 1989; Vermersch et al., 1996). In 2001 Sergeant and colleagues showed that there were splicing alterations in the microtubule-associated tau pre-mRNA in CNS tissue from DM1 patients (Sergeant et al., 2001). They also observed lower amounts of tau isoforms containing the exon 2 and exon 3 at both mRNA and protein levels, compared with controls. Role of *tau* in DM was also validated by using a mouse model which expressed CTG repeats in *DMPK* 3′ -UTR. Like DM1 patients, the transgenic mice showed abnormal expression of tau in brain (Seznec et al., 2001).

1.6.1.5 Myotubularin-related protein 1 (*MTMR1*)

The *MTMR1* gene belongs to a conserved family of phosphatase genes including 14 members in human, mainly *MTM1* and *MTMR1-13*. Alternative splicing of *MTMR1*, produces three major isoforms A, B and C. During muscle differentiation, the expression of *MTMR1* is developmentally regulated by alternative splicing of two fetal isoforms A and B, which switches to the adult isoforms C in adult skeletal muscle and cardiac muscles during development (Buj-Bello et al., 2002). No mutations in the *MTMR1* gene have been linked with human diseases so far, but aberrant splicing of *MTMR1* pre-mRNA has been reported in differentiating muscle cell cultures in congenital DM1 patients. Buj-Bello and colleagues (2002) observed that there was a significant reduction of the normal muscle adult C isoforms, increased levels of the fetal A and B isoforms and the presence of a new aberrant G isoforms containing novel exon 2.2 in skeletal muscle biopsies of congenital DM1 patients and in differentiating muscle cell cultures.

Ho *et al*. (2005) also reported that the transgenic mice overexpressing CUG-BP1 showed disrupted splicing of *MTMR1* gene, consistent with that observed in DM heart and skeletal muscle. Analysis of splicing by RT-PCR indicated that the mice expressed more of fetal A and B isoforms, compared to the wirld type mice, which expressed more of adult normal C isoforms (Ho et al., 2005a).

1.6.1.6 Ryanodine receptor (RyR) and Sarcoplasmic/endoplasmic reticulum Ca^{2+}-ATPase (SERCA)

Ryanodine receptor 1 (RyR1) and sarcoplasmic/endoplasmic reticulum Ca^{2+}-ATPase (SERCA), the two sarcoplasmic reticulum (SR) proteins are responsible for regulating intracellular Ca^{2+} homeostasis in skeletal muscle cells (Kimura et al., 2005). There are multiple isoforms of ryanodine receptors in mammals. RyR1- primarily expressed in skeletal muscle. RyR2 is expressed in heart muscle and RyR3 is expressed more widely, but particularly in the brain. The expression of RyR1 isoform is regulated both developmentally and in a tissue specific manner (Futatsugi et al., 1995). In case of SERCAs, there are 3 major paralogs, SERCA1, SERCA2 and SERCA3. They are all expressed at different levels in different cell types. Alternative splicing for transcripts from these genes is regulated developmentally and in tissue specific manner. This results into isoforms that differ in their C-terminal region (MacLennan et al., 1997). SERCA1a, which is an adult isoform and SERCA1b, which is a neonatal isoform are primarily expressed in fast-twitch (type2) skeletal muscle (Wuytack et al., 1992). SERCA2a is expressed in slow –twitch (type1) skeletal and cardiac muscles, but SERCA2b expression is more extensive. SERCA3 is found in many non-muscle tissues at different levels (Lytton et al., 1992).

Several splice variants for RyR1 has been described by Futatsugi *et al.*(1995). The variant ASI (-), which lacks exon 70 and a splice variant ASI (+), which has the exon 70. Kimura and colleagues (2005) reported that the fetal variant, ASI (-) of RyRI which lacked the exon 70 was significantly increased in

skeletal muscles from DM1 patients and the transgenic mouse model (HSA^{LR}) (Kimura et al., 2005).

In the case of the other SR protein, SERCA, the proportion of SERCA1b (-exon 22) was significantly elevated in DM1 muscles compared to control. This was consistent to what was observed in transgenic mouse model of DM1 (HSA^{LR}). Data from these studies suggested that aberrant splicing of RyR1 and SERCA1 mRNAs played a role in misregulation of intracellular Ca^{2+} homeostasis in DM1 muscle (Kimura et al., 2005).

1.6.1.7 Fast Skeletal Troponin T (*TNNT3*)

Kanadia and colleagues (2005) reported aberrant splicing of TNNT3 in adult DM1 muscle. This was further verified by reporting the presence of fetal (F) exon isoform in muscleblind-like knock out mouse model ($Mbnl^{\Delta E3/\Delta E3}$) (Kanadia et al., 2003).

1.7 Role of RNA-binding proteins in DM

RNA-binding proteins play an important role in many cellular processes and functions. They are involved in many post-transcriptional activities like splicing, polyadenylation, mRNA stabilization and localization and translation. The two main families of RNA-binding proteins implicated in DM pathogenesis are MBNL and CELF proteins. hnRNP H, another RNA-binding protein, has also been shown to be implicated in DM pathogenesis.

1.7.1 CUG-BP1 and pathogenesis of DM

CUG-BP was the first protein to be reported and analysed by Timchenko and colleagues in 1996. Bandshift analyses using cell extracts of HeLa cell, fibroblasts and myotubes were used as protein source to identify CUG-BP. CUG-BP protein was found to specifically bind to triplet repeats (CUG) present in *DMPK* mRNA, so was termed CUG-BP (CUG binding protein). Two isoforms of CUG-BP were identified; CUG-BP1 and CUG-BP2, both are isoforms of a novel heterogeneous nuclear ribonucleoprotein (hNab50) (Timchenko et al., 1996). CUG-BP is a member of the CELF (CUG-BP1 and ETR-3-like factors) family of RNA-processing factors that regulates alternative splicing (Ladd and Pliam, 2001). Six CELF (also known as BRUNOL) genes have been identified in humans by screening human EST databases (Ladd et al., 2001; Ladd et al., 2004). All six CELF proteins were reported to regulate pre-mRNA alternative splicing and two of them (CUG-BP1 and ETR-3/CUG-BP2) were also involved in cytoplasmic RNA-associated functions (Lu et al., 1999).

The CELF family proteins can be sub grouped into two groups, first group consisting of CUG-BP and ETR-3 (which are 78% identical amongst each other) and a second group consisting of three novel proteins CELF3, CELF4 and CELF5 (CELF3 has 60.8 % sequence similarity with CELF4 and CELF5 has 63.8% sequence similarity with CELF4).

The *in vivo* experiments involving CUG-BP/hNab50 showed that CUG-BP interacts with mRNAs and are involved in the processing or transport of many other transcripts. It was initially thought that CUG-BP proteins were

sequestered by the expanded CUG repeats in *DMPK* RNA just like MBNL proteins. However, it was reported by Michalowski and colleagues (1999) that CUG-BP is not sequestered by RNA containing the expanded CUG repeats. They used electron microscopy to examine the structure of $CUG_{75\text{-}130}$ repeat containing RNA and CUG-BP together and reported that binding of CUG-BP was only at the base of the RNA hairpin and not on the hairpin stem (Michalowski et al., 1999). It was postulated that the binding of CUG-BP protein was not proportional to the CUG repeat length and it was also observed in yeast three-hybrid system that it preferentially binds to the UG motifs rather than CUG repeats. Furthermore, Fardaei and colleagues (2001) reported using indirect Immunofluorescence and GFP tagged proteins that the CUG-BP does not colocalize with the expanded CUG repeats in DM1 cells (Fardaei et al., 2001).

As reported in previous studies, two phosphorylated forms of CUG-BP- a hyperphosphorylated form (CUG-BP1) and a hypophosphorylated form (CUG-BP2) exist (Roberts et al., 1997). CUG-BP is in fact a substrate for DMPK. An increase in the level of hypophosphorylated form (CUG-BP2) in the nucleus was observed as result of the reduced levels of DMPK protein in DM patients and DMPK knockout mice (Roberts et al., 1997).

In a recent study, it was shown that the expression of DMPK-CUG-repeat RNA activates protein kinase C (PKC), which leads to CUG-BP1 hyperphosphorylation and increased CUG-BP1 steady state levels in DM1 (Kuyumcu-Martinez et al., 2007).

Several studies have pointed towards a gain of CUG-BP1 activity in DM1. They have all reported an increase in CUG-BP1 steady state levels in DM1 myoblasts, heart tissues and skeletal muscle (Dansithong et al., 2005; Savkur et al., 2001; Timchenko et al., 2001). CUG-BP1 is known to regulate alternative splicing of pre-mRNAs like cTNT, IR and Clc1, which are aberrantly spliced in DM1 striated muscles (Charlet et al., 2002; Philips et al., 1998; Savkur et al., 2001). To test whether increase in CUG-BP1 steady state levels was sufficient to cause the misregulation of alternative splicing of specific transcripts in DM, Ho and colleagues (2005) generated a transgenic mice overexpressing CUG-BP1 (MCKCUG-BP1) in heart and skeletal muscles. These mice showed aberrant splicing for *TNNT2, MTMR1* and *CLCN1*, consistent with that observed in DM. They also showed histological abnormalities like chains of central nuclei and degenerating fibers, resembling congenital DM1 (Ho et al., 2005a). Timchenko *et al*. (2004) generated CELF1 overexpressing lines (CUGBP1-TR). They reported that there was a significant increase of MEF2A and p21 levels compared to wild type controls, in CELF1 overexpressed CUGBP1-TR lines. These lines also displayed delayed myogenesis and growth retardation that correlated with the level of CELF1 upregulation (Timchenko et al., 2004).

In addition, to these CUG-BP1 overexpression models, there have been two recent mouse models which showed inducible tissue- specific expression of RNA containing CUG repeats in the context of the DMPK 3′-UTR (Mahadevan et al., 2006; Orengo et al., 2008; Wang et al., 2007) . To better study the role of CUG-BP1 in spliceopathy in DM pathogenesis, Mahadevan and colleagues (2006) generated an inducible model overexpressing the DMPK

3′-UTR with CTG_5 or CTG_{200} repeats (figure1.5, c). The mice with CTG_{200} repeats showed RNA foci and MBNL1 sequestration. The mice with CTG_5 repeats showed no RNA foci or MBNL1 sequestration but it displayed profound myotonia and heart and skeletal muscle abnormalities on transgene expression (Mahadevan et al., 2006). Unlike HSA^{LR} mice, the splicing defects in GFP-DMPK-$(CTG)_5$ mice were associated with CELF1 upregulation (Mahadevan et al., 2006).

Wang *et al*. (2007) and Orengo *et al*. (2008) both used the inducible Cre-Lox system to produce tissue-specific expression of expanded CUG repeats (figure 1.5, b). Orengo and colleagues (2008) suggested that the increased CUG-BP1 levels were associated with aberrant alternative splicing of CLCN1 (inclusion of the fetal exon 7a which contains a premature stop codon), SERCA1 (exclusion of exon 22) and CYPHER (inclusion of exon 11) in the mouse model (EpA960) after tamoxifen-induced transgene expression (Orengo et al., 2008). Unlike HSA^{LR} mice, which didn't show any CELF1 upregulation or muscle weakness, the EpA960 mice (figure1.5, b) showed CUG-BP1 hyperphosphorylation and upregulation after the transgene expression. This suggested that the genomic context of CTG expansion may be contributing to CELF1 upregulation, which then results into misplicing of CUG-BP1 dependant transcripts.

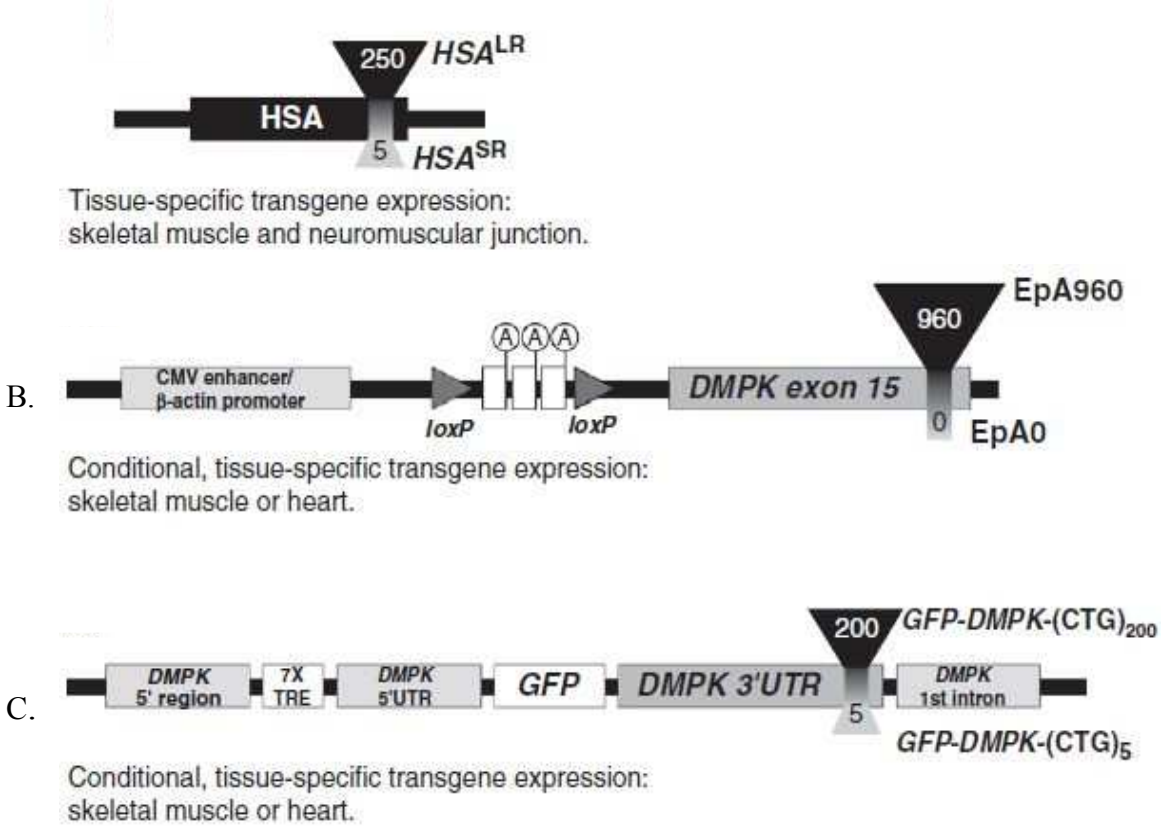

Figure 1.5 Schematic representation of CTG-expressing transgene constructs (modified from Mario Gomes-Pereira, 2011). A) HSA^{SR} and HSA^{LR} transgenic mice carrying a fragment of human skeletal actin (HSA) gene with 5 CTG and 200 CTG repeats inserted in its final exon respectively. **B)** Inducible EpA mice carrying human version of DMPK exon 15, with (960 CTGs) or without repeats. **C)** *GFP-DMPK-(CTG)$_n$* mice which expresses a *GFP* transcript fused to the *DMPK* 3´-UTR containing 5 or 200 CTG repeats.

1.7.2 MBNL and pathogenesis of DM

Another family of RNA-binding proteins, one which bind with high affinity to RNAs containing the expanded CTG repeats in a size-dependent manner, is Muscleblind-like protein (MBNL), a mammalian homologue of *Drosophila* muscleblind protein (Mbl) which is necessary for development of muscle and differentiation of photoreceptor cells in *Drosophila* (Miller et al., 2000). *Drosophila* Mbl proteins contain two tandem zinc finger (TZF) motifs, members of the zinc finger family of nucleic acid binding motifs. These zinc-finger motifs presumably confer on Mbl the ability to bind to their RNA targets (Begemann et al., 1997; Miller et al., 2000). Unlike Drosophila Mbl protein, human MBNL protein has four tandem zinc finger (TZF) motifs instead of two.

Muscleblind-like proteins in humans are encoded by three different genes, which are known as *MBNL1 (*formally *MBNL), MBNL2 (MBLL)* and *MBNL3 (MBXL)*, located on chromosomes 3, 13 and X respectively (Fardaei et al., 2002; Miller et al., 2000). It has been shown that MBNL1 is primarily expressed in muscle and heart, unlike MBNL2, which shows a similar level of expression across all tissues like heart, brain, lung, placenta, liver, skeletal muscle and kidney. MBNL3 has a strong expression in placenta (Fardaei et al., 2002). All three MBNL proteins have been shown to co-localize with expanded CUG/CCUG repeats RNA foci in *vivo* (Fardaei et al., 2002; Mankodi et al., 2001; Miller et al., 2000). Reduction of MBNL proteins, due to sequestration by the RNA containing expanded CTG/CCTG repeats may account for some of the pathological features of DM. In support for this hypothesis, Kanadia *et al.* (2003) generated a mouse knockout model ($MBNL^{\Delta E3/\Delta E3}$). The mouse showed

myotonia, cataracts and misregulation of splicing observed in DM1 and DM2. Consistent with the hypothesis that MBNL1 sequestration causes aberrant splicing of specific RNAs, Kanadia *et al.* (2006) used adeno-associated virus (AAV) - mediated transduction to overexpress MBNL1 protein. They showed that overexpression of MBNL1 in transgenic HSA^{LR} mice rescued the myotonia and splicing defects of CLCN1, CYPHER/Ldb3, SERCA1 and TNNT3 (Kanadia et al., 2006). More recently Chamberlain and colleagues (2012) generated the first transgenic MBNL1 overexpression mouse model to check the safety and therapeutic potential of MBNL1 overexpression. They reported that the high levels of MBNL1 overexpression was well accepted by skeletal muscle and it ameliorated skeletal muscle myopathy (Chamberlain and Ranum, 2012).

MBNL1 protein has been shown to play a main role in DM pathogenesis in various studies. Dansithong and colleagues (2005) tested the role of MBNL proteins in the maintenance of DM1 foci integrity by down regulating the levels of MBNL1 and MBNL2 in DM1 myoblasts using siRNAs. They reported that depletion of MBNL1 protein resulted in reduction of foci by nearly 70 %, ~25% reduction in foci number in case for MBNL2 depletion and together (MBNL1 and MBNL2 depletion) it resulted in reduction of foci number by 80% (Dansithong et al., 2005). Loss of MBNL1 function due to its sequestration has been implicated in misregulated splicing of many transcripts like *CLCN1*, *IR* and *cTNT* which leads to the disease symptoms like myotonia, insulin resistance and cardiac conduction abnormalities in patients with DM (Charlet et al., 2002; Dansithong et al., 2005; Ho et al., 2004) but it was not clear if the phenotype was caused by direct or indirect effects on splicing. To

test this, Ho *et al.* (2004) used siRNA to downregulate MBNL1 levels in HeLa cells. Analysis revealed that depletion of endogenous MBNL1 altered alternative splicing of *cTNT* and *IR* (Ho et al., 2004). Furthermore, it had already been shown that overexpression of MBNL1 and MBNL2 played a predominant role in the rescue of IR splicing defects in DM1 myoblasts (Dansithong et al., 2005).

But there are studies which indicate that sequestration of MBNL proteins alone cannot account for all clinical features seen in the DM. A study performed by Ho *et al.* (2005) showed that both CUG and CAG RNA repeats were able to form foci that contain both exogenously expressed GFP-MBNL1 and endogenous MBNL1, but only CUG repeats altered splicing of cTNT and IR transcripts (Ho et al., 2005b).

A MBNL1 knockout mouse model was generated by Kanadia and colleagues (2003) which mimicked the DM1 situation where MBNL1 protein is sequestered and is functionally unavailable for normal use. The mice displayed myotonia (*CLCN1* aberrant splicing and ClC-1 protein reduction), cataracts and missplicing of certain other transcripts. However, muscle weakness was not detected in this model which results from different mechanisms, like CELF upregulation (Kanadia et al., 2003). Thus, some features of DM phenotype may not result from loss of MBNL1 function alone and other factors might be involved in DM pathogenesis.

1.7.3 MBNL and CUG-BP1 proteins are antagonistic regulators of alternative splicing

The expanded CUG repeats have a trans-dominant effect on alternative splicing regulation through at least two RNA-binding proteins: Muscleblind-like 1 (MBNL1) and CUG-BP1. These proteins are antagonistic regulators of splicing events that are misregulated in DM1. In DM normal developmental splicing events are disrupted which results in expression of fetal protein isoforms instead of adult isoforms in adult tissues. It has been shown that the MBNL levels are reduced due to sequestration by expanded CUG repeats RNA and steady state levels of CUG-BP1 are increased in DM cells. Loss of MBNL1 function and CUG-BP1 elevation has been implicated in misregulated splicing of pre-mRNAs like *IR* and *cTNT* which leads to the disease symptoms like insulin resistance and cardiac conduction abnormalities in patients with DM (Ho et al., 2004; Lin et al., 2006; Philips et al., 1998; Savkur et al., 2001).

CUG-BP1 induces inclusion of both human and chicken cTNT exon5 and exon skipping of human IR exon 11 whereas, MBNL proteins promotes exon skipping of human and chicken cTNT exon5 and inclusion of human IR exon 11 (Charlet et al., 2002; Ladd et al., 2001; Philips et al., 1998; Savkur et al., 2001). The antagonism is not due to the direct competition for the same binding site, but both MBNL and CUG-BP1 proteins recognize discrete *cis*-acting parts in human and chicken cTNT (Ho et al., 2004). CUG-BP1 can regulate splicing of minigenes even if there is a mutation in MBNL1-binding site. Likewise, MBNL can regulate splicing of minigenes with CUG-BP1-binding site mutation that block CUG-BP1 responsiveness. This suggest that

MBNL and CUG-BP1 proteins act independently and they don't have a direct competition for the common binding site (Ho et al., 2004).

The RNA dominance model describing the pathogenesis of myotonic dystrophy is summarized in Fig. 1.6

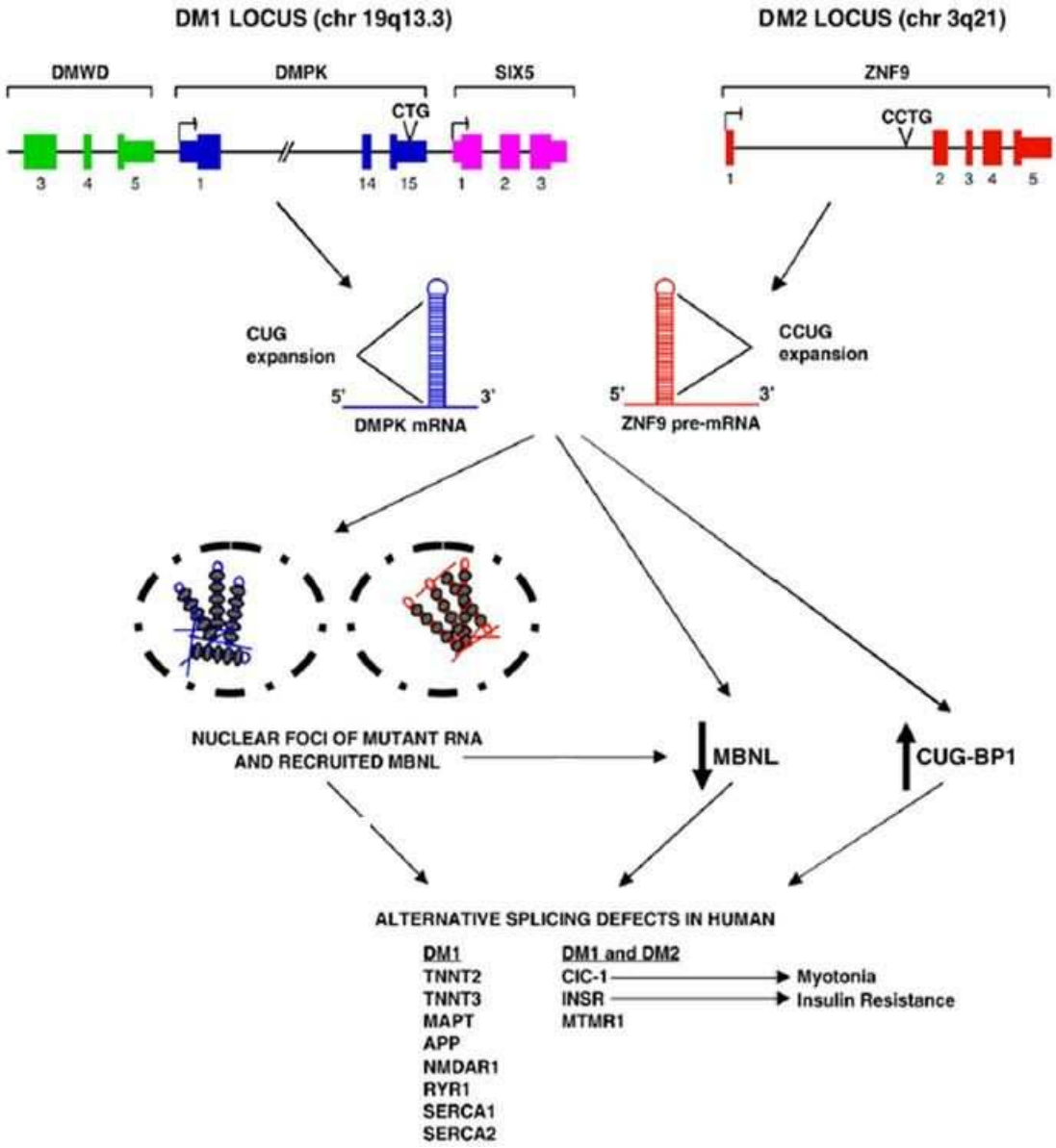

Figure 1.6 RNA toxic gain of-function for DM (modified from Diane and Tapscott, 2007). The RNA dominance mutation model proposes that the expanded CTG repeats results in a toxic gain of function at the RNA level by disrupting the activities of RNA-binding proteins implicated in regulating alternative splicing and mRNA translation. Alteration of various RNA-binding proteins such as MBNL1-3, CUG-BP1 and hnRNP H leads to misregulation of many developmentally regulated transcripts, which causes the symptoms in DM.

1.8 Possible Targets for Therapeutic Intervention in DM

Currently there is no treatment for either form of DM. Molecular therapeutic strategies for DM1 can be directed specifically at the level of RNA or protein. There have been many publications involving biochemical and oligonucleotides based therapy directed against molecular effects of repeat expansion. They aimed at either correcting of aberrant splicing (Wheeler et al., 2007) or disrupting the interaction between MBNL and the repeats (Arambula et al., 2009; Gareiss et al., 2008; Mulders et al., 2009; Pushechnikov et al., 2009; Warf et al., 2009; Wheeler et al., 2009). Also there have been studies which utilized the use of cell based assays in conjunction with fluorescent splicing reporters for compound screens (O'Leary et al., 2009; Orengo et al., 2006).

Our own lab designed and developed cell-based assays that were utilized for screening molecules and compounds for DM therapy. These assays allowed the screening of thousands of small molecules and compounds on large scale in High Throughput Screens (HTS) to identify compounds that eliminate nuclear foci and may have potential for further development as DM therapies (Ketley et al., 2013). The initial primary screen analysed compounds from 3 different libraries. 13200 compounds were screened from a Chembrige Diverset library, 2724 compounds from the NPC library and 80 kinase inhibitors and 33 phosphatase inhibitors from Enzo Life sciences. Table 1.4 shows the number of compounds screened as part of primary screening and the positive hits which were taken forward to secondary assays.

Library	Compounds screened	Primary Hits	Secondary Assays	Tertiary Assays
Chembridge library	13200	364	0	0
FDA approved drugs collection	2724	120	2	2
Kinase Inhibitors	80	2	2	2
Phosphatase Inhibitors	33	0	0	0

Table 1.4 Shows the number of compounds screened and the numbers taken forward to the secondary and tertiary assays (Ketley et al., 2013).

1.9 Aim of project

Myotonic dystrophy (DM) is the most common adult-onset muscular dystrophy that affects the muscles and various other body systems. Strong evidence supports a pathogenic RNA dominance model in which RNAs containing expanded CUG/CCUG forms stable hairpin structures which alters the activities of various RNA binding proteins like CUGBP1/ETR3-like factors (CELF) and MBNL proteins. The RNAs containing the expanded repeats accumulates in the nucleus where they sequester all three MBNL proteins (MBNL1, MBNL2 and MBNL3). MBNL1 plays an important role in regulating alternative splicing in skeletal and cardiac muscle (O'Rourke and Swanson, 2009). Thus, its depletion from the nuclear pool results in misregulated alternative splicing of many other transcripts. In my thesis I have focussed mainly on the sub-cellular distribution of MBNL1 protein and its role in DM. The main aims of my research were:

1. To compare different separation methods to study the sub-cellular (Nuclear v/s Cytosolic) distribution of Muscleblind-like protein 1 in Normal and DM cells. I have compared two separation techniques, the first one involves use of Nonidet P-40 buffer and the second one involves use of physical shearing method using a ‘syringe’ to separate nuclear and cytoplasmic fractions.
2. To assess the effect of compounds that came up as ‘positive hits’ in primary screening on MBNL1 nucleo-cytosolic distribution in DM1 fibroblasts and myoblasts. I have used western blot analysis to determine this.

3. To determine the effect of compounds (positive ‘hits’) on the MBNL1 protein in the foci (MBNL foci) using immunocytochemistry studies.
4. To assess the effect of MBNL1 and 2 down regulation on the nuclear foci in DM1 cells.
5. To assess the effect of Antisense oligonucleotides (AONs) on MBNL1 protein sub-cellular distribution in DM myoblasts
6. To determine the phosphorylation state of MBNL1 protein and to map the phosphorylated site (s) using Mass Spectrometry and IP.

Chapter -2: Methods and Materials

2.1 Cell culture

Tissue cell culture was carried out inside a laminar flow cabinet in tissue culture room.

2.1.1 Cell lines

Cell lines used in the study include human fibroblasts cell lines from DM1 (KB-Telo MyoD) and DM2 (KAGO-Telo) patients. Two wild type lines were also used NIRA-Telo and SB-Telo MyoD; contains an inducible MyoD gene, which is expressed in the presence of doxycyclin promoting the differentiation of fibroblast cells into myoblasts cells. All the cells used in the study had been previously telomerised that is they express telomerase so they were able to grow continuously in culture over extended period of time. DM myoblasts and control myoblast cells were also used in our study. CTG repeat sizes were; KBTeloMyoD - 400 repeats and DM15 – 3000 repeats.

2.1.2 Media and solutions

Medium used in the study was Dulbecco's minimum essential media (DMEM) from Gibco life technologies containing 4500 mg/L glucose, L-glutamine and pyruvate. Other solutions used in tissue culture were Foetal bovine serum (FBS) from Gibco life technologies, Antibiotics Penicillin and Streptomycin from Gibco, Phosphate buffer saline (PBS), 0.25% Trypsin-EDTA solution from Sigma and Dimethyl Sulphoxide (DMSO) from Sigma.

2.1.3 Media for fibroblasts and myoblasts

Dulbecco's Modified Eagles Medium (DMEM) with penicillin (10,000 units of Penicillin G) and streptomycin (10,000 µg/ml), and 10% fetal calf serum (FBS) was used to grow fibroblast cells. In the case of myoblasts, the cells were first grown in Ham's F10 containing penicillin and streptomycin with 20% FBS and then differentiated for 5-6 days into myotubes in DMEM containing low serum (1% FBS) to stop them from proliferating.

2.1.4 Passaging of cells

For fibroblast and myoblast cell lines, cells were sub-cultured after reaching 80%-100% confluency, which was determined by visualizing the cells under the microscope. Firstly, the media was decanted and the cells were mildly rinsed with 10 ml pre-warmed PBS followed by addition of 2 ml of 0.25% Trypsin-EDTA to the flask containing the cells. The cells were then incubated in the 37°C and 5% CO_2 incubator for 2 min in order to remove the cells from the base of the flask. The cells were visualized under microscope to confirm dissociation and 11 ml of new medium was added to the flask and gently pipetted up and down to dissolve the cells homogenously. The cells were then split into new sterile 75 cm^3 flasks depending on the required cell concentration which was usually 1/3 in our studies.

2.1.5 Cryopreservation and Storage of Cells

DMSO was used as a cryopreservant for human fibroblasts and myoblasts. For freezing the cells, medium was decanted and cells were washed with 10 ml of pre-warmed PBS. Cells were then trypsinized with 2 ml of 0.25% trypsin EDTA to dissociate them from the bottom of flask by incubating the flask at 37°C incubator. Following trypsinization the cells were resuspended in 10 ml of fresh media and pelleted by centrifugation at 2000 rpm for 3 minutes. Supernatant was discarded and the cells were resuspended in 1 ml of fresh media containing 10% (v/v) DMSO. The cells were then instantly transferred to cryotubes for storage at -80°C for 24 hours and finally transferred to liquid nitrogen for storage.

2.1.6 Defrosting and reviving cells from liquid nitrogen

Cryovials containing the frozen cells were removed from liquid nitrogen and immediately placed into a 37°C water bath. The cells were quickly thawed (<1 minute) by gently swirling the cryovial in the water bath. The vial was immediately transferred into the laminar hood. 1 ml of pre-warmed complete media was added dropwise to the vial containing the thawed cells. The solution was then again transferred to a universal tube containing 9 ml of complete media. The cell suspension was then centrifuged at approximately 1000 rpm for 1-2 minutes. After the centrifugation the supernatant was decanted aseptically without disturbing the cell pellet. The cell pellet was then gently resuspended with 20 ml of new complete media and transferred into a T-75 flask and incubated overnight in 37°C incubator.

2.1.7 Transfection of Cells

Human fibroblasts cells were transfected with plasmid DNA or siRNA using the Amaxa Transfection system, according to the manufacturer's instructions. siRNAs oligonucleotides used for MBNL1 and MBN2 down-regulation were ordered from Invitrogen, UK. The sequences of siRNAs used in my study were: for MBNL1, 5′-CACUGGAAGUAUGUAGAGAdTdT-3′; for MBNL2, equimolar amounts of two siRNAs, 5′-CACCGUAACCGUUUGUAUGdTdT-3′ and 5′ GAGGAACAUGCUCACGCUCdTdT-3′ were used; and for scrambled siRNA, 5′-GCGCGCUUUGUAGGAUUCGdTdT-3′ was used (Dansithong et al., 2005).

2.2 Immunocytochemistry

2.2.1 Seeding of cells into 96-well plate

The cells were seeded into 96-well plates and allowed to grow for 24 hours to attain 80% confluency. After 24 hours incubation, the cells were ready for compound treatments (48 hours exposure) followed by either Immunofluorescence or RNA Fluorescence *in situ* Hybridisation (RNA-FISH).

2.2.2 Fixation

Media was taken off 96-well plates and cells were washed thrice with PBS. Fixation of the cells was performed using ice cold methanol: acetone (1:1) for 30 minutes at room temperature. The wells were again washed three times (5 mins each wash) with PBS before blocking step.

2.2.3 Blocking

The cells were blocked with 3% BSA + 5% goat serum in PBS for 1 hour at room temperature to decrease the non specific interactions.

2.2.4 Antibody staining

After blocking, the cells were washed thrice with PBS (5 mins each wash) and incubated with 1% BSA containing diluted primary MBNL1 antibody (1:2000) for overnight at 4°C. Next day the cells were then rinsed thrice with PBS and incubated at room temperature with 1% BSA containing diluted secondary antibody (1:500), Alexa 647 goat anti-mouse IgG. The cells were washed with PBS thrice and incubated again with Hoechst dye for 10 mins to stain the nuclei. The Hoechst was then replaced with PBS and stored at 4°C for future scanning on the plate reader.

2.3 RNA Fluorescence *in situ* Hybridisation (RNA-FISH)

RNA-FISH was performed on wild type, DM1 fibroblasts and DM myoblasts cells to visualize bright spots/foci which contained RNA transcripts with expanded CUG repeats. Cells were exposed to compounds for 48 hours after which *in situ* hybridisation was performed to identify foci using Cy5 labelled $(CAG)_{10}$ probe for DM1. Cells were first washed with PBS thrice followed by fixation with 4 % PFA for 30 mins at room temperature. After fixation, the cells were again washed thrice with PBS to get rid of any excess of PFA. To permeabilise the cells, 80% ethanol was used for 15 mins at room temperature followed by three washes with PBS. The cells were then treated with prehybridisation (Prehyb) mixture for 15 mins which contained formamide and

20 x SSC in DEPC water. After treatment with Prehyb solution, the cells were treated with hybridisation (Hyb) solution containing Formamide, 20x SSC, BSA, salmon sperm DNA, Vanadyl Adenosine complex (VAC) and Cy5 labelled oligonucleotides probe. The exact recipe for Prehyb and Hyb used is described in table 2.1. The cells were then incubated overnight at 37°C in a moist chamber. Next day the cells were washed with thrice with 5mM $MgCl_2$ in PBS. This was followed by Hoescht staining for 10-15 mins and stored at 4°C for future scanning at plate reader. Plates were analysed on a Molecular Devices Micro High Content Imaging system. Number of cells imaged in a single well was approximately ~100.

Recipe for 10 ml		
Prehyb solution		Hyb solution
4 ml	Formamide	4 ml
1 ml	20 X SSC	1 ml
5 ml	DEPC H_20	5 ml
-	BSA	20 µl
-	ssDNA	100 µl
-	VAC	10 µl
• Probe (Cy5 or Cy3) -1 µl per every 2ml Hyb. Solution used.		

Table 2.1 Recipe for Prehyb and Hyb solution used in *in situ* experiments

2.4 Compound treatment of DM cells

384 well plates were used to screen each compound in triplicate. Each well contained approximately 1.6 x 10^4 cells. For Chembrige Diverset library, compounds were tested at concentration of 40 μM. For the NPC library, compounds were tested at three different concentrations; 40μM, 8μM and 1.6μM in 384-well format. The kinase and phosphatase libraries were screened in 96-well format with compound concentrations of 100μM, 10μM, 1μM and 100nM. All the secondary validation screens were done over a 12 point dilution range, following a 1:3 dilution protocol, ranging from 40 μM to 200 pM in 96-well format.

In case of western blotting experiments showing the effect of compounds on MBNL1 distribution before and after the treatment, the cells in 75cm^3 flasks were first grown to a confluency of 80-90% cell density. The media was then removed and replaced with the new media containing compounds and the cells were then exposed further for 2 days before extracting sub-cellular proteins from them. The compounds were used at different concentrations, such as RO 31-8220 (10μM), hypericin (10μM), gemcitabine (10μM), chromomycin A3 (40nM), and IMOX (10μM).

2.5 Immunoprecipitation

2.5.1 Cell lysis

Cells were grown in T75 tissue culture flask for 3 days. Total cell extract was obtained as described in section **2.6.1.** The cell pellet obtained was treated with 1ml of RIPA buffer for complete lysis before conducting the immunoprecipitation experiments with serine, tyrosine and threonine phospho-specific antibodies.

2.5.2 Preparation of Dynabeads Protein G

Dynabeads were completely resuspended by pipetting up and down or by rotating on a roller for 2 mins. 50µl of Dynabeads were transferred to a new eppendorf and separated on a magnet until the supernatant was clear and then removed.

2.5.3 Binding of Antibody

10µl of MBNL1 (MB1a) antibody was added to a fresh tube containing 200µl of Ab binding and Washing buffer (already supplied with the kit, # 100.07D, Invitrogen, UK). The whole mixture was then incubated with rotation for 10 mins at room temperature. The tube was then placed on the magnet and supernatant was removed. The beads were washed again by resuspending in 200 µl Ab binding and washing buffer before removing the supernatant and proceeding to immunoprecipitation.

2.5.4 Immunoprecipitation of Target Antigen

Sample (total cell extract) containing the antigen (Ag) (typically 1000 µl) was added to the tube containing the beads and antibody and gently pipetted to resuspend the Dynabeads-Ab complex. The whole mixture was incubated at 4°C for overnight. Next day, the supernatant was removed by placing the tube on magnet and the Dynabeads-Ab-Ag complex washed three times using 200 µl washing buffer (included in the kit) for each wash.

2.5.5 Elution of Target Antigen

After the washing steps, the tube was placed on magnet and supernatant removed. 20µl of elution buffer and 10 µl of premixed NuPAGE LDS sample buffer were added to the Dynabeads-Ab-Ag complex. NuPAGE sample reducing buffer was also added to the tube (as per manufacturer's instructions). The whole mixture was heated for 10 min at 70 °C before loading the supernatant onto a western gel. After completing the western blot, the membrane was probed with phospho-specific antibodies to investigate if MBNL1 protein was phosphorylated and at which residue.

2.6 Protein Analysis

2.6.1 Preparation of total cell protein from Fibroblast and Myoblast cells

The cells were grown in a T75 flask, 75 cm^2 tissue culture flasks. The media was decanted and the cells rinsed once with 10 ml of pre-warmed PBS. 2ml of trypsin was added to the flask and incubated for 3 min until the cells detached from the base of the flask and started rounding up. 1 ml of trypsin was discarded and the flask was gently shaken to detach the cells from bottom of the flask. 9 ml of fresh media was added to neutralize trypsin and pipetted up and down. The entire volume was transferred into a universal tube and centrifuged for 3 mins at 2000 rpm. The supernatant was discarded and the pellet was resuspended with 10 ml of PBS to remove any residual media. Whole volume was centrifuged for 3 mins at 2000 rpm. The supernatant was again discarded and pellet was stored in -80°C for subsequent use. The pellet was then treated with RIPA buffer for complete lysis followed by 2 cycles of freeze-thaw before loading it on western blotting.

The recipe for RIPA buffer used:

- Tris 50mM, pH 8.0
- NaCl 150 mM
- SDS 0.1%
- Deoxycholic acid 0.5%
- Nonidet P40 1%
- Protease inhibitors such as PMSF or protease inhibitors cocktail which are commercially available.

2.6.2 Subcellular fractionation using buffers (Nuclear and cytosolic fractions)

Subcellular fractionation was carried out to separate nuclear and cytosolic proteins. Cultured DM1, DM2 and control cells were separated into subcellular fractions using Nonidet P-40 solution (0.65% Nonidet P-40, 0.01 M Tris-HCL, pH- 7.9, 0.15 M NaCl and 1.5 mM $MgCl_2$ in Sterile Distilled Water). This concentration of detergent was able to break the cytoplasmic membrane but was not powerful enough to break the nuclear membrane. So it was used to obtain the cytoplasmic contents of a cell. Media was decanted from the flask containing the cells. The cells were then washed once with 10 ml of cold PBS. 1 ml of Nonidet P-40 solution was added to the flask and incubated for 2 mins at room temperature. Without disturbing the cells, the entire 1 ml volume was pipetted out in an eppendorf as cytosolic fraction. 5 ml of Nonidet P-40 solution was added to the flask and transferred to a universal tube followed by centrifugation at 2000 rpm for 5 mins. Supernatant was discarded and the visible pellet was resuspended in 200 µl of RIPA buffer to obtain the nuclear fraction.

2.6.3 Subcellular fractionation using the physical shearing method

The subcellular distribution of MBNL1 can vary with the culture conditions. The subcellular distribution of MBNL proteins may be responding to local signals or culture conditions, rather than any internal myogenic program. So I decided to use physical shearing method using a 'syringe'. The cells were grown in T75 tissue culture flask. Media was decanted and the cells were

washed with PBS. 500µl of ice cold PBS (+ PMSF or protease inhibitors cocktail) was added to the flask. The cells were then scraped off the bottom of the flask using a cell scraper and the lysate collected in a 1.5 eppendorf tube. 20 Gauge needle with a 5 ml syringe was assembled. The lysate was carefully passed through the needle 12-15 times to disrupt the cytoplasmic membrane of the cells. Care was taken not to use the same needle for a different cell line or compound treatment. The suspension was then centrifuged at 13000 rpm at 4°C to collect the supernatant (as cytosolic fraction) and the pellet was resuspended in 500 µl of RIPA buffer to obtain the nuclear fraction. Two free-thaw cycles were performed on nuclear extract to completely break the nuclear membrane before loading both the samples on western blots.

2.6.4 Quantification of Protein

Protein was quantified using the BioRad DC protein Assay. The DC™ (detergent compatible) protein assay is a colorimetric assay for protein concentration following detergent solubilisation. It is based on the Lowry assay but modified to save time. A standard BSA curve was plotted with known concentration of BSA ranging from 10µg/ml to 70µg/ml in RIPA buffer or any other buffer used while extracting cytosolic or nuclear fractions and the concentrations of protein in the samples were extrapolated using the standard curve.

2.6.5 Western Blot

A commercial NuPage system from Invitrogen, UK was used to perform western blotting according to the instructions provided in their manual.

Sample preparation

Protein samples were mixed with LDS sample buffer and with reducing agent. The protein samples containing the LDS were then heated at 70 °C for 15 mins. The total reaction volume was not exceeded over 17µl due to holding capacity of the wells in the pre-cast Invitrogen gels.

SDS-PAGE

Before running the SDS-PAGE, running buffer was prepared by mixing 40 ml of MOPS buffer (10X) with 760 ml of sterile distilled water to make a final volume of 800 ml. Pre- cast 10% bis-Tris gels from Invitrogen, UK were used for western blotting. Before loading the samples on the gel, the comb was carefully removed without disrupting the wells. The gels were then rinsed in running buffer thrice before arranging it in X-cell Surelock mini-cell system. The chamber was put in right position and the clamp was carefully closed. The chamber was filled with SDS running buffer till the top. The samples were then loaded (10µl- 15µl) into the wells. Pre-stained marker (acts as a control for visualization during protein transfer step) and Magicmarker were loaded in the first two wells. SDS-PAGE was performed using a NuPAGE gel program which was set for 50 min to run at a constant voltage of 200 V.

Transferring proteins to PVDF membrane after SDS-PAGE

40 ml of transfer buffer (10 X) was mixed with 80 ml of methanol in 680 ml of SDW (Sterile Distilled Water) to prepare transfer buffer. Four bloating pads were immersed completely into transfer buffer until they reached saturation. Any visible air bubbles were removed carefully by tapping on them. Removing the air bubbles is important as they can obstruct the transfer of proteins from gels to PVDF membrane. PVDF membrane was soaked in methanol for 30 seconds before the transfer which was followed by wash with sterile distilled water and then placed in a container containing 200 ml of transfer buffer to equilibrate. After gel electrophoresis was completed, the gel cassette's two plates were separated by inserting the gel knife. Finally the gel membrane sandwich was set according to the instructions in the Invitrogen, NuPAGE manual. The entire sandwich was placed in the inner chamber which was then filled with transfer buffer. Care was taken to fill the outer chamber with sterile distilled water. The proteins were then transferred for 1 hour at 30 V.

Detection

Post transfer step, the membrane was rinsed thrice in dH_20 for 10 min each followed by blocking step in 20 ml of TBS-T (TBS-Tween buffer) containing 5% blotto (dry milk powder, Invitrogen, UK) or BSA for overnight at 4°C on a shaker. The following day, the membrane was rinsed again with TBS-T buffer twice (10 min each) and incubated with 10 ml of primary antibody solution containing 3% BSA for 4 hours at room temperature on shaker. After incubation with primary antibody the membrane was rinsed thrice (10 min each) with TBS-T buffer followed by incubation with 10 ml of TBS-T buffer

containing 3 % BSA and secondary antibody (Anti-rabbit IgG or anti-mouse IgG). The membrane was then rinsed thrice with TBS-T buffer (10 min each) to wash off any residual secondary antibody. The membrane was then finally placed on a cling film and incubated with detection reagent (ECL plus) for 5 minutes. The membrane was then dried with filter paper to drain any excess ECL solution. In the end the membrane was placed in a photographic cassette and exposed to X-ray film.

Name of antibody	Antigen/Isotype	Details	Dilution
MB1a (a kind gift from Dr. Ian Holt (Holt et al., 2009))	Human MBNL1 protein	Mouse monoclonal culture supernatant	1:5000
α- tubulin (Santa Cruz)	Human α -tubulin	Mouse monoclonal concentration- 200µg/ml	1:500
Lamin-B (Santa Cruz)	Human Lamin B	Mouse monoclonal culture supernatant	1:500
MB1a	4A8 IgG1	Mouse monoclonal culture supernatant	1:5000
MB2a	3B4 IgG2b	Mouse monoclonal culture supernatant	1:100
Phospho-serine (Acris Antibodies)	IgM	Monoclonal	1:100
p-Tyr Antibody (Santa Cruz)	IgG_{2b}	Monoclonal	1:100
p-Thr (H-2) (Santa Cruz)	IgG1	Monoclonal	1:100

Table 2.2 Details of primary antibodies used in western blot.

2.7 RNA Analysis

2.7.1 Total RNA extraction

Cells were grown in T75 tissue culture flasks before they were trypsinized and pelleted at 2000 rpm for 5 mins. Supernatant was discarded and the pellet was resuspended in 1 ml of TRI-Reagent (# AM9738, Applied Biosystems). TRI Reagent solution combines phenol and guanidine thiocyanate in a monophasic solution to quickly inhibit RNase activity. Addition of bromochloropropane (BCP) leads to the separation of homogenate into aqueous phase (containing RNA), interphase (containing DNA) and organic phase (containing proteins). After resuspending the pellet in TRI Reagent, the tube was incubated for 5 mins at room temperature before adding 100µl of BCP. Followed by incubation for 15 mins at room temperature, it was subsequently centrifuged for 12000 g for 10-15 mins at 4 °C. The aqueous phase was then collected in a fresh tube and 600 µl of isopropanol was added and vortexed immediately at moderate speed. After incubating the tube for 5-10 mins at R/T, it was centrifuged again for 12000 g for 8 mins at 4 °C. Supernatant was discarded and 1 ml of 75 % ethanol was added to wash the pellet. The pellet was air dried for 3-5 mins before dissolving the pellet with 100 µl of DEPC water. The amount of RNA was quantified on the nanodrop and used for subsequent reverse transcription experiments. The remainder was stored in -80°C for future use.

2.7.2 Fractionated RNA Extraction

RNAse-free pipettes and tips were used for extracting Nuclear and Cytoplasmic RNA fractions from cell culture. Cells grown in T75 Tissue culture flask were washed once with 10 ml of cold PBS.1 ml of solution 1 (Nonidet P40, 0.65%; 0.01M Tris HCl, pH 8.0; 0.15M NaCl and 1.5mM $MgCl_2$ in DEPC H_2O) was then added to cover the cells (to break cell wall). Cells were incubated for 1 min at room temperature, before transferring the entire volume into a fresh tube labelled with cytoplasmic fraction. 2ml of solution 1 was again added to the flask, with gentle tap on the side of flask to collect everything into a fresh tube (Nuclear fraction). Tubes were placed on ice throughout. Both the tubes were then centrifuged for 5 mins at top speed at 4°C. 800 µl of cytoplasmic fraction was pipetted out and was mixed with 200 µl of solution 2 (10% SDS, 0.05M EDTA and 0.5M Tris/HCl pH 8.0) in a fresh tube. In case of nuclear fraction, supernatant was discarded and pellet was resuspended in 400 µl DEPC H_20 and 100 µl of solution 2.

In Fume Hood

Tubes were then transferred to the fume hood. 500 µl chloroform and 500 µl phenol were added to the tube containing cytoplasmic fraction. In case of nuclear fraction, 250 µl of chloroform and 250 µl phenol were added. The tubes were then vortexed at top speed for 5 min at 4°C. The aqueous layer from both the tubes was then transferred into 2 fresh tubes. Centrifugation step was repeated 2 times. The tubes were again centrifuged for 30 min and supernatants discarded.

Out of Fume Hood

To the cytoplasmic fraction, 1 ml of isopropanol and 200 µl of 3M NaOAc were added. 0.5 ml isopropanol and 100 µl of 3M NaOAc were added to the nuclear fraction, followed by centrifugation at top speed for 30 min at 4°C. The supernatants were then discarded from both the tubes and the pellets were washed with 75 % ethanol. In the end the pellets were air dried and dissolved in 25 µl of DEPC H_20, prior to RNA quantification on nanodrop.

2.7.3 DNase Treatment

Total RNA and cytoplasmic RNA samples were treated with DNase1 to remove contaminating DNA from RNA preparations. 1µl of 10x RNase-free DNase buffer (New England BioLab protocols) (400mM Tris-HCl/pH-8.0, 100 mM $MgSO_4$ and 10 mM $CaCl_2$) and 1µl of enzyme RNase-free DNase (1U/µl for every 1 µg of RNA used) was added to RNA samples and incubated at 37°C for 30 min. After incubation 1µl of DNase stop solution was added to the mixture and again incubated at 65°C for 10 min to inactivate the DNase1 enzyme prior to using for reverse transcription reaction.

2.8 Molecular Biology Techniques

2.8.1 Reverse Transcription PCR

After treatment with DNase1, the RNA sample (1-2 µg preferably) was added to a fresh eppendorf tube containing 4 µl of 1mM dNTPs, 4 µl of Random hexamors with DEPC H_20 to give a final volume of 16µl. The mixture was then incubated for 5 mins at 70 °C, centrifuged and put on ice immediately. 2µl of 10X reverse transcriptase buffer (NEB) (500nM Tris-HCl, 750mM KCl, 30mM $MgCl_2$ and 100nM dithiothreitol), 1µl of RNase inhibitor (New England BioLabs,UK) and 1 µl of 200 Units/µl reverse transcriptase enzyme were added to the tube. The mixture was then incubated at 42°C in water bath for 90 mins followed by incubation at 90°C to inactivate the enzyme before PCR.

For BpmI analysis of DMPK, $1/20^{th}$ of the synthesized cDNA was used for PCR amplification with MegaMix (Microzone) using N11 as forward primer (5′- CACTGTCGGACATTCGGGAAGGTGC) with 133 as reverse primer (5′- GCTTGCACGTGTGTGGCTCAAGCAGCTG). Amplification was done with a Tm of 58°C, by modifying the protocols used by Hamshere *et al* (1997). The PCR product was then heated to 95 °C for 2 minutes followed by cooling to 4°C. For BpmI restriction digestion analysis of DMPK PCR products, 4µl of the PCR mixture was digested overnight with restriction enzyme BpmI (New England BioLabs, UK) in a total reaction mixture of 20 µl at 37°C followed by incubation for 10 minutes at 65°C. The final products were then analysed by electrophoresis at 80-90V using a 3% agarose gel. Finally the density of bands quantified using ImageJ software.

2.8.2 Gel Electrophoresis

Gel electrophoresis was used to separate and analyze DNA and their fragments, based on their size and charge. Depending on the size, the DNA fragments were analysed on 1-3% (w/v) gels. For DNA of 1Kbp and above, a standard 1% gel was prepared by dissolving 0.4 gms of agarose in 40 ml of 1X TAE buffer (40 mM Tris-HCl, 50 mM EDTA/pH-8.0, 0.1% (w/v) glacial acetic acid) in the microwave oven and then cooled. 3% agarose gel was used to separate DNA sizes of less than <300 bp. 10µl ethidium bromide, most common dye to visualize DNA or RNA bands was added. Before loading the DNA samples, loading buffer (30% glycerol, 0.025% bromophenol blue and 0.025% xylene cyanol) was added to each sample (final concentration 1X). Finally DNA samples and marker (1Kb ladder) were loaded and gels electrophoresed at 60-90V for 1-1.5 hour in 1X TAE buffer. DNA fragments were visualized under ultra-violet (UV) irradiation using BioRad GelDoc system.

2.9 Microscopy

2.9.1 Brightfield Microscopy

Cell imaging in tissue culture was performed using a brightfield microscope fitted with 4x, 10x and 40x objectives.

2.9.2 High Throughput Imaging

Cells were visualized on Molecular Devices ImageXpress Micro widefield high content plate reader fitted with Nikon 40x ELWD. Cells after immunofluorescence and *RNA-FISH* analysis were imaged using this machine.

2.10 Electronic Databases

National Centre for Biotechnology Information (NCBI) and Ensembl were used to access information about transcripts and nucleotide and protein sequences. Primers were designed using a web version 4.0 of primer3 Input.

Chapter- 3: Results

Distribution of Muscleblind-like proteins in normal and DM cells.

3.1 Introduction

Expanded CTG and CCTG repeats expression is proposed to have a trans-dominant effect, which alters the activity of RNA-binding proteins like Muscleblind-like (MBNL) proteins. These proteins play an important role in mediating pre-mRNA alternative splicing regulation. Besides its nuclear role, MBNL2 was found to have a role in localisation of integrin α 3 RNA to focal adhesion complexes in cytoplasm. MBNL2 was reported to bind to an ACACCC motif in the 3′ UTR of integrin alpha 3 mRNA to transport it to the adhesion complexes. It has been shown that all Muscleblind-like proteins have similar structures, thus it is quite possible that they may have similar functions also (Pascual et al., 2006). As already shown by Saloni Mittal (2008), MBNL1 is not confined to the nucleus but shuttles between the nucleus and the cytoplasm. The ability of MBNL1 to shuttle between the nucleus and cytoplasm implies that in addition to its role in regulating alternative splicing, it may also be involved in mRNA transport across the nuclear envelope, have cytoplasmic functions such as translational regulation, and affect mRNA stability or mRNA localization. In this section I have attempted to assess the sub-cellular (Nuclear v/s Cytosolic) distribution of Muscleblind-like proteins in Normal and DM cells. Holt and colleagues (2009) showed that different fixation methods can affect the visualization of MBNL1 in the nucleus compartment. They used acetone: methanol fixation method which allowed

partial loss of 'soluble' MBNL proteins from both cytoplasm and nucleoplasm for reliable visualization of nuclear foci without high nucleoplasmic MBNL staining (Figure 3.1). Thus, In view of these findings, I decided to compare different separation methods to study the sub-cellular (Nuclear v/s Cytosolic) distribution of Muscleblind-like protein 1 in Normal and DM cells.

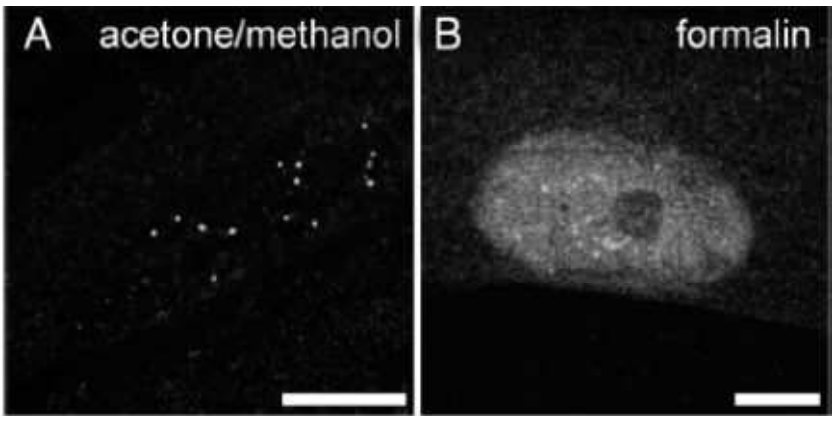

Figure 3.1 Comparison of acetone: methanol and formalin fixation methods. **(A)** Cultured human DM1 myoblasts (800 CTG) fixed and permeabilized with acetone: methanol showing clear foci without high nucleoplasmic MBNL staining **(B)** or with formalin followed by Triton X-100 which resulted in quite high nucleoplasmic MBNL1 staining, which can obscure the foci (Images taken from Holt *et al*., 2009) (Holt et al., 2009) .

3.2 Comparison of different sub-cellular separation methods

In this section I have compared different separation methods to study the sub-cellular (Nuclear v/s Cytosolic) distribution of Muscleblind-like protein 1 in normal and DM cells. In section 3.2.1, I have used Nonidet P-40 buffer to extract nuclear and cytosolic fractions whereas in section 3.2.3, I have used physical shearing method to extract nuclear and cytosolic protein fractions.

3.2.1 Separation into two compartments i.e. Nuclear and Cytosolic fractions using Nonidet P-40 buffer

To give a clear indication of MBNL1 distribution in individual sub-cellular compartments, it was important to perform western blotting with representative loading rather than equal loading. As the nucleus forms a small part of the entire cell and majority of space is cytosolic, therefore it would be misleading to load (in western blotting) equal amounts of proteins for both nuclear and cytosolic fractions. Thus, a detailed representative loading for each compartment was performed. Nuclear and cytosolic fractions were extracted separately from 2 x 10^6 cells and re-suspended each of them in equivalent volumes (Table 3.1). The total amount of protein in each fraction was measured and an equivalent volume loaded on to a gel. Typically this would be one hundredth of the total, equivalent to 2 x 10^4 nuclei and similar numbers of 'cytoplasms'. For example 3µl of total cell extract ($1/100^{th}$ of the total volume in the tube), 2µl of nuclear extract ($1/100^{th}$) and 10µl of cytosolic extract ($1/100^{th}$) was loaded on gels because they all were extracted in different volumes of buffers (either RIPA or Nonidet P-40) during their preparation as

described in Table 3.1. Thus, the protein loaded on gels is from an equivalent number of nuclei and 'cytoplasms' for each cell line. It is therefore representative of the distribution of all cellular proteins.

Cultured DM1, DM2 and control fibroblasts were extracted with Nonidet P-40 solution, to prepare nuclear and cytosolic fractions for western blotting. Lamin B and Tubulin were used as controls to determine the extent of cross-contamination of nuclear and cytosolic compartments during extraction.

Initial analysis revealed that both the DM and control cells show a greater proportion of MBNL1 protein in the cytosolic fraction than in nuclear fraction (Fig. 3.2). In both DM1 and DM2 cells the amount of cytosolic MBNL1 was 97% and 96 % respectively and proportion of the nuclear MBNL1 was much less (3-4%). The same pattern was observed in control (NIRA) cells, where 98% of MBNL1 was present in cytosolic fraction with much less (2%) present in nuclear fraction (Fig.3.4).

Analysis for MBNL2 distribution also showed a greater proportion of MBNL2 in the cytosolic fraction than in nuclear fraction for both DM and non-DM fibroblast cells (Fig. 3.3). Histograms compiled from intensity scans of triplicate samples suggested that majority of MBNL is cytosolic (free MBNL) with much less present in nuclear compartment for both DM and non-DM cells (Fig.3.5).

Type of extract	Resuspension volume	Volume loaded on W.B
Total cell extract (Normal and DM cells)	300 µl (RIPA buffer)	3 µl (equivalent of ~2 x 10^6 cells)
Nuclear extract (Normal and DM cells)	200 µl (RIPA buffer)	2 µl (equivalent of 2 x 10^4 nuclei)
Cytosolic extract (Normal and DM cells)	1000 µl/ 1ml (Nonidet P-40)	10 µl (equivalent of 2 x 10^4 cytoplasms)

Table 3.1 Volumes used for representative loading during western blotting.

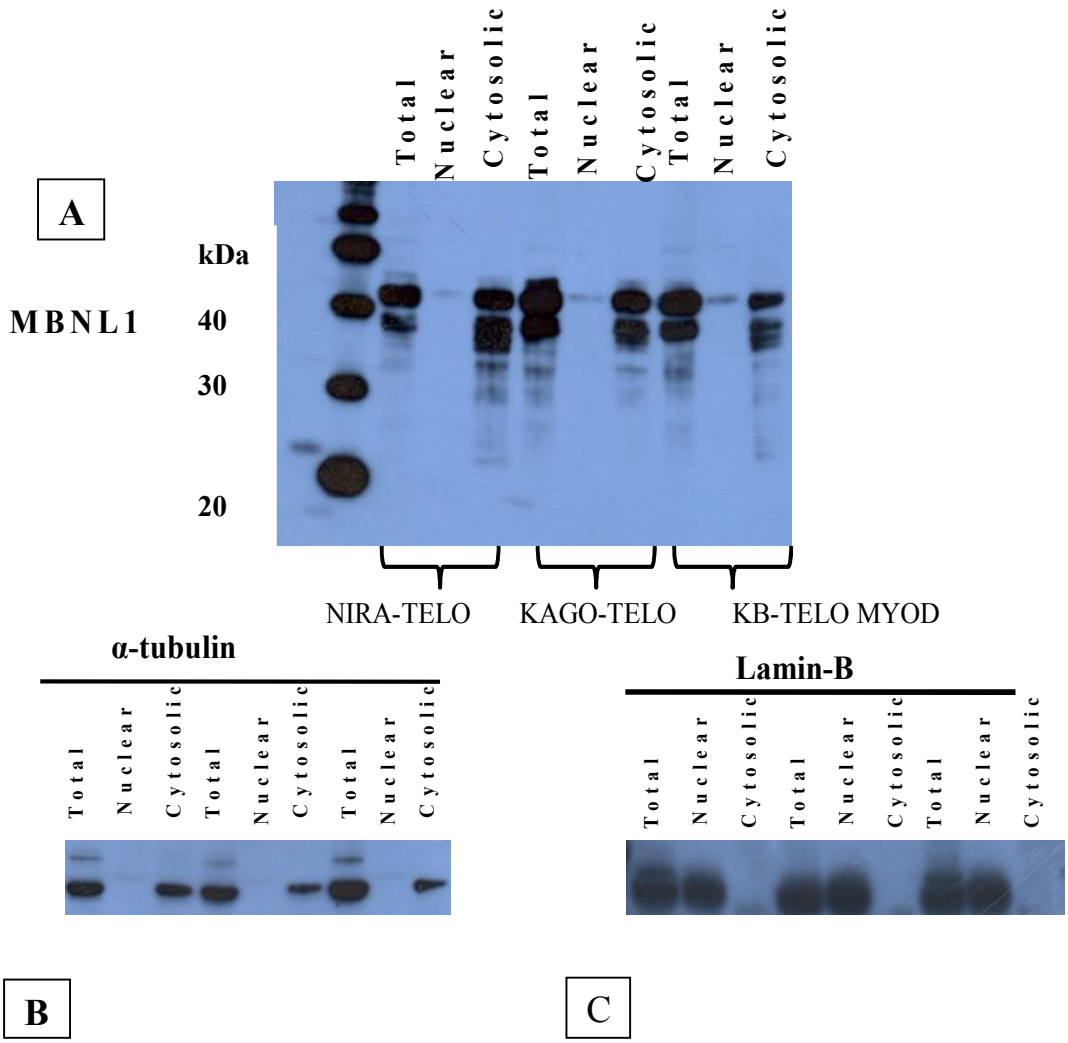

Figure 3.2 Sub-cellular distribution of MBNL1. (A) Distribution of MBNL1 in NIRA-TELO (Normal), KAGO-TELO (DM2) and KB-TELO MYOD (DM1) cell lines **(B)** Control α- tubulin at ~50 kDa (cytosolic protein) **(C)** Control Lamin- B (nuclear protein).

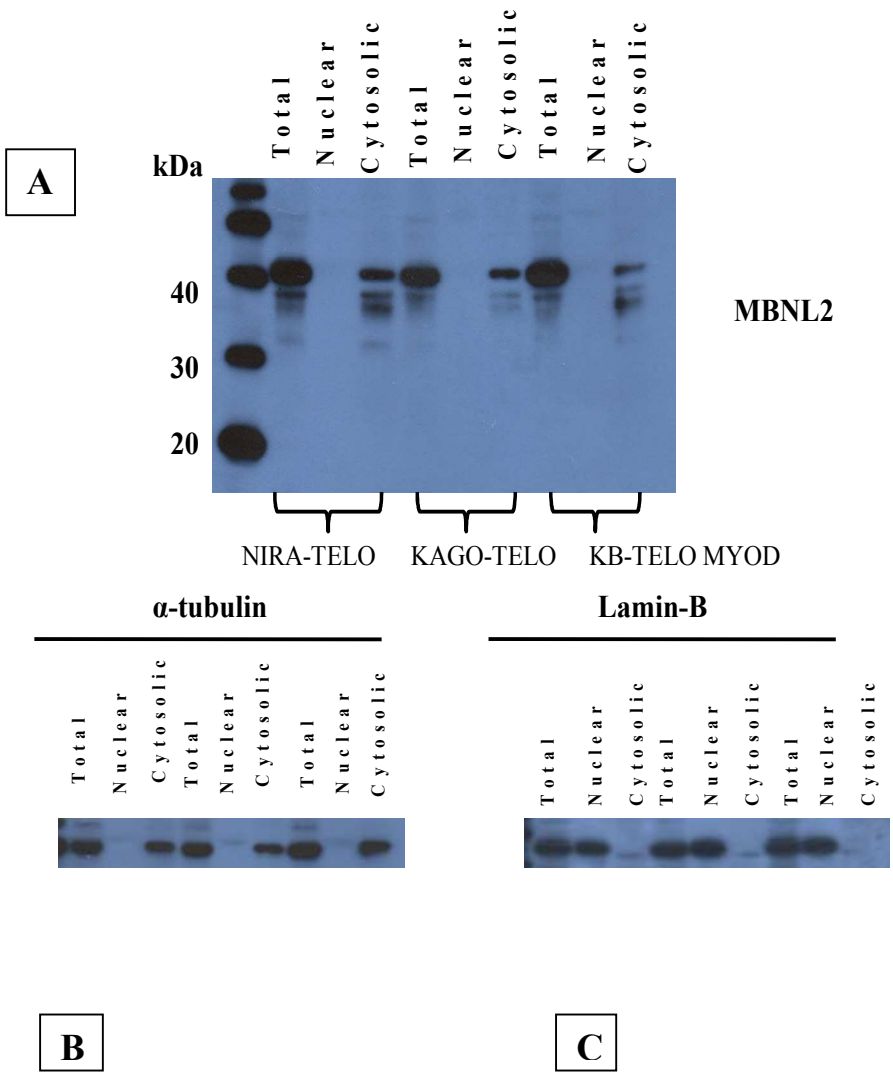

Figure 3.3 Sub-cellular distribution of MBNL2. (A) Distribution of MBNL2 (MB2a) in NIRA-TELO (Normal), KAGO-TELO (DM2) and KB-TELO MYOD (DM1) cell lines **(B)** Control α- tubulin **(C)** Control Lamin-B.

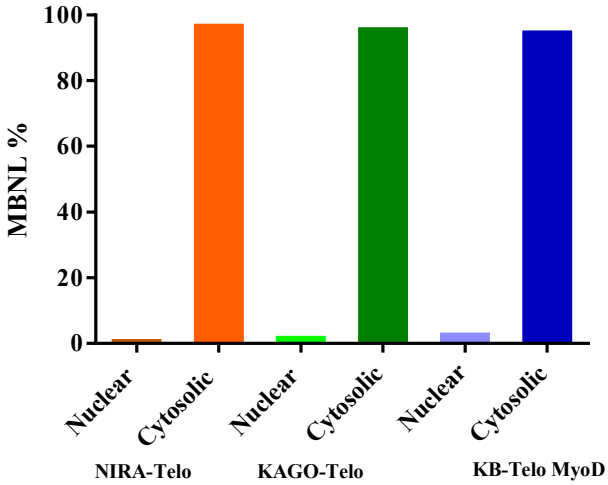

Figure 3.4 The sub-cellular distribution of MBNL1. Histograms show data compiled for MBNL1 sub-cellular distribution in NIRA-Telo (Normal), KAGO-Telo (DM2 cell line), and KB-Telo MyoD (DM1 cell line) from intensity scan of blot in Fig. 3.2 (A), normalized against values for lamin-B and tubulin.

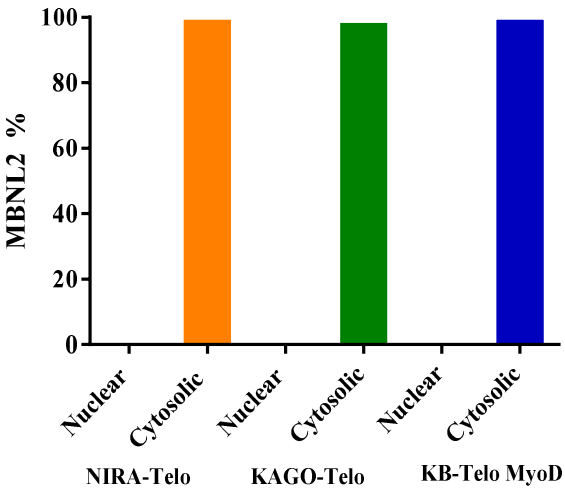

Figure 3.5 The sub-cellular distribution of MBNL2. Histograms show data compiled for MBNL2 sub-cellular distribution in NIRA-Telo (Normal), KAGO-Telo (DM2 cell line), and KB-Telo MyoD (DM1 cell line) from intensity scan of blot in Fig. 3.3 (A), normalized against values for lamin-B and tubulin.

3.2.2 Separation into two compartments i.e. nuclear and cytosolic fractions using Nonidet P-40 (Ice cold conditions)

The fractionation using buffer Nonidet P-40 worked quickly and I watched through an inverted microscope as the lysis took place on the cell monolayer. In general this whole procedure took 2-3 min. However, I decided to repeat the extraction on ice to test whether the MBNL1 protein distribution was an artifact of the procedure. The sub-cellular fractionation was performed again to separate nuclear and cytosolic proteins at 4ºC on ice. Cultured DM1, DM2 and control fibroblasts were extracted with Nonidet P-40 solution as before. The cultured DM1 and DM2 fibroblasts were kept on ice throughout the separation protocol. Care was taken to use ice cold buffers every time. Figure 3.6 shows the subcellular distribution of MBNL1 in KAGO Telo (DM2) and in KB-Telo MyoD (DM1) cell line, nuclear and cytosolic fractions prepared under ice cold conditions. Again representative loading was followed as indicated in Table 3.1. Consistent with previous experiments, MBNL1 appeared to predominate in the cytosolic fractions with much less in the nuclear fractions (Fig.3.6A).

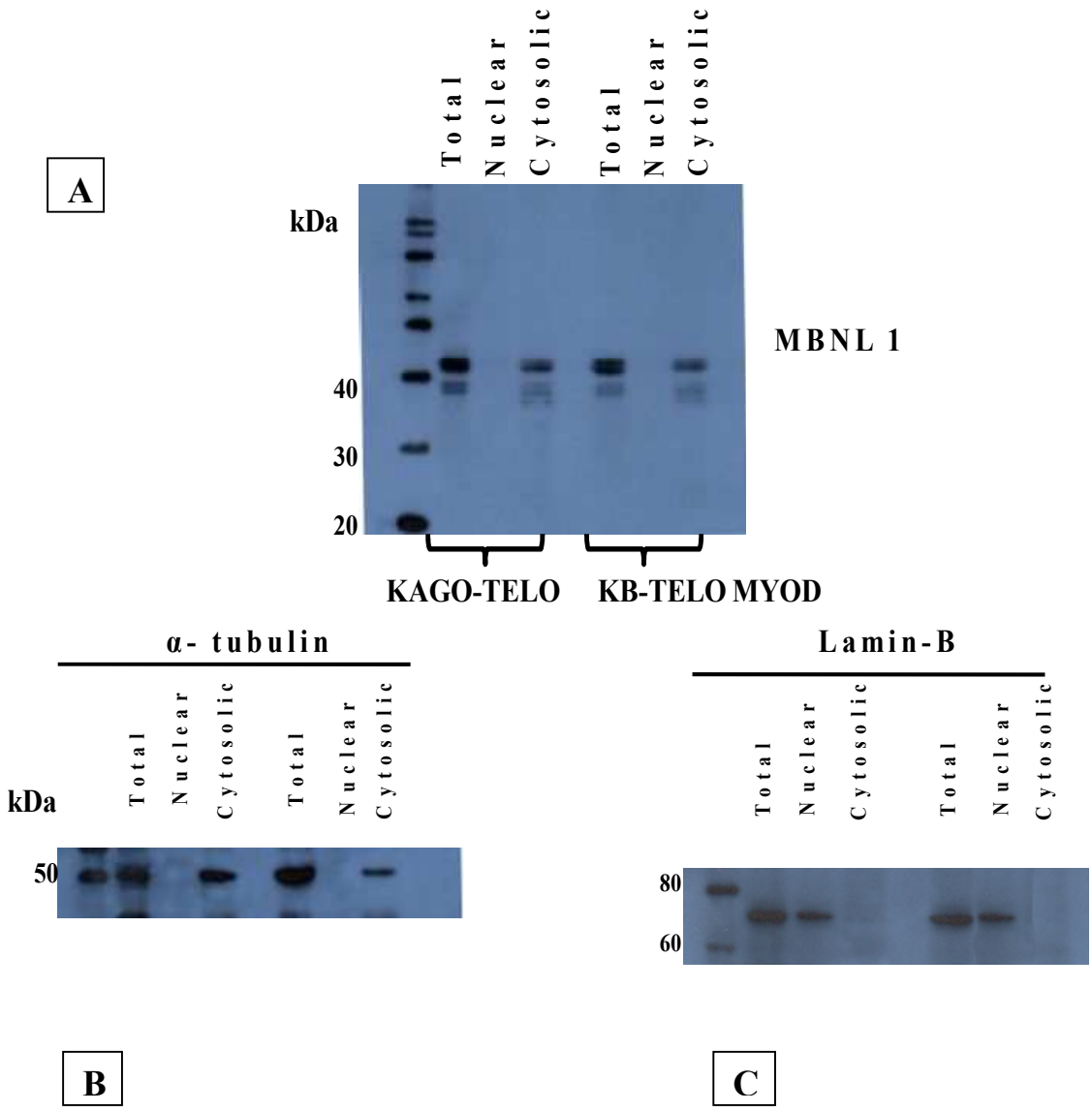

Figure 3.6 Effect of ice cold conditions on subcellular distribution of MBNL1 protein. (A) Subcellular distribution of MBNL1 in KAGO-TELO (DM2) and in KB-TELO MYOD (DM1) cell line **(B)** Control- α tubulin (~50 kDa) **(C)** Control Lamin-B. MBNL1 protein was still found to be predominant in cytosolic fractions than in nuclear fractions.

3.2.3 Separation into two compartments i.e. Nuclear and Cytosolic fractions using physical separation method

In the previous experiments, endogenous MBNL1 and MBNL2 were found to be predominantly cytosolic in normal and DM cell lines. In order to test whether the subcellular distribution of MBNL1 can vary with the culture conditions, I decided to use physical shearing method using a 'syringe' instead of the buffers/detergents. Representative loading was followed for western blots as described in Table 3.2. To calculate the percentage of nuclear MBNL1, I extracted nuclear and cytoplasmic protein fractions separately from 2 x 10^6 cells and re-suspended each of them in equivalent volumes. The total amount of protein in each fraction was measured and an equivalent volume loaded on to a gel. Typically this would be one fiftieth of the total, equivalent to 4 x 10^4 nuclei and similar numbers of 'cytoplasms'. Following western blotting the proteins were detected with MBNL1 antibody (MB1a), a mouse monoclonal antibody against MBNL1 (generated by Dr. Ian Holt). The validity of this antibody in normal and DM fibroblasts has already been tested by Dr. Ian Holt (Holt et al., 2009). MB1a antibody recognises a band corresponding to molecular weight of 41~42 kDa on western blots. MBNL1 protein consists of several isoforms of similar size and in protein extracted from our cell lines. Therefore, MBNL1 always appeared as a double band in all our blots. The relative intensity of nuclear and cytosolic bands was estimated using Image J software. The values were normalised by comparison to lamin (for nuclear) and alpha tubulin (for cytoplasmic) to indicate the extent of cross contamination (usually less than 3%), and expressed as the percentage of nuclear MBNL1 relative to the cytoplasmic.

The histogram data compiled from the intensity scans of triplicate samples show that the percentage of nuclear MBNL1 was 16.45% in NIRA-Telo (non-DM) fibroblast cells (Fig. 3.7). But in case of sub-cellular distribution of MBNL1 in KAGO-Telo (DM2 cell line) and KB-Telo MyoD (DM1 cell line) the percentage of nuclear MBNL1 was found to be 38.43% (N=3) and 36.63 % (N=3) respectively (Fig. 3.8 and 3.9).

Western blot analysis therefore revealed that the DM cells show a greater proportion of MBNL1 protein in the nuclear compartment compared to non-DM cells. In both DM1 and DM2 cells the amount of nuclear MBNL1 was found to be at least 50% greater than seen in non-DM cells.

Type of extract	Resuspension volume	Volume loaded on W.B
Nuclear extract (Normal and DM cells)	500 µl (RIPA buffer)	10 µl (equivalent to 4 x 10^4 nuclei)
Cytosolic extract (Normal and DM cells)	500 µl (PBS)	10 µl (equivalent to 4 x 10^4 'cytoplasms')

Table 3.2 Volumes used for representative loading during western blotting.

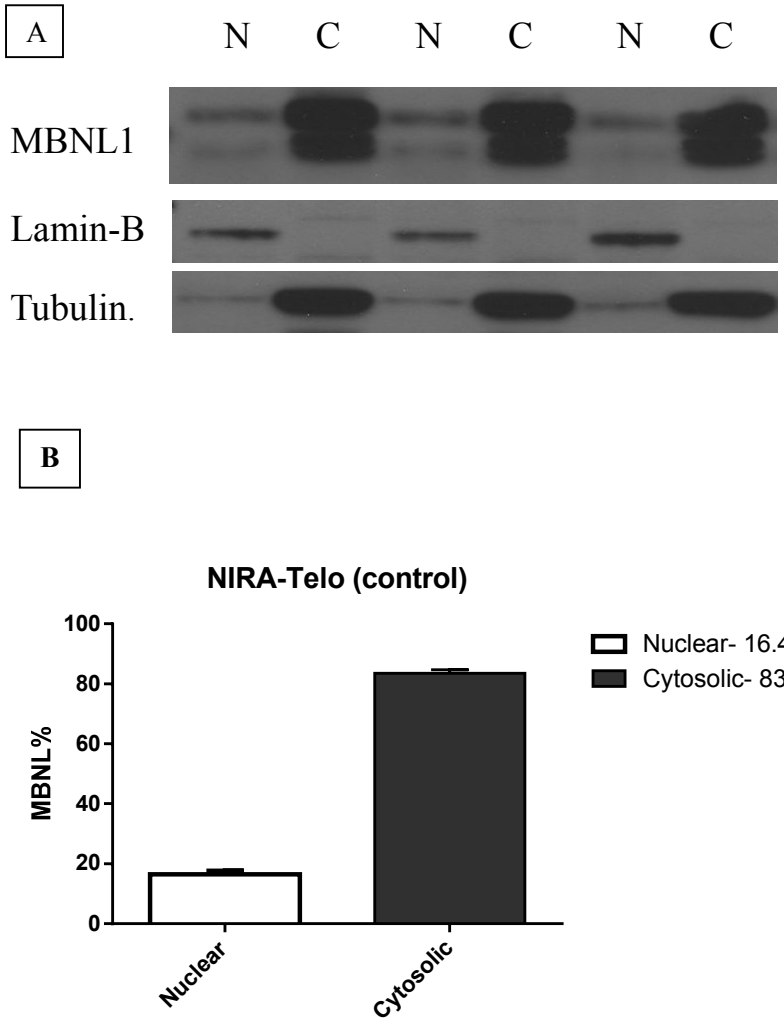

Figure 3.7 Distribution of MBNL1 in NIRA-Telo (control) fibroblast. **(A)**Western blots showing separated sub-cellular fractions (Nuclear and Cytosolic). MBLa (MBNL1) antibody recognises a band corresponding to molecular weight of 41~42 kDa in all the triplicates. Controls for the fractionation procedure are shown by blotting by Lamin-B and α-tubulin antibody. **(B)** Histograms show data compiled from intensity scans of triplicate samples, normalized against values for lamin-B and tubulin.

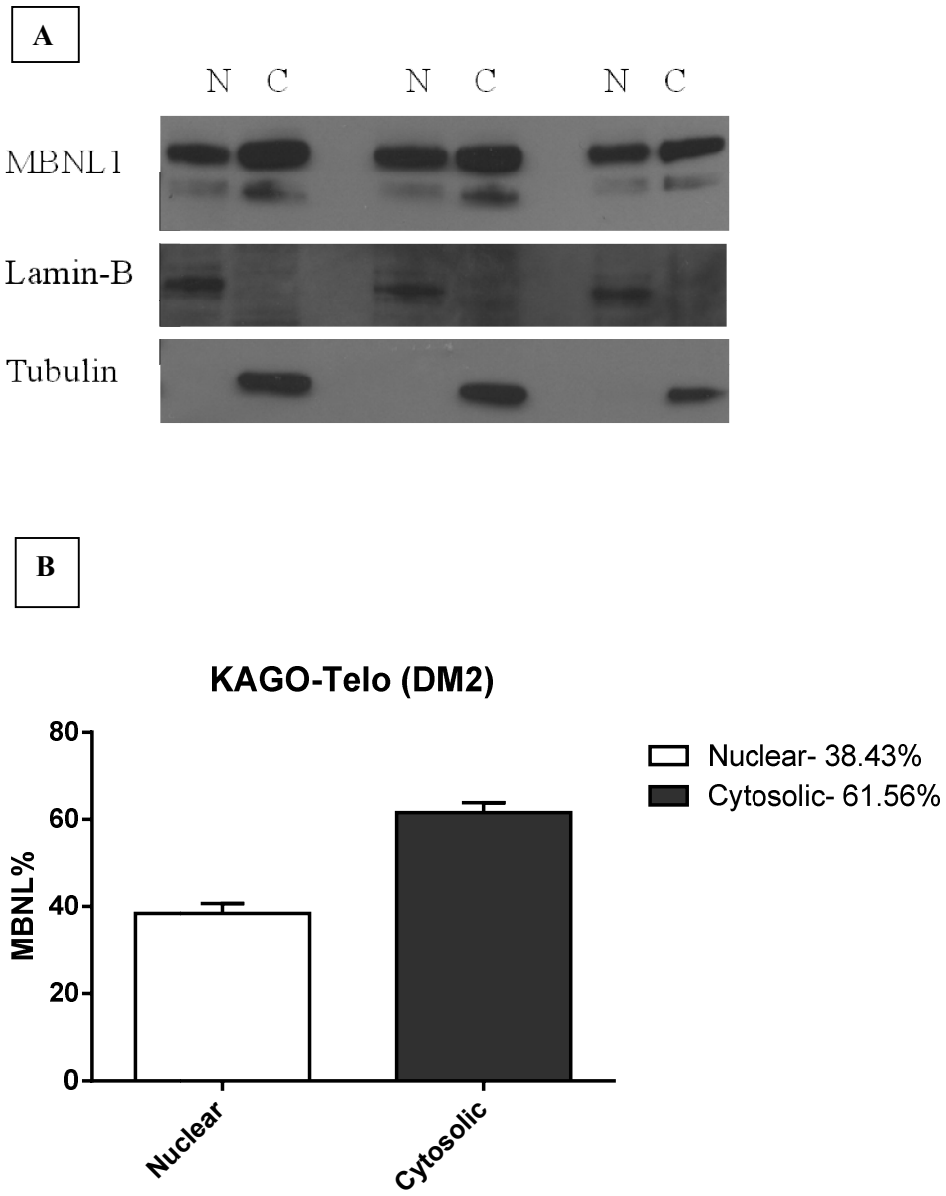

Figure 3.8 The sub-cellular distribution of MBNL1 in DM2 cell line. (A) Western blots showing the distribution of MBNL1 in nuclear (N) and cytosolic (C) compartments of cell line KAGO-Telo (DM2). **(B)** Histograms show data compiled from intensity scans of triplicate samples, normalized against values for lamin-B and tubulin.

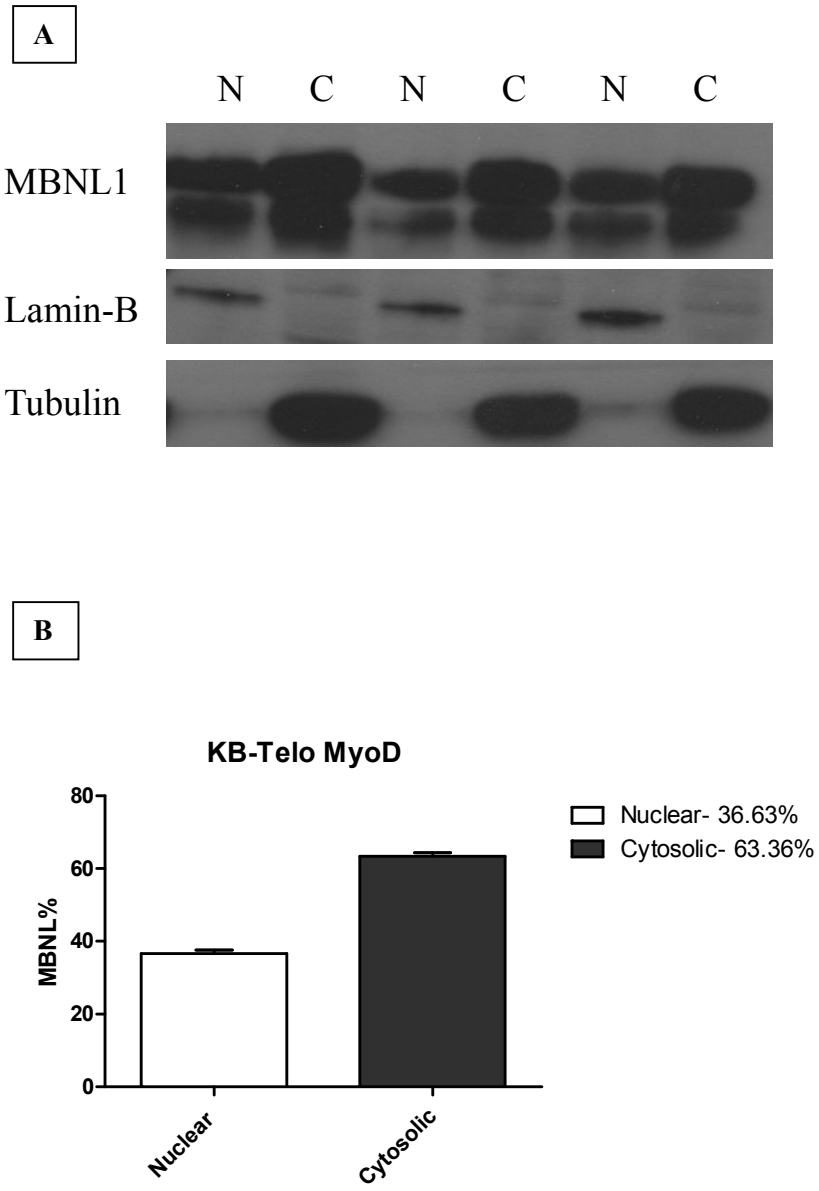

Figure 3.9 The sub-cellular distribution of MBNL1 in DM1 cell line. (A) Western blots showing the distribution of MBNL1 in nuclear (N) and cytosolic (C) compartments of cell line KB-Telo MyoD (DM2). **(B)** Histograms show data compiled from intensity scans of triplicate samples, normalized against values for lamin-B and tubulin.

3.3 Summary

In this chapter two different separation methods have been used to compare the sub-cellular (Nuclear v/s Cytosolic) distribution of Muscleblind-like protein 1 in normal and DM cells. The first method uses Nonidet P-40 buffer and the second method uses physical shearing method with a 'syringe' to separate nuclear and cytosolic fractions. MBNL1 protein appeared to predominate in cytosolic fractions in both DM and non-DM cells after extraction with Nonidet P-40 buffer but the sub-cellular distribution of MBNL1 appeared different after physical shearing method, with a significant amount of MBNL1 present in nuclear fractions. This may suggest that the detergent treatment might be affecting the sub-cellular distribution of protein. Increased nuclear presence is consistent with the current RNA model for DM pathogenesis which states that the MBNL proteins are sequestered in the nucleus by the expanded CUG/CCUG repeats forming foci in DM cells. Thus, physical shearing method to separate nuclear and cytosolic protein fractions was used for all further studies.

Chapter-4: Effect of compounds on Muscleblind-like protein 1 distribution

4.1 Introduction

A popular model of DM pathogenesis suggests that MBNL proteins are sequestered in nuclear foci by mutant RNA which results in its depletion from the nucleoplasm and in turn causes misregulated alternative splicing of various other transcripts. It would be hypothesised that MBNL1 protein sub-cellular distribution would be restored to that of an unaffected cell following reduction/disruption of RNA nuclear foci. Thus, I decided to use western blots to examine the distribution of MBNL1 protein in nuclear and cytosolic fractions of DM cells before and after treatment with compounds, identified during the primary screen.

4.2 Effect of compounds on MBNL1 nucleo-cytosolic distribution in DM1 fibroblasts.

Following the primary and secondary screens RO 31-8220, gemcitabine, chromomycin A3, IMOX and hypericin were highlighted as best potential compounds that remove nuclear foci. In order to assess whether they affected other aspects of DM pathophysiology these compounds were subjected to additional assays such as MBNL1 distribution in nuclear and cytosolic compartments. Initial analysis revealed that in both DM1 and DM2 cells the amount of nuclear MBNL1 was at least 50% greater than observed in the non-

DM cells (Fig. 3.7, 3.8 and 3.9), consistent with protein sequestration by the repeat expansion RNA in nuclear foci. Treatment with these 5 compounds resulted in reduced total levels of protein in KB-Telo MyoD (fibroblast) cell extracts. However, this reduction was equivalent in both nuclear and cytoplasmic fractions following compound treatments.

The conditionally immortalized fibroblast derived from DM1 patients (KB-Telo MyoD) were used for drug treatment. Cells were grown for 3-4 days in high serum media, before they were treated with compounds for 2 days. After exposing the cells for 2 days with compounds, the nuclear and cytosolic protein was extracted using physical shearing method (Fig. 4.1).

Following a two day treatment of DM1 fibroblast cells with each compound significantly reduced the proportion of nuclear MBNL1 compared to DMSO treated cells. The MBNL1 protein distribution in treated DM cells resembled that of non-DM cells with a much higher percentage in the cytoplasm, around ~80% and only ~20% in the nuclear fraction.

DM cells showed a greater proportion of MBNL1 in the nuclear fraction compared to non-DM cells. In DM1 cells the amount of nuclear MBNL1 was at least 50% greater than observed in non-DM cells (NIRA-Telo, control fibroblast) (Fig. 4.2A-B). Treatment of DM1 fibroblasts (Fig. 4.2C-D) with chromomycin A3, RO 31-8220 and hypericin significantly reduced the proportion of nuclear MBNL1 compared to DMSO treated cells (Fig. 4.2B).

Compound treatment of DM1 cells (Fig.4.3A-B) with gemcitabine and IMOX also shifted that pattern observed in DM cells to be more like those observed in non-DM cells i.e. they both significantly reduced the proportion of nuclear MBNL1 compared to DMSO treated cells (Fig. 4.2B).

Compound treatment affected the distribution of MBNL1 protein compared to DMSO treated KB-Telo MyoD cells (DM1 fibroblasts) (Fig. 4.4). Treatment with chromomycin A3 ($p=0.0046$) significantly reduced the nuclear MBNL1 protein to 22.24 % compared to 39.92% in nuclear DMSO treatment. Similarly there was a significant difference between nuclear RO 31-8220 treatment ($p=0.0004$) and nuclear DMSO treatment. Also there was significant reduction in nuclear MBNL1 protein in case of hypericin ($p=0.0009$) and gemcitabine ($p=0.0202$) compound compared to DMSO control treatment. Statistical analysis showed a significant reduction in nuclear MBNL1 protein in case of IMOX compound compared to DMSO control ($p= 0.0003$), the nuclear MBNL1 protein after IMOX treatment got reduced to 10.16%. * represents a significant difference from the control DMSO (Student's two tailed t test; *$P<0.05$)

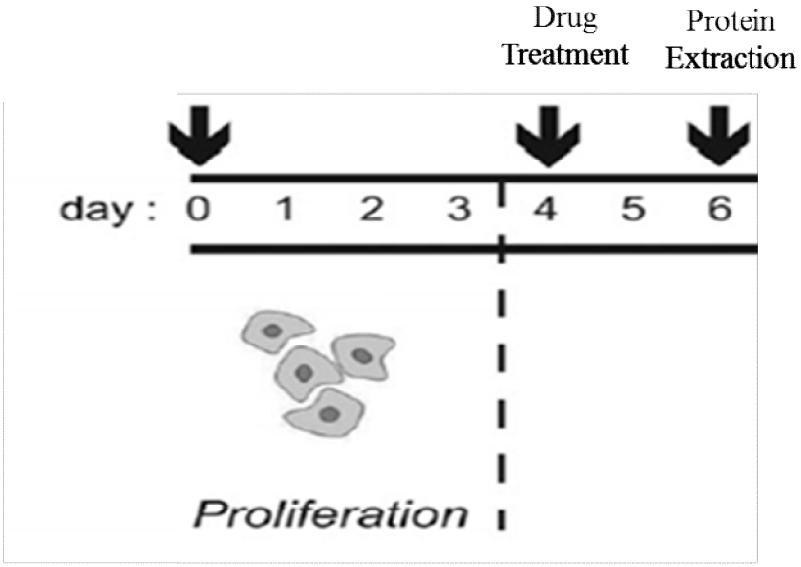

Figure 4.1 Immortalized fibroblast cells derived from DM1 patients were used for drug treatment. The cells were treated with compounds at day 4 and protein was extracted at day 6.

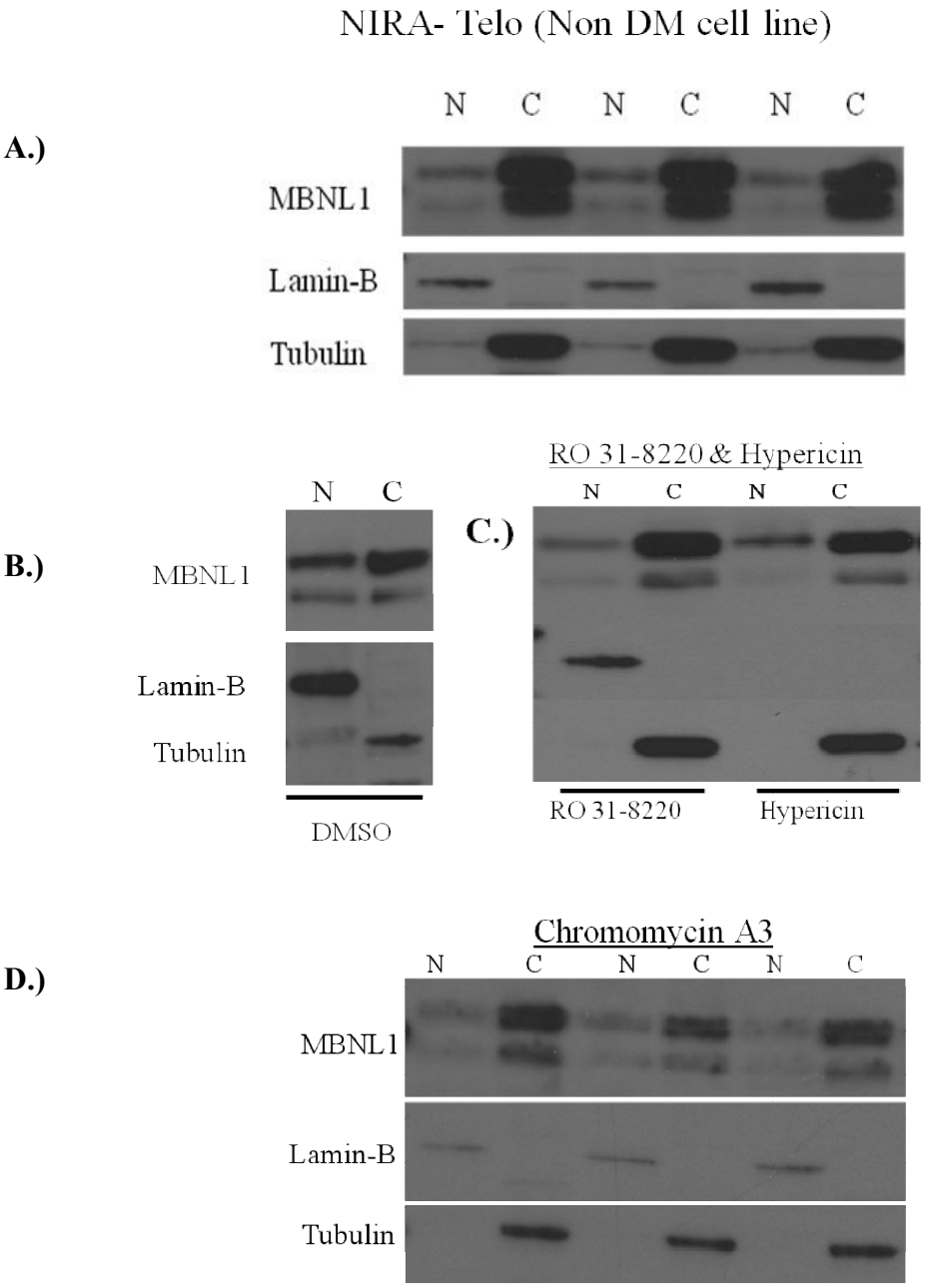

Figure 4.2 The sub-cellular distribution of MBNL1 before and after compound treatment. (A) Western blots showing the distribution of MBNL1 in nuclear (N) and cytosolic (C) compartments in NIRA-Telo (Non-DM) fibroblast cells **(B)** and in KB-Telo MyoD (DM1) cells following treatment with DMSO **(C)** compound Ro 31-8220 and Hypericin **(D)** and Chromomycin A3.

A.)

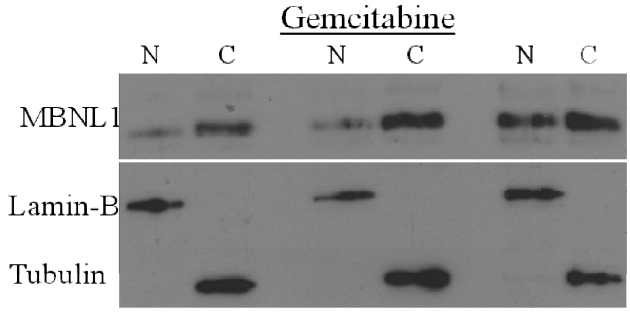

B.)

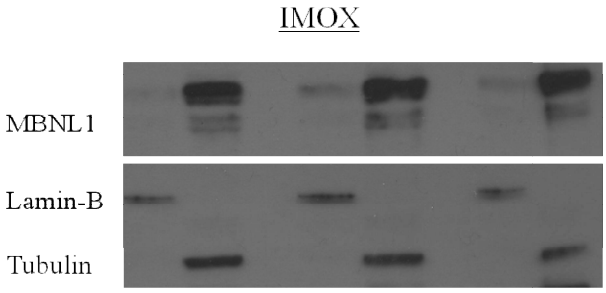

Figure 4.3 The sub-cellular distribution of MBNL1 after compound treatment. (A) Western blots showing the distribution of MBNL1 in nuclear (N) and cytosolic (C) compartments in KB-Telo MyoD (DM1) cell line following treatment with compound gemcitabine **(B)** and compound IMOX.

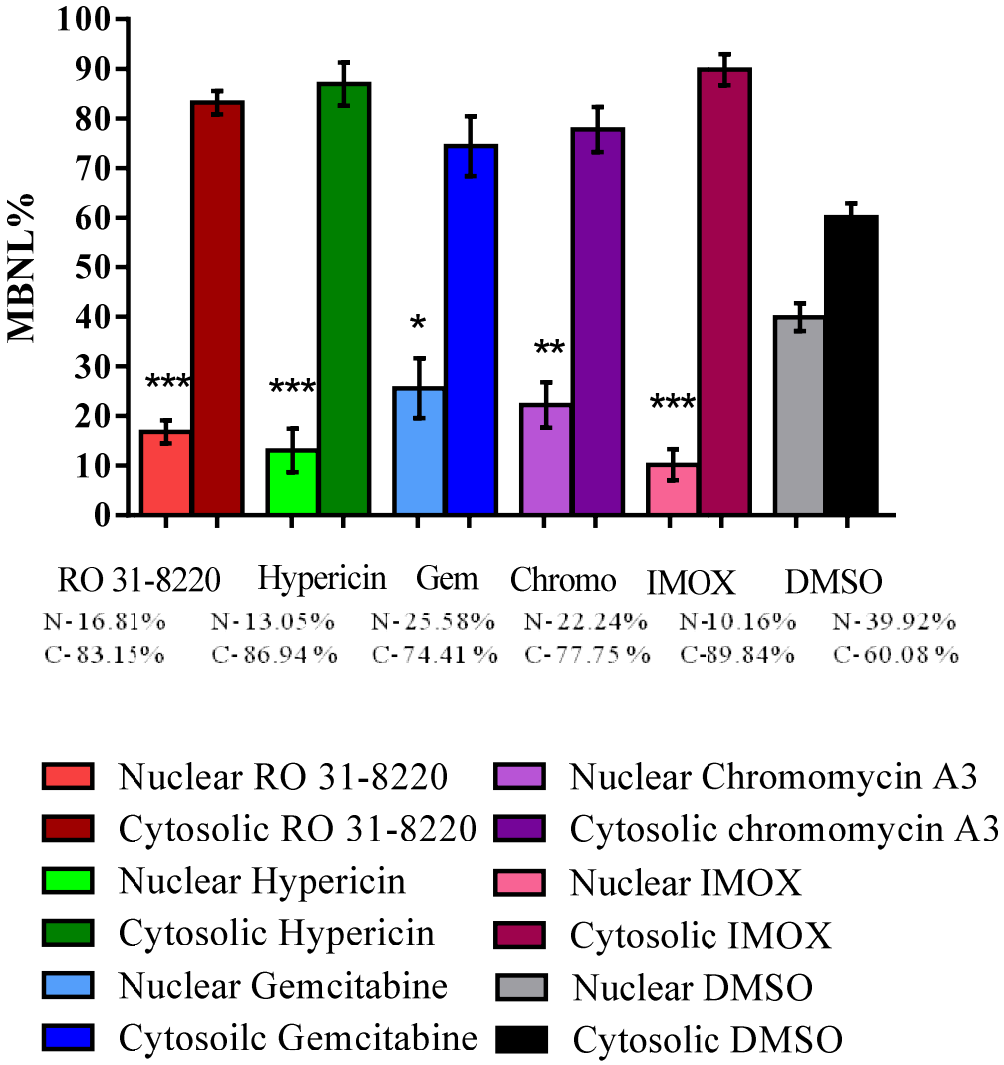

Figure 4.4 The distribution of MBNL1 in nuclear and cytosolic fractions after compound treatment in DM fibroblasts. Histograms show data compiled from intensity scans of triplicate blots for KB-Telo MyoD cell line (DM1), normalized against values for lamin-B and tubulin following treatment with RO 31-8220 (10µM), hypericin (10µM), gemcitabine (10µM), chromomycin A3 (40nM), IMOX (10µM) and DMSO. All the statistical comparisons are done to the DMSO treatment. * represents a significant difference from the control DMSO (Student's two tailed *t* test; *P<0.05)

4.3 Effect of compounds on MBNL1 nucleo-cytosolic distribution in DM myoblasts

In view of findings described in sections 4.1 and 4.2 that compound treatment affected MBNL1 distribution in fibroblasts, I decided to test whether the same affect was consistent in DM myoblast cells. Immortalized myoblast cells (DM15) derived from DM patients were used for compound treatments. The cells were first differentiated for 5 days into myotubes under low serum conditions to stop them from proliferating. The differentiated cells were then exposed to compound treatments for 2 days. After 2 days of exposure the protein was extracted to give the nuclear and cytosolic fractions (Fig. 4.5).

Western blot shows that DM15 myoblasts (DM) have a greater proportion of MBNL1 in the nuclear fraction compared to Me16 (non-DM) myoblast cells. In DM15 myoblast cells the amount of nuclear MBNL1 was much greater than observed in Me16 myoblast cells (non-DM, control myoblast) (Fig. 4.6A-B). Treatment of DM15 myoblasts (Fig. 4.6C, 4.7A-D) with compounds chromomycin A3, gemcitabine, IMOX, RO 31-8220 and hypericin resulted in a very significant shift of the ratio of nuclear to cytoplasmic MBNL1 (Fig. 4.6B).

In case of chromomycin A3 ($p= 0.0129$) and RO 31-8220 ($p=0.0035$), the nuclear MBNL1 was reduced to 21.73% and 4.17% respectively compared to 38.40 % MBNL1 in nuclear DMSO treatment in DM15. Statistical analysis showed a significant reduction of nuclear MBNL1 protein after the treatment with compounds hypericin ($p=0.0033$), gemcitabine ($p=0.0321$), IMOX

(p=0.0017) compared to nuclear DMSO treatment. In case of gemcitabine and hypericin, the nuclear MBNL1 was reduced to 8.59% and 28.05% respectively compared to nuclear MBNL1 (38.40%) in DMSO treatment. All the statistical comparisons are done to the DMSO treatment (*P<0.05).

The values have been normalized against Tubulin and Lamin-B. Thus, although there has been a reduction in overall protein level after compound treatments, this reduction in protein level was equivalent in both nuclear and cytosolic fractions following compound treatments, with a substantial reduction in the proportion of MBNL1 that is nuclear.

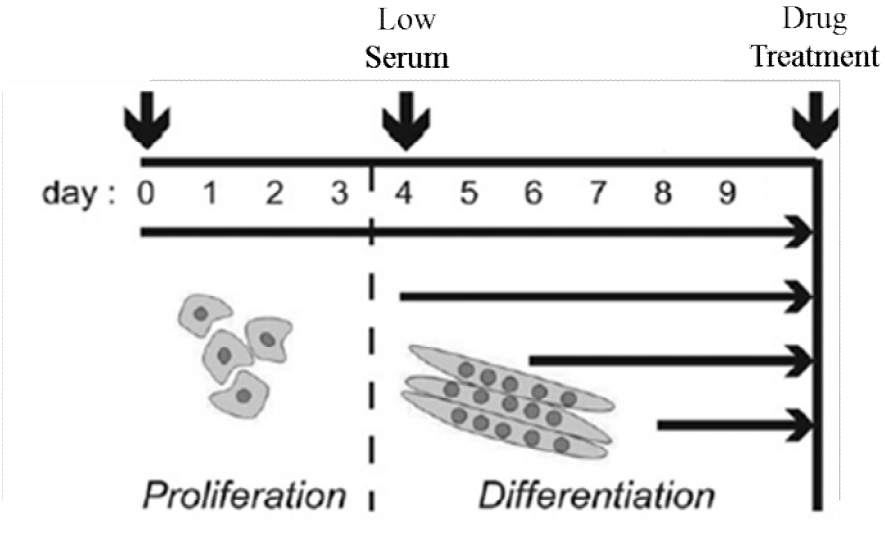

Figure 4.5 Immortalized myoblast cells (DM15) derived from DM patients were used for drug treatment. The cells were first differentiated for 5 days into myotubes under low serum conditions. The differentiated cells were then exposed to compounds treatment before extracting the nuclear and cytosolic proteins.

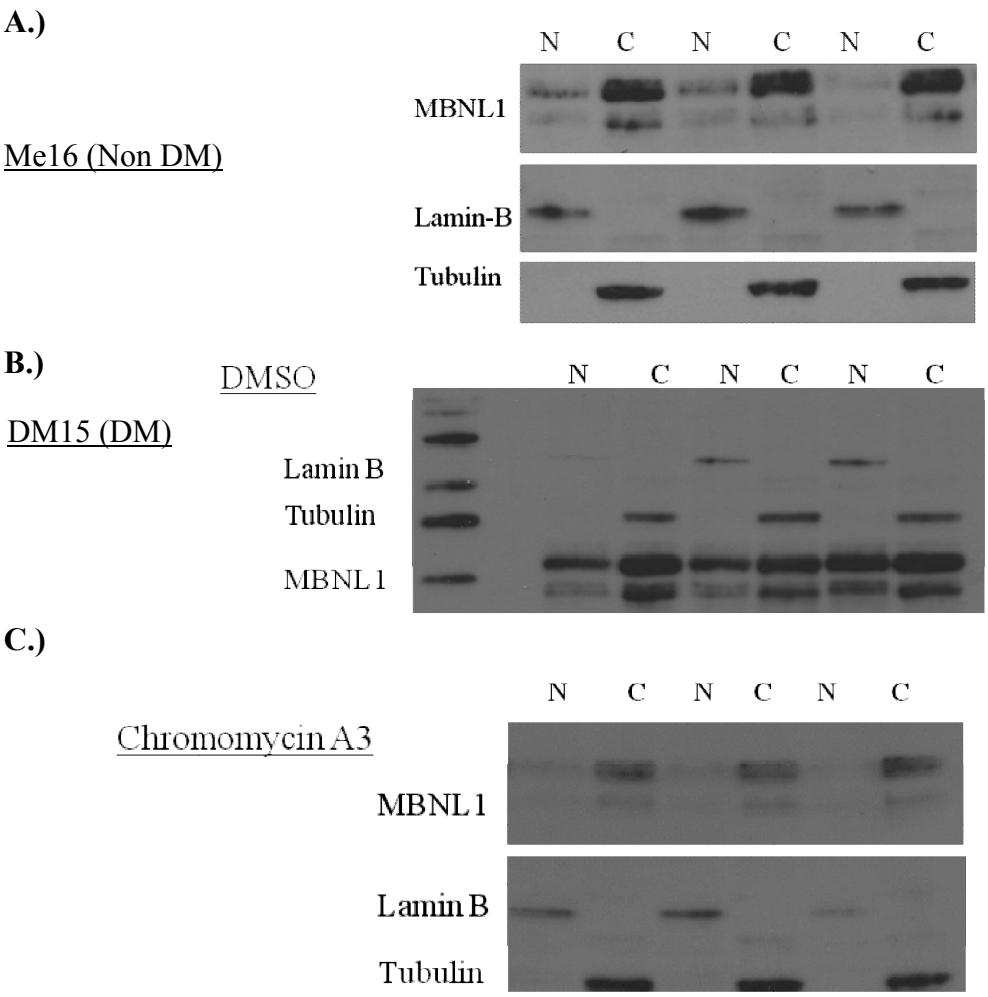

Figure 4.6 The sub-cellular distribution of MBNL1 before and after compound treatment. (A) Western blots showing the distribution of MBNL1 in nuclear (N) and cytosolic (C) compartments in Me16 (non-DM) myoblast cells **(B)** and in DM15 (DM) myoblast cells following treatment with DMSO, **(C)** and chromomycin A3 (40 nM).

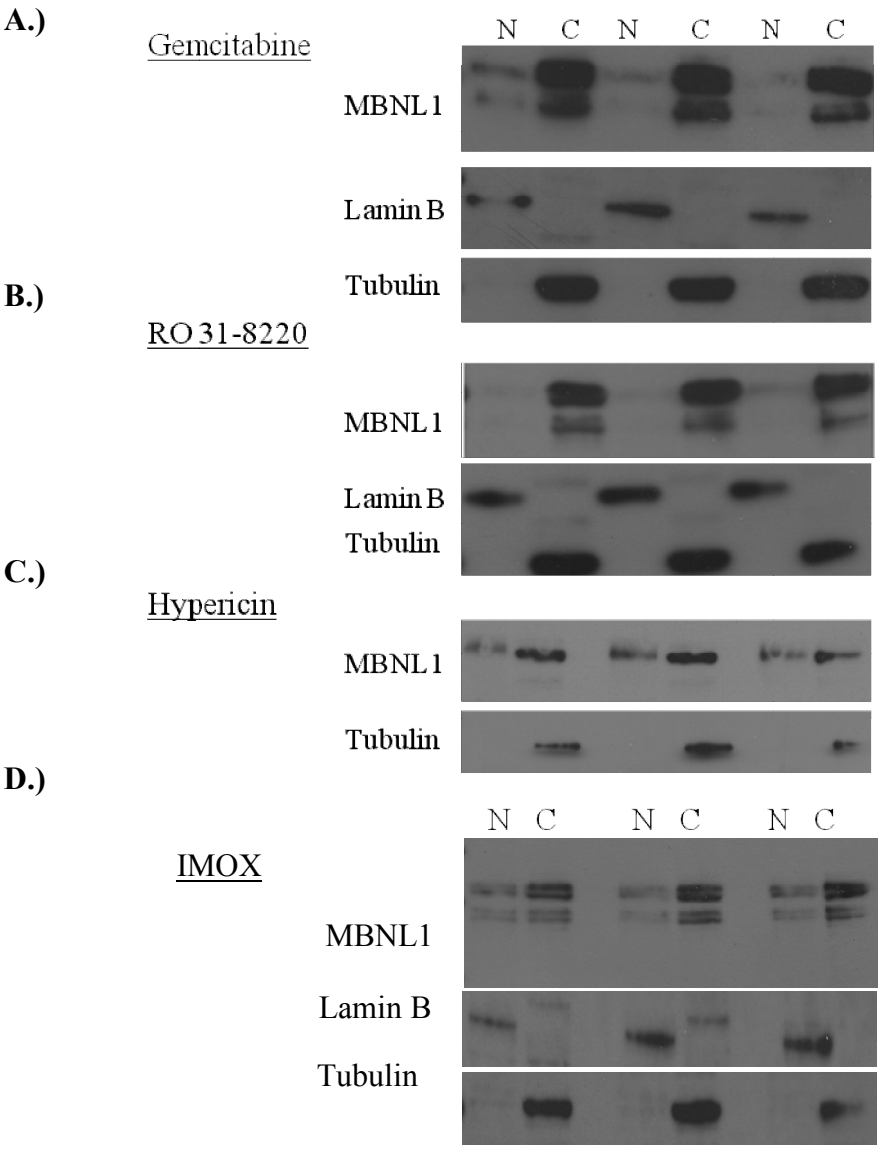

Figure 4.7 The sub-cellular distribution of MBNL1 after compound treatment. **(A)**Western blots showing the distribution of MBNL1 in nuclear (N) and cytosolic (C) compartments in DM15 myoblast cell line following treatment with compound gemcitabine, **(B)** RO 31-8220 (10μM), **(C)** hypericin (10μM), **(D)** and IMOX.

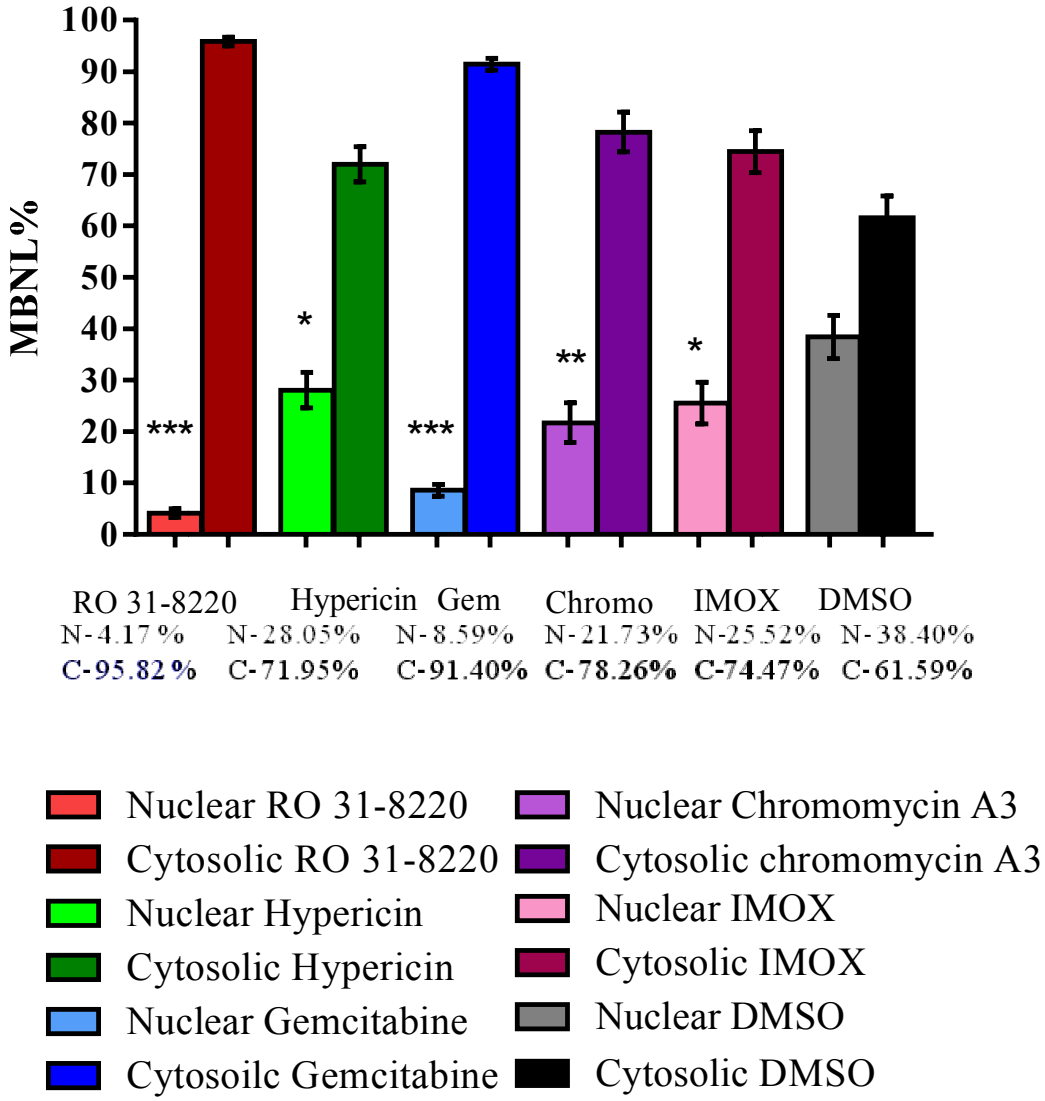

Figure 4.8 The distribution of MBNL1 in nuclear and cytosolic fractions after compound treatment in DM myoblast. Histograms show data compiled from intensity scans of triplicate blots for myoblast cell line DM15, normalized against values for lamin-B and tubulin following treatment with RO 31-8220 (10μM), hypericin (10μM), gemcitabine (10μM), chromomycin A3 (40nM), IMOX (10μM) and DMSO. * represents a significant difference from the control DMSO (Student's two tailed *t* test; *P<0.05)

4.4 Comparing the effects of Ro 31-8220 and GF 109203X

Two of the 80 compounds from the kinase inhibitor library; GF 109203X and Ro 31-8220 were identified as PKC inhibitors, although structurally very similar but they had different effects on nuclear foci. Both being highly potent PKC inhibitor, a similar effect would be expected but Ro 31-8220 was effective at removing nuclear RNA foci whereas GF 109203X had only a slight effect at the highest concentrations. It showed no effect at concentrations lower than 40 μM (Ketley et al., 2013). Thus, I decided to compare its effect on the distribution of MBNL1 protein in nuclear and cytosolic compartments. Consistent with its effect in the nuclear foci assay, GF 109203X treatment did not reduce or remove nuclear MBNL1 protein as shown by western blots (Fig.4.9). Statistical analysis showed there was no significant difference between treatments of GF 109203X and mock control DMSO.

A.)

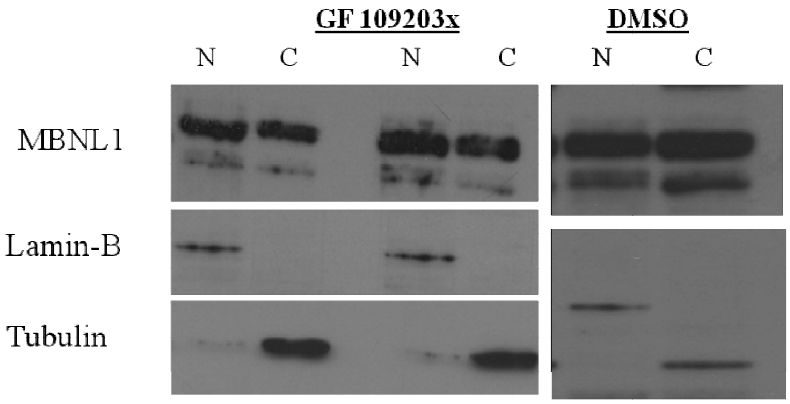

B.)

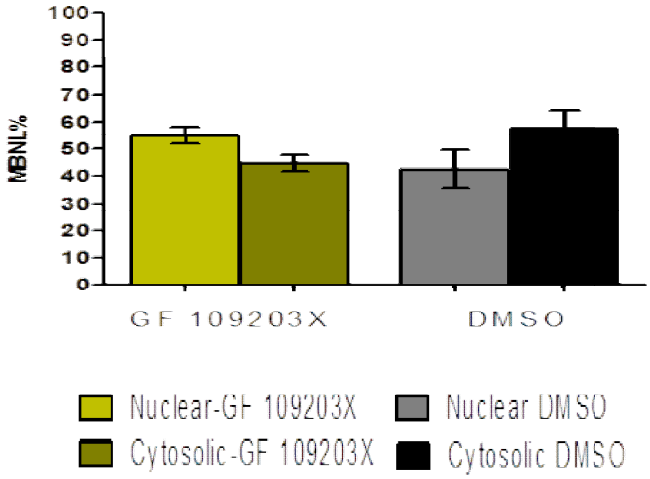

Figure 4.9 The sub-cellular distribution of MBNL1 before and after compound treatment. (A) Western blots showing the distribution of MBNL1 in nuclear (N) and cytosolic (C) compartments in DM1 fibroblast cell line (KB-Telo MyoD) after treatment with GF 109203X and DMSO (control) **(B)** Histograms show data compiled from intensity scans of triplicate blots for KB-Telo MyoD cell line, normalized against values for lamin-B and tubulin following treatment GF 109203X (10μM).

4.5 Effect of compounds on the MBNL1 protein in the foci (MBNL foci)

The accepted model of DM suggests that the expanded repeat RNA leads to the sequestration of RNA binding protein like Muscleblind-like protein 1 (MBNL1), which prevents MBNL1 from performing its other normal cellular functions in the nucleus or cytoplasm. Indeed MBNL has been shown to co-localize with expanded CUG and CCUG repeat RNA (Fardaei et al., 2001). To examine the effect of compound treatment on the MBNL1 protein content of nuclear foci, immunocytochemistry of DM cells before and after exposure to compounds was performed. Immunocytochemistry was carried out using the MBLa antibody, a mouse monoclonal antibody against MBNL1. Immunofluorescence analysis in fibroblast cells from DM1 patients (KB-Telo MyoD) showed 'MBNL foci' within nuclei (Fig 4.10). It would be hypothesized that if compounds can restore the MBNL1 protein distribution then they might be able to reduce or remove the 'MBNL1 foci' which is primarily composed of sequestered MNBL1 protein in the DM1 patient's cells. Consistent with their effect on nuclear RNA foci and depletion of MBNL1 from the nuclear compartment of DM cells, the MBNL1 foci disappeared or got reduced significantly following compound treatment.

Compounds R0 31-8220 and chromomycin A3 resulted in significant reduction in number of MBNL1 foci in KB-Telo MyoD cells after the treatment when compared to untreated KB-Telo MyoD cells (Fig. 4.11).

Also the cells treated with compounds hypericin and IMOX either lack or have much reduced numbers of MBNL1 foci, as seen in immunofluorescence

images (Fig. 4.12 and 4.13). Though no obvious reduction was observed in case of GF109203X treatment, which is consistent to its effect on RNA nuclear foci and MBNL1 sub-cellular distribution.

Statistical analysis revealed there was no significant effect of GF109203X and gemcitabine treatment on MBNL1 foci in comparison with controls (DMSO treated cells). However, the compounds hypericin ($p=0.0001$) and IMOX ($p=0.0001$) showed a significant difference compared to controls (DMSO treated). A very siginificant difference was observed in case of chromomycin A3 ($p<0.0001$) and R0 31-8220 ($p<0.0001$) compounds as compared to the DMSO treated cells (Fig. 4.14).

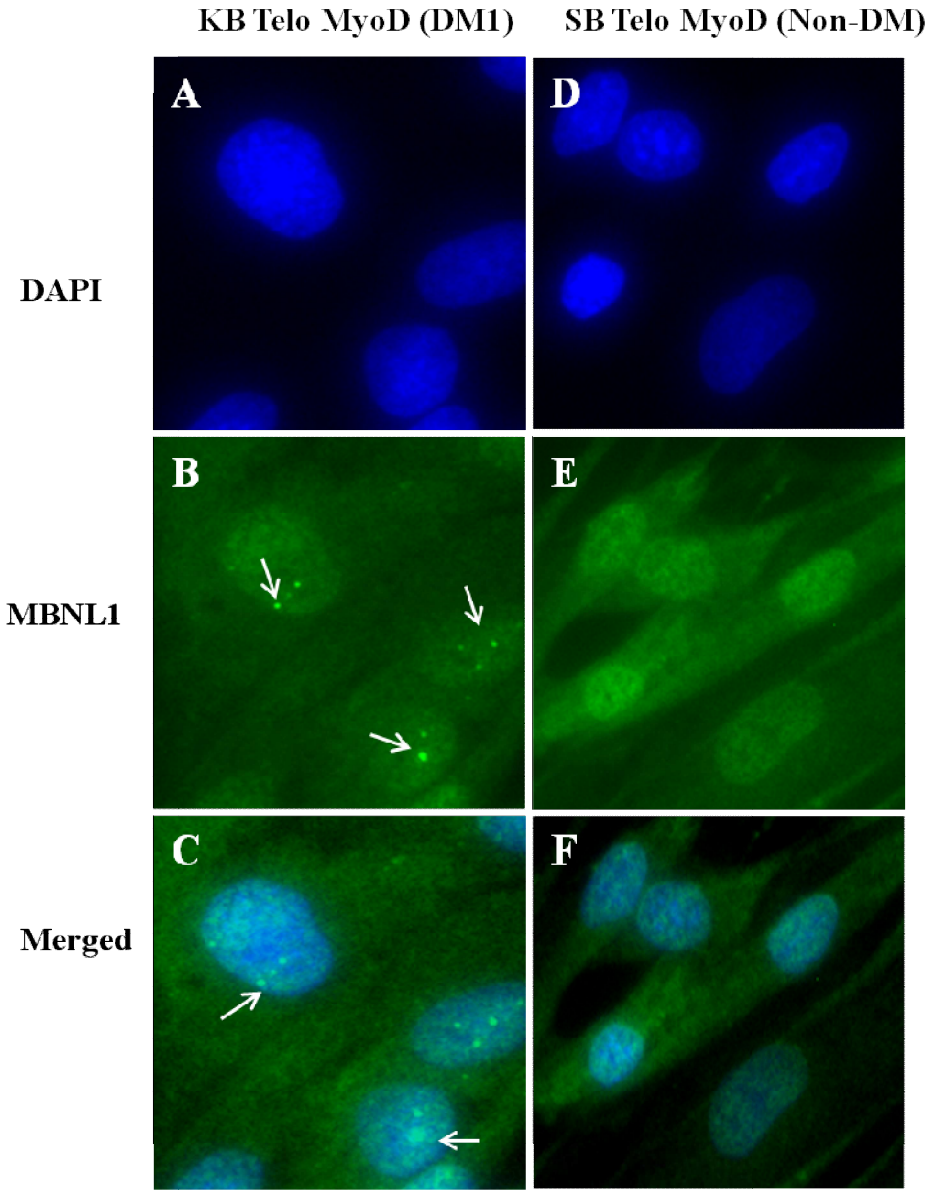

Figure 4.10 MBNL1 (protein) foci in DM and non-DM cells. (A-C) Immunostaining with MB1a antibody reveals MBNL1 foci in DMSO treated KB Telo MyoD cells, marked with white arrows. **(D-F)** Immunofluorescent images for control non -DM cells (SB-Telo MyoD) are lacking MBNL1 foci.

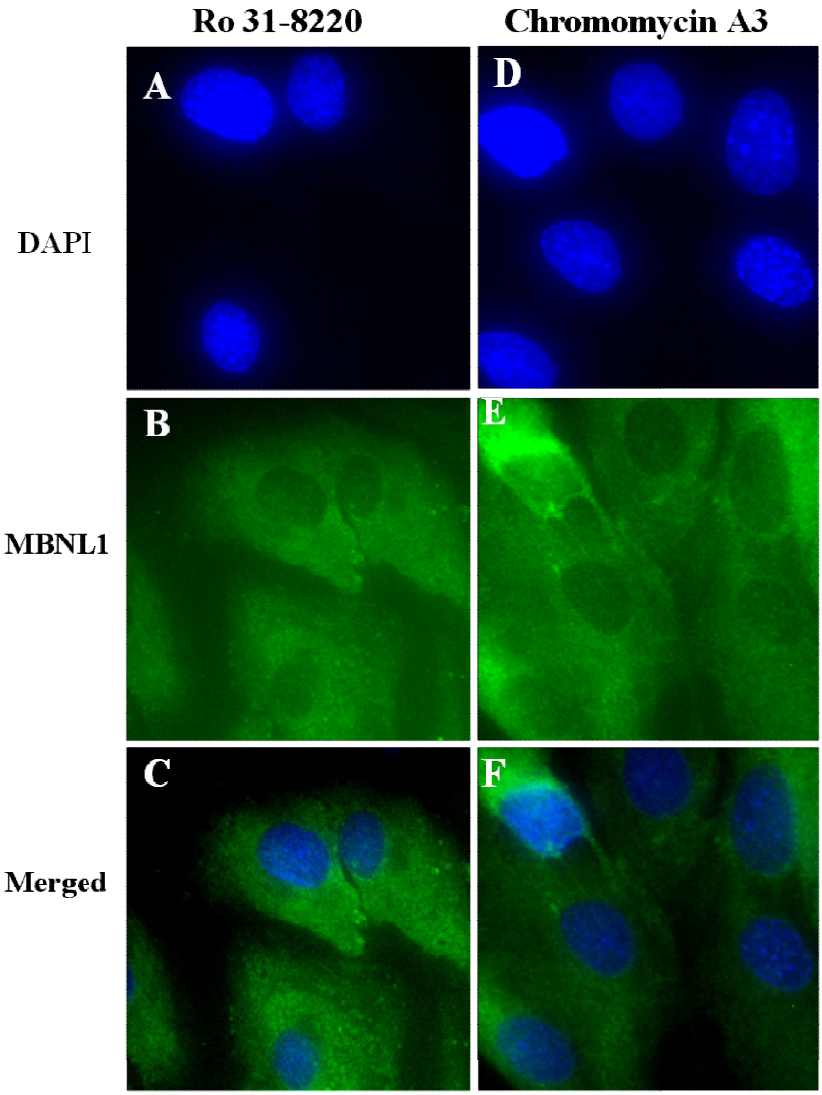

Figure 4.11 The effect of RO 31-8220 and chromomycin A3 on MBNL1 foci (MBNL1 foci). Cells treated with compound RO 31-8220 **(A-C)** and chromomycin A3 **(D-F)** either lack, or have very much reduced numbers of protein foci.

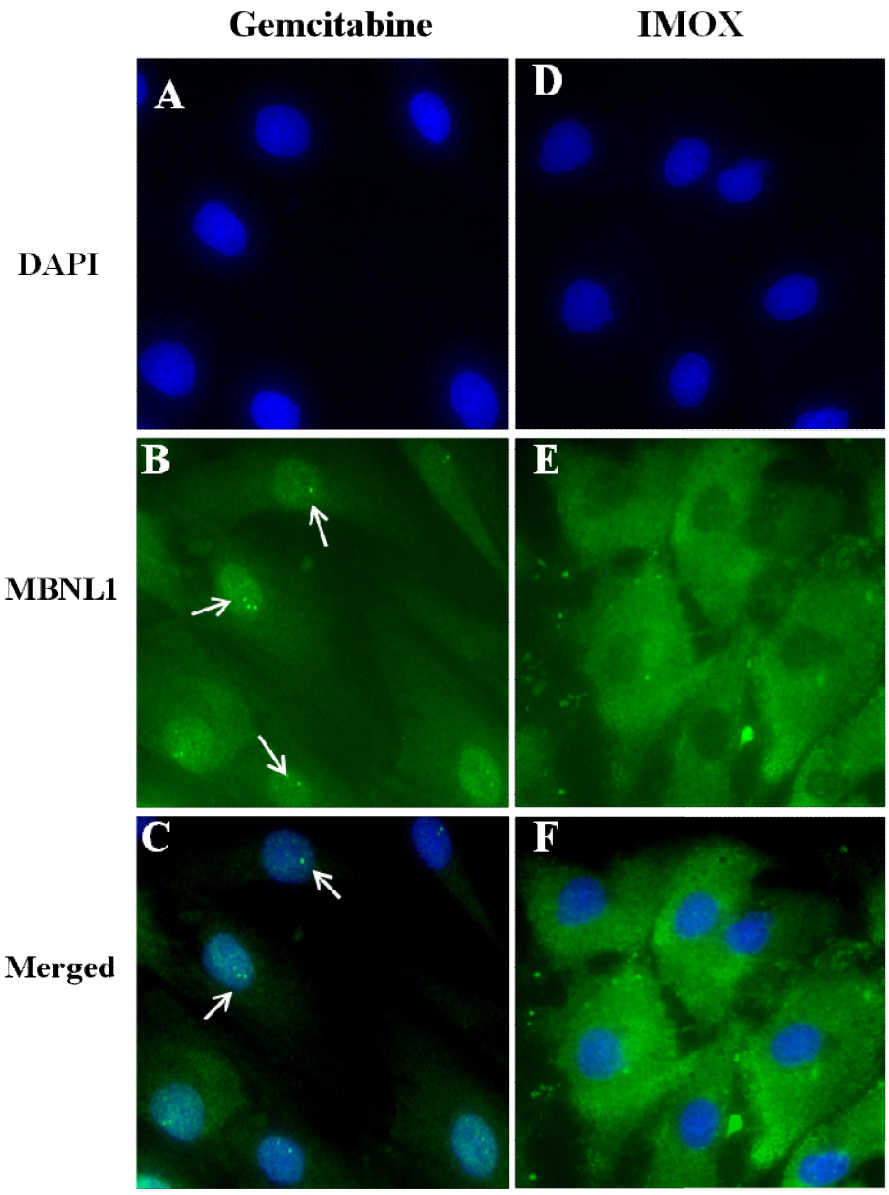

Figure 4.12 The effect of Gemcitabine and IMOX on protein foci (MBNL1 foci). Cells treated with compound gemcitabine **(A-C)** and IMOX **(D-F)** either lack, or have reduced numbers of protein foci compared to DMSO treated KB-Telo MyoD cells (DM1).

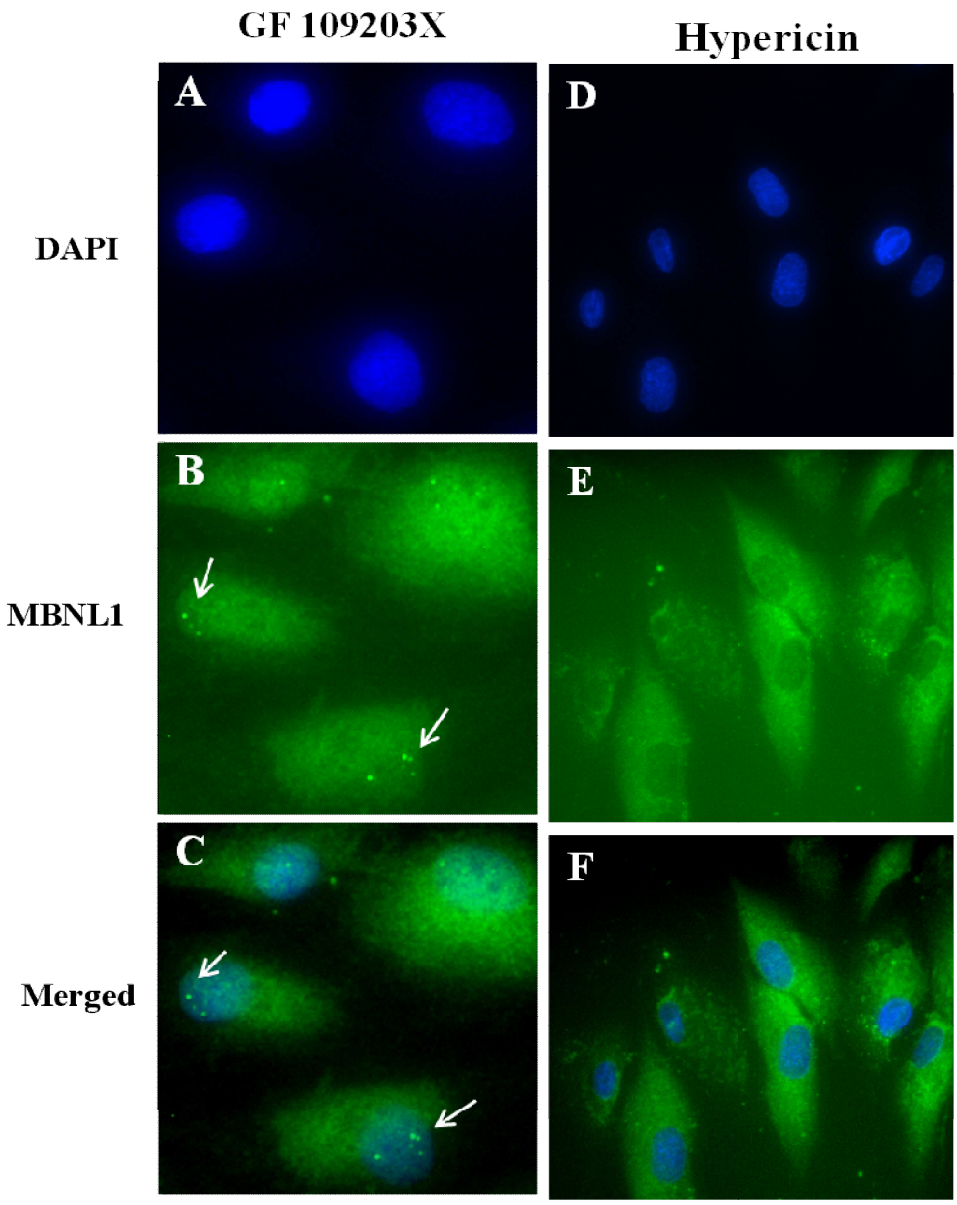

Figure 4.13 The effect of GF109203X and hypericin on MBNL1 foci (MBNL1 foci). Cells treated with compound GF109203X **(A-C)** had no effect on numbers of protein foci whereas **(D-F)** hypericin treated KB-Telo MyoD cells (DM1) showed significant reduction of number of protein foci.

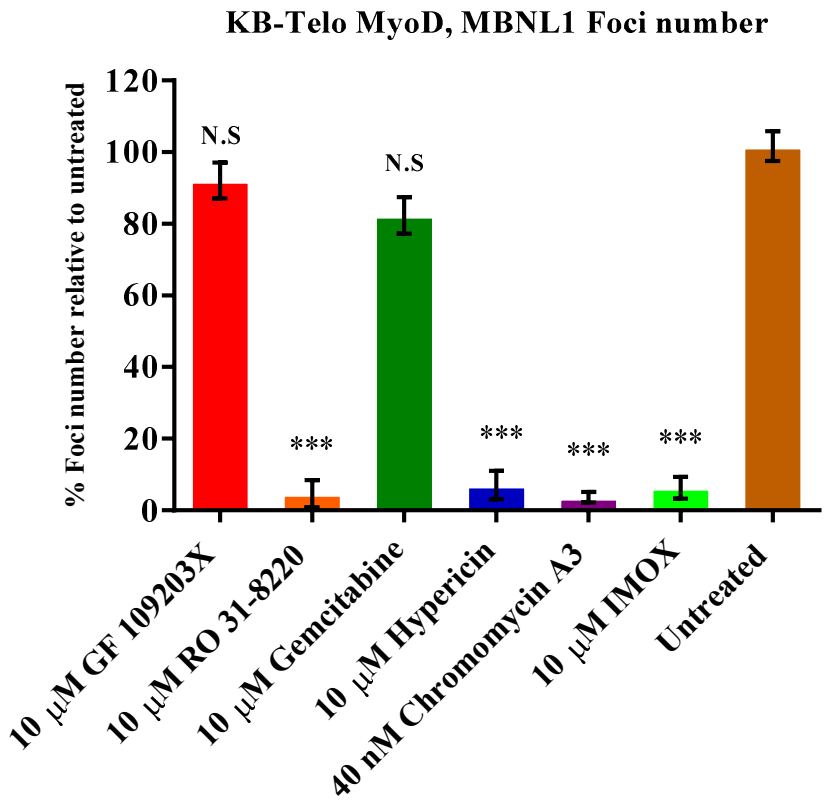

Figure 4.14 Effect of compounds on MBNL1 foci. Histograms show data compiled from the immunocytochemistry images after compound treatments in KB-Telo MyoD cells. * represents a significant difference from the control untreated (Student's two tailed *t* test; *P<0.05).

4.6 Immunocytochemistry studies on LR-Telo MyoD before and after compound treatment

Two of the compounds identified; gemcitabine and hypericin appeared toxic in the nuclear foci assay. Their toxicity profiles matched the reduction of foci, whereas compounds RO 31-8220, chromomycin A3 and IMOX reduced foci in the nuclear foci assay at concentrations that did not match the toxicity profile (Ketley et al., 2013). Chromomycin A3 reduced the foci and didn't affect the cell viability over 2 day exposure, whereas RO 31-8220 had a higher toxicity profile in general but showed a sharper reduction in foci number over a narrow concentration range. Similarly for IMOX, the toxicity profile didn't match the reduction of foci. Thus, RO 31-8220, chromomycin A3 and IMOX were selected for further analysis for immunocytochemistry studies in another DM1 cell line derived from a different patient, LR-Telo MyoD. Consistent with their effect on KB-Telo MyoD cell line, RO 31-8220, chromomycin A3 and IMOX were able to reduce MBNL1 foci compared to DMSO treated LR-Telo MyoD cells (Fig. 4. 15).

Following the treatment with compounds RO 31-8220, chromomycin A3 and IMOX, there was a significant reduction in the MBNL1 foci number over the dilution range. Immunocytochemistry study of 12 point dilution series with a 1:3 dilution protocol, ranging from 200 pM to 40 μM concentration at series of time intervals (2, 4, 8, 16, 24 and 48 hours after compound exposure) for compounds chromomycin A3, IMOX and Ro 31-8220 was performed in LR-Telo MyoD cells (DM1). In Figures 4.16- 4.18, foci number is represented

relative to the DMSO treatment on the 'y' axis and concentration (log μM) on 'x' axis.

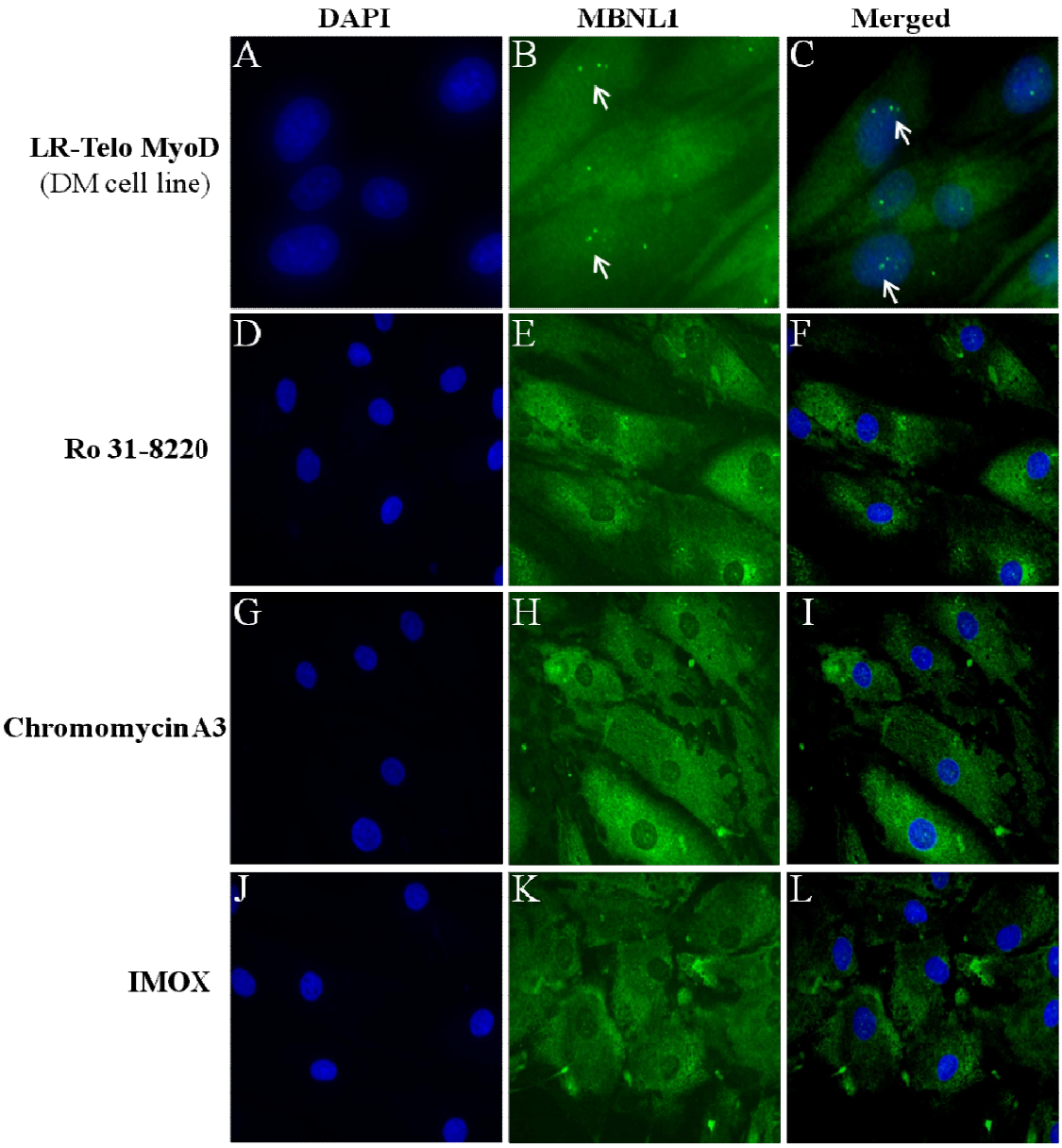

Figure 4.15 The effect of RO 31-8220, chromomycin A3 and IMOX on protein foci (MBNL1 foci). (A-C) Immunostaining with MBLa antibody reveals protein foci in DMSO treated LR Telo MyoD cells. Cells treated with RO 31-8220 **(D-F)**, chromomycin A3 **(G-I)** and IMOX **(J-L)** either lack, or have very much reduced numbers of protein foci.

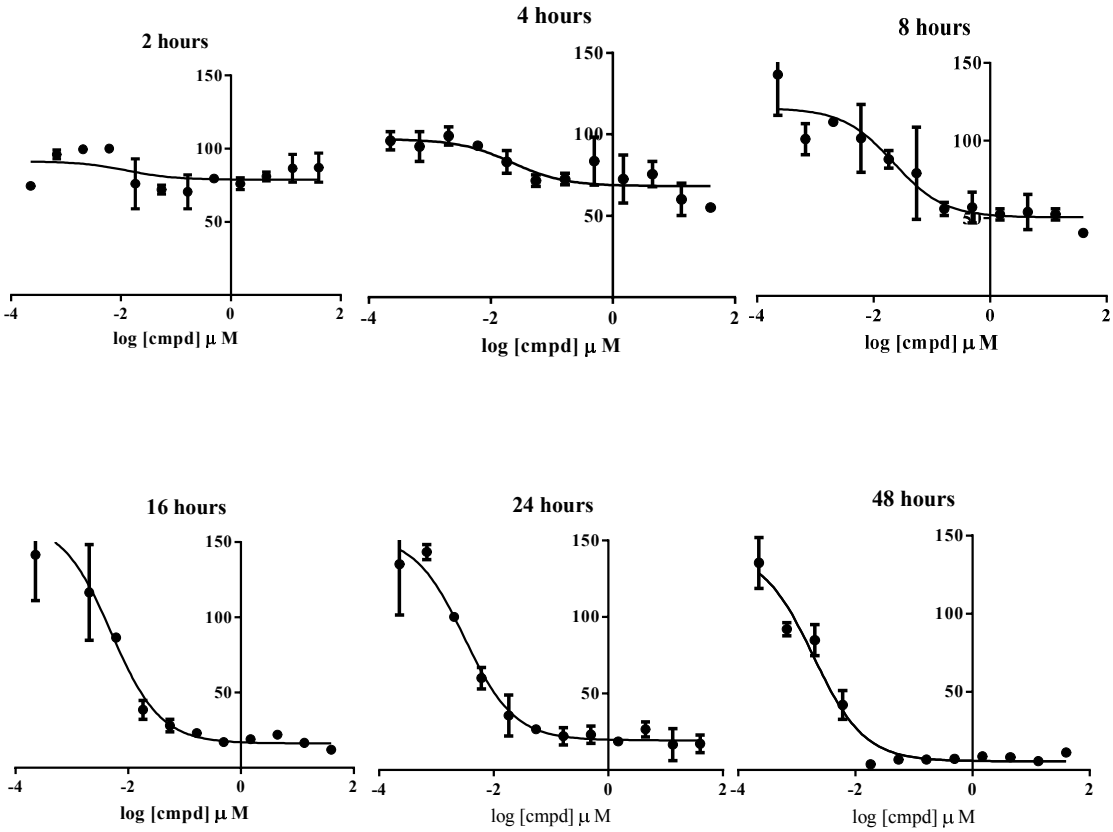

Figure 4.16 Standard concentration curves showing the effect of chromomycin A3 treatment in LR-Telo MyoD cells. Chromomycin A3 treatment showing reduction in protein foci in 12 point titration ranging from 200pM to 40 μM in triplicates to determine its concentration response on reduction of MBNL1 protein foci at different time intervals after compound exposure

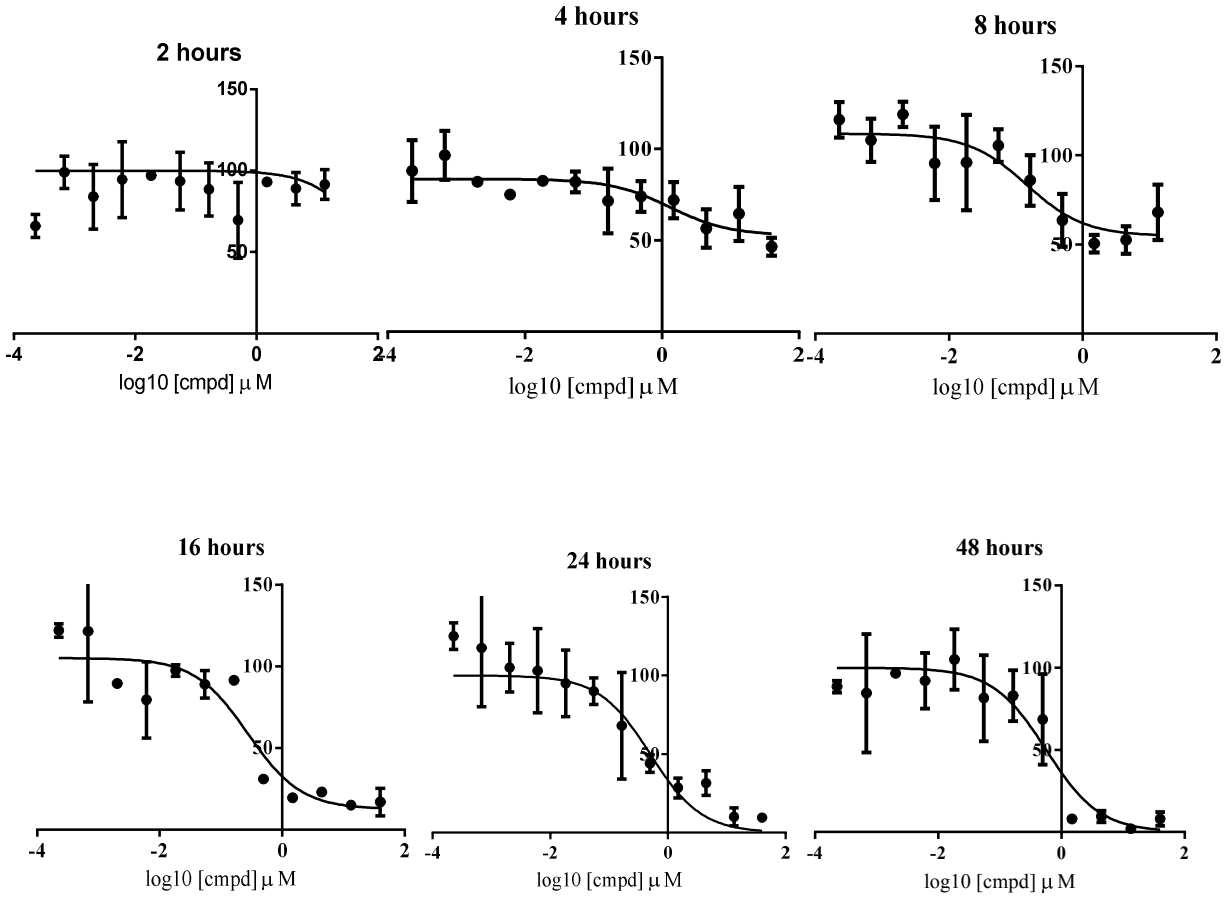

Figure 4.17 Standard concentration curves showing the effect of RO 31-8220 treatment in LR-Telo MyoD cells. RO 31-8220 treatment showing reduction in protein foci in 12 point titration ranging from 200pM to 40 µM in triplicates to determine its concentration response on reduction of MBNL1 protein foci at different time intervals after compound exposure

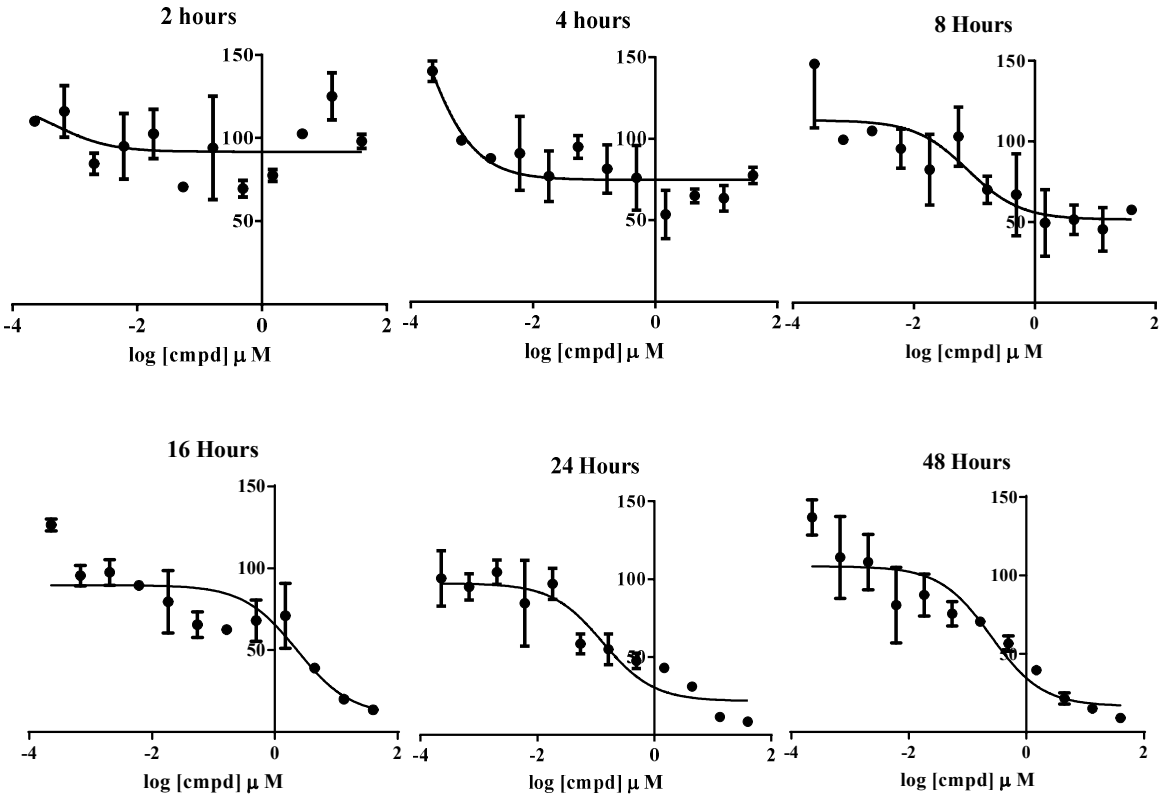

Figure 4.18 Standard concentration curves showing the effect of IMOX treatment in LR-Telo MyoD cells. IMOX treatment showing reduction in protein foci in 12 point titration ranging from 200pM to 40 µM in triplicates to determine its concentration response on reduction of MBNL1 protein foci at different time intervals after compound exposure

4.7 Effect of MBNL1/2 down regulation on the nuclear foci in DM cells

The aim of this study was to establish whether MBNL1/2 depletion via RNA interference would result in reduction of the nuclear foci as previously reported by Dansithong *et al.* (2005) and to test the role of MBNL1 and MBNL2 in formation of DM foci. *MBNL1* and *MBNL2* double knockdown was conducted three times over a 7 day period using siRNA oligonucleotides to ensure removal of MBNL. DM1 fibroblasts were transfected with siRNA's directed against both MBNL1 and MBNL2, on days 0, 3 and 6 and after the 3 rounds of knockdown, total protein was extracted which was subjected to Western blot analysis for validation of successful knockdown. At the same time nuclear and cytoplasmic RNA was also extracted for RT-PCR analysis and Bpm1 polymorphism assessment which will be discussed later in section 4.8. *In situ* hybridization and immunocytochemistry studies were also performed on cells to assess the effect of MBNL1/2 down regulation on both RNA nuclear foci and MBNL (protein) foci in KB-Telo MyoD cells (DM cells).

12 μg of protein was subjected to SDS-PAGE followed by Western blot with anti-MBNL1 and anti-MBNL2 monoclonal antibodies to measure the % silencing achieved for both. In case of *MBNL1*, the % silencing achieved was 99% when compared to SCR (scrambled) or untreated cells whereas ~98% silencing was achieved in case of *MBNL2* knockdown (Fig. 4.19). Both the blots were also probed with tubulin as an internal control for loading.

In contrast to results reported by Dansithong and colleagues (2005), there was no reduction in the nuclear (RNA) foci number compared to SCR or untreated

cells in knockdown experiment that I conducted (Fig. 4.21). The results from the *in situ* hybridization images showed that there was a significant increase ($p=0.0005$) in the number of smaller nuclear RNA foci after the MBNL1 and MBNL2 knockdown as compared to SCR (scrambled) or untreated cells (Fig 4.20). Data for foci area and intensity were also obtained in the form of excel spreadsheets. The histograms in figure 4.22 show data compiled for average pixel intensity and average foci area for a single RNA foci after MBNL1 and MBNL2 knockdown.

siRNA- mediated down-regulation of MBNL1 and MBNL2 resulted in a 40% increase in the number of nuclear RNA foci than observed in scrambled siRNA treated cells or untreated cells (Fig. 4.21). However, the average intensity and the average area for single focus decreased significantly following MBNL1 and MBNL2 knockdown compared to untreated cells (Fig 4.22).

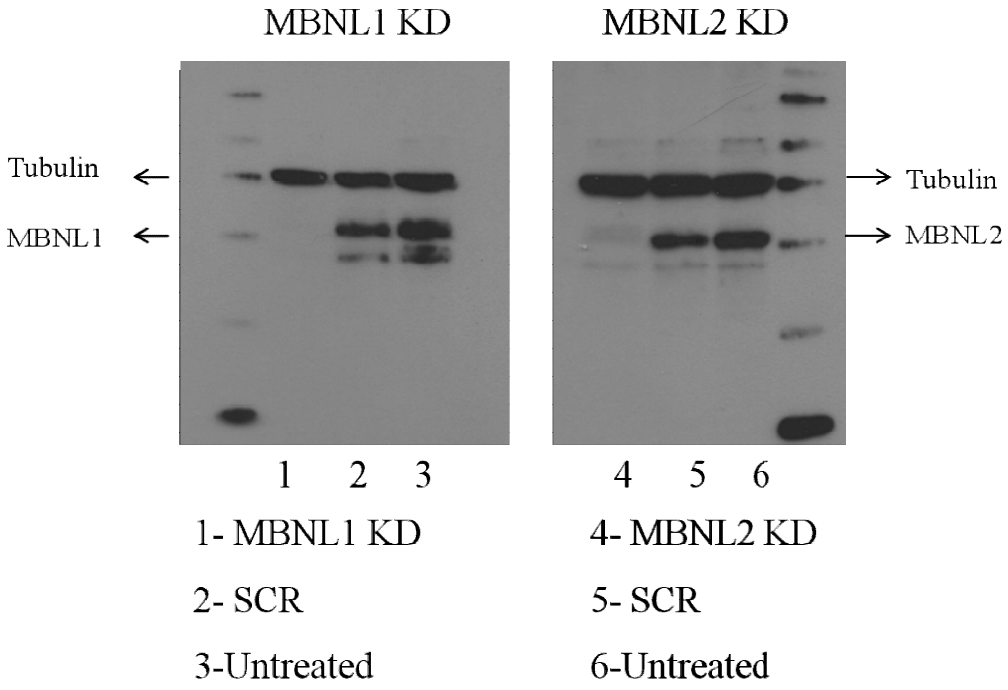

Figure 4.19 Western blots showing MBNL1 and MBNL2 knockdown. 99% of silencing was achieved in case of the MBNL1 knockdown and 98% in case of MBNL2. Tubulin was included as a loading control for both blots.

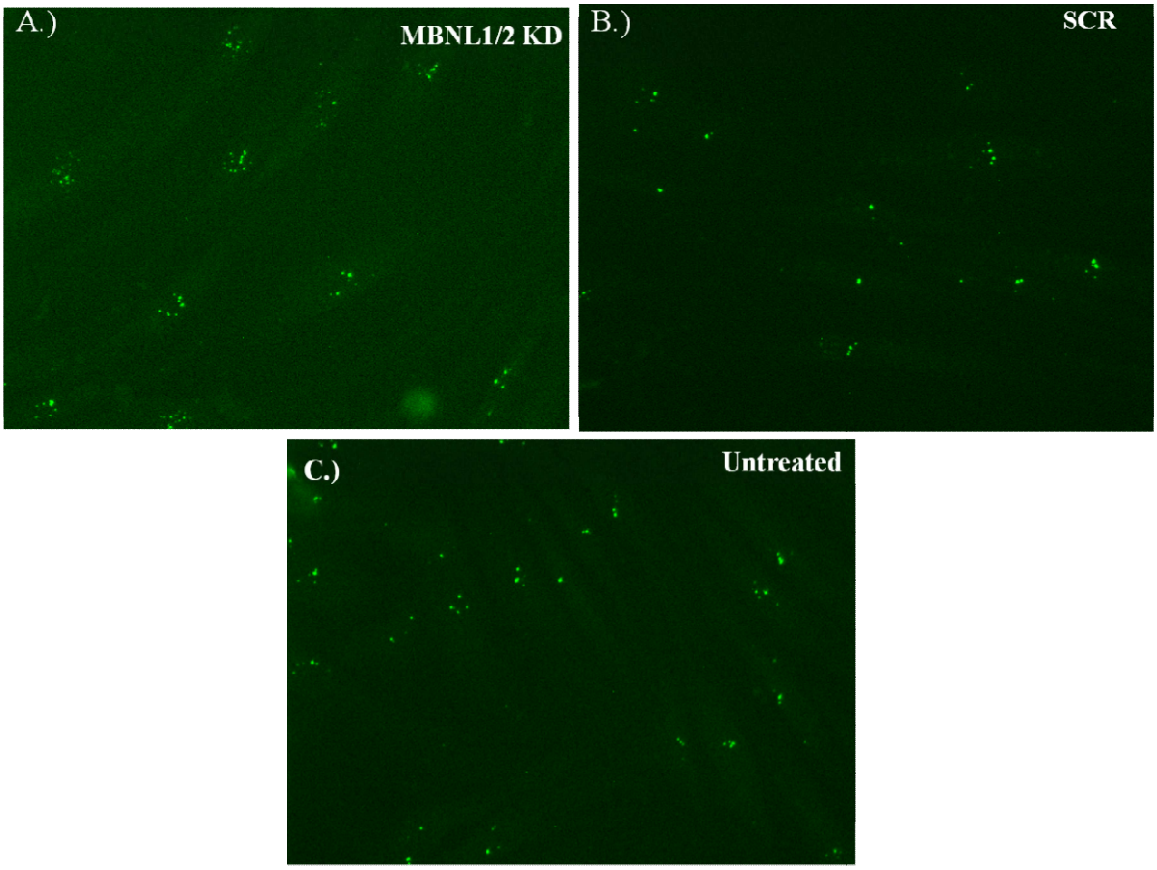

Figure 4.20 Effect of MBNL1 and MBNL2 double knockdown on RNA foci. MBNL1 and MBNL2 double knockdown increases the number of smaller nuclear RNA foci whereas scrambled (SCR) knockdown does not have any effect on RNA foci in KB-Telo MyoD cells (DM1 cells).

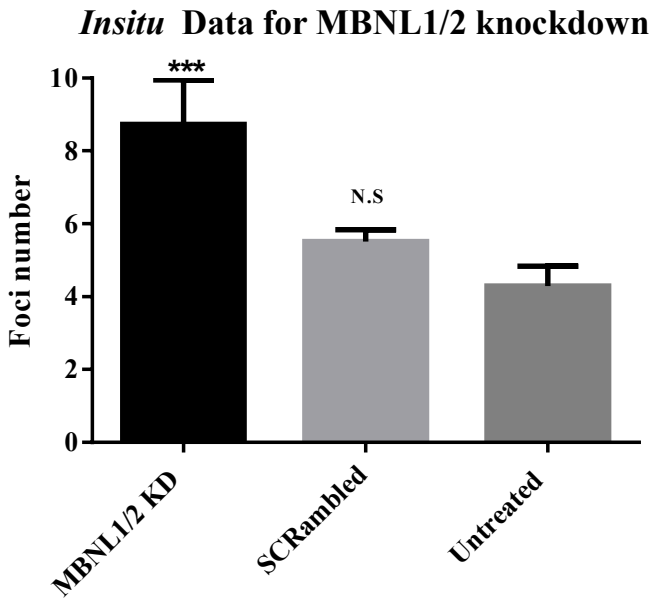

Figure 4.21 Histograms show data compiled from the *in situ* hybridization images after MBNL1 and MBNL2 knockdown. Data suggests that there was a significant increase (p=0.0005) in the number of nuclear RNA foci after the MBNL1 and MBNL2 double knockdown when compared to SCR (scrambled) or untreated cells. * represents a significant difference from the control untreated (Student's two tailed *t* test; *P<0.05, where N.S denotes data not significant.

A.)

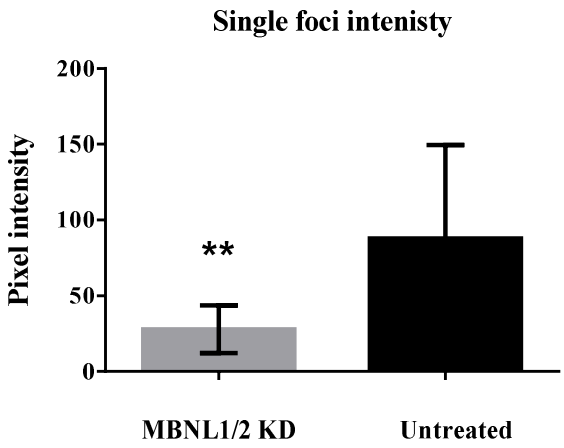

B.)

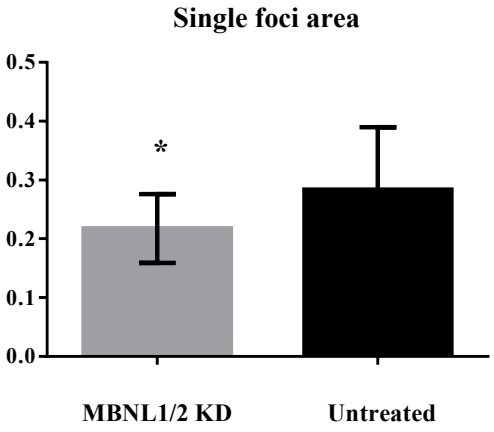

Figure 4.22 Histograms show data compiled for average pixel intensity and average foci area for a single nuclear RNA foci after MBNL double knockdown. A significant reduction in the average area and average intensity was observed for a single foci following MBNL double knockdown. * represents a significant difference from the control untreated (*P<0.05).

In a second set of experiment I attempted to assess the effect of MBNL1 and MBNL2 down-regulation on MBNL1 (protein) foci. Immunocytochemistry data shows that *MBNL* double knockdown in DM1 cell line (KB-Telo MyoD cells) resulted in a significant reduction of MBNL1 (protein) foci compared to SCR (scrambled, non-specific siRNA) or untreated cells as shown by immunofluorescence images ($p=0.0001$) (Fig. 4.23). Though the western blot data indicates 98% removal of MBNL protein, we still see the presence of a few MBNL (protein) foci in the immunocytochemistry images, which may be due to the residual 2% MBNL protein in the cells before the MBNL double knockdown.

Statistical analysis showed there was a significant reduction in the average area and average intensity of a single foci (MBNL foci) following MBNL double knockdown as seen in figure 4.24.

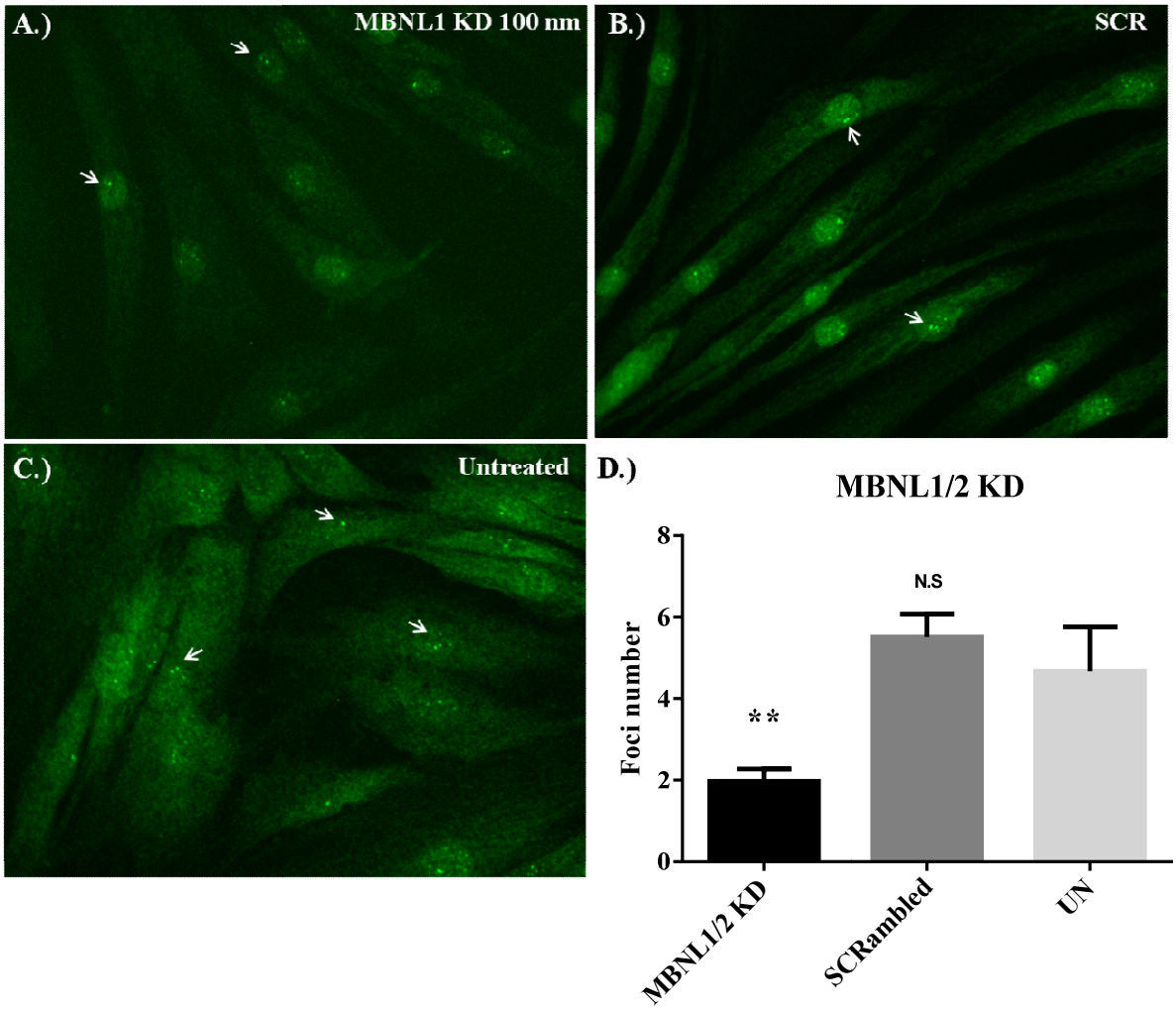

Figure 4.23 Effect of MBNL1 and MBNL2 double knockdown on MBNL1 foci. (A) Immunostaining with MBNL1 (MBLa) antibody reveals fewer MBNL1 (protein) foci after MBNL1/2 knockdown, marked with white arrows. **(B-C)** while scrambled knockdown which is non-specific to MBNL does not have any effect on nuclear foci in DM1 fibroblasts (KB-Telo MyoD cells). **(D)** Histograms show data compiled from the immunocytochemistry images. * represents a significant difference from the control untreated (Student's two tailed *t* test; *P<0.05).

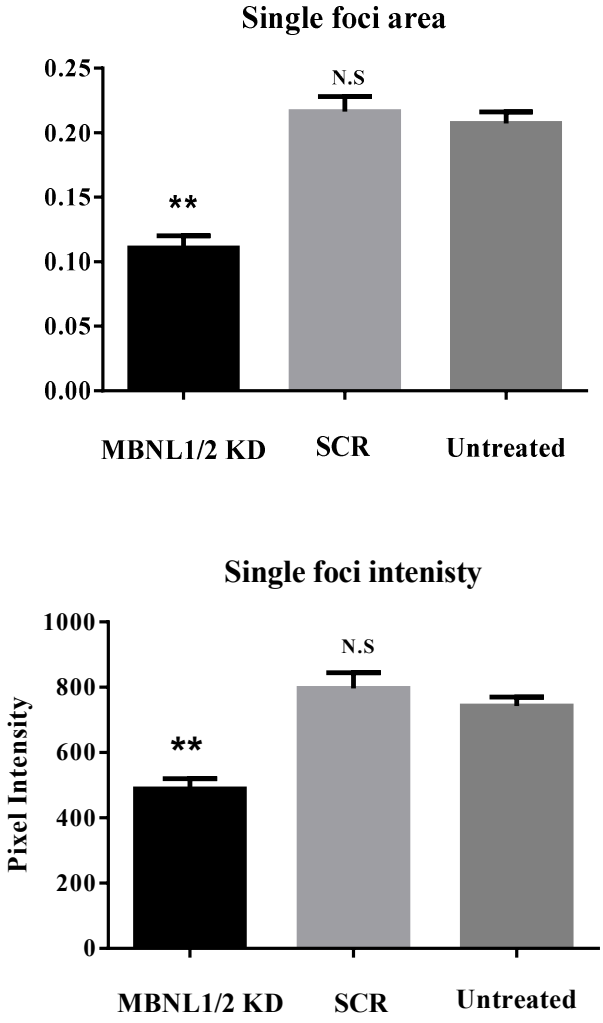

Figure 4.24 Histograms show data compiled for average foci area and average pixel intensity for a single MBNL (protein) foci after MBNL double knockdown. A significant reduction in the average area and average intensity was observed for a single foci following MBNL double knockdown compared to scrambled or untreated cells. * represents a significant difference from the control untreated (Student's two tailed *t* test; *P<0.05, where N.S denotes data not significant.

4.8 Bpm1 Polymorphism Analysis

BpmI polymorphism assay is based on the previous work from our lab (Hamshere et al., 1997). This essay enabled us to differentiate between the expanded and wild-type DMPK transcript based on the presence or absence of a coding *BpmI* polymorphism. Primers were designed on exon 9 and exon 10 which flanked the *BpmI* polymorphic site on exon 10 of DMPK (Fig 4.25).

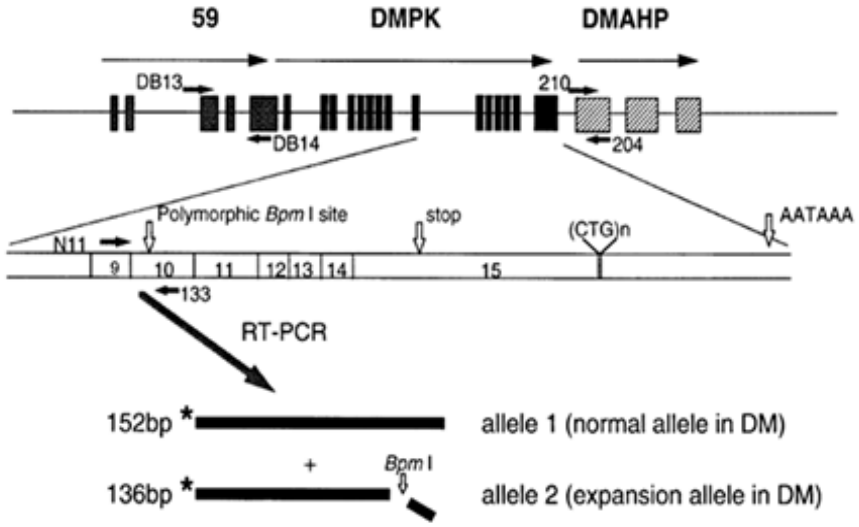

Figure 4.25 BpmI polymorphism assay. The positions for primers N11 and 133 are indicated by black arrows. The mutant and normal DMPK transcripts are indicated as allele 1 and allele 2 (Hamshere et al., 1997).

The DM cell line which was informative for a *BpmI* polymorphism in exon 10 and a wild type cell line, SB-Telo MyoD, which was established from an individual who did not have DM but who is heterozygous for *BpmI* polymorphism were used for this study . The RNA was extracted from both nuclear and cytosolic fractions of KB-Telo MyoD (DM) cells and SB-Telo MyoD (WT) cells. RNA was then reverse transcribed which was followed by PCR using oligonucleotides for DMPK at 28 cycles. A 154bp amplicon was generated by PCR amplification. Overnight digestion with *BpmI* enzyme of 154 amplicon resulted into two bands on 3% ethidium stained agarose gel, one at 154bp and other at 138 bp which represented the normal and mutant expanded allele respectively. Figure 4.26 clearly shows that in case of wild type cells the mutant transcript is present in both nuclear and cytosolic fractions of the cell whereas, in case of DM cells the mutant transcripts is just present in nuclear fraction and is absent from cytosolic fractions.

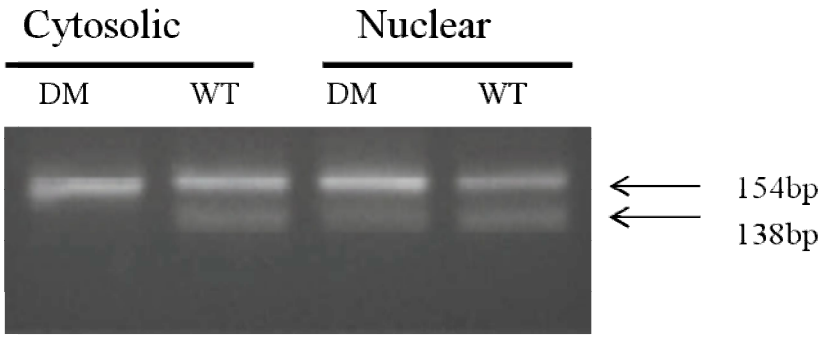

Figure 4.26 Bpm1 polymorphism analysis of nuclear and cytoplasmic fractions from DM (KB-Telo MyoD) cells and wild type (SB-Telo MyoD) cells.

4.8.1 Effect of MBNL1 and MBNL2 down-regulation on the mutant repeat expansion transcript.

To determine the effect of MBNL1 and MBNL2 down-regulation on the mutant repeat expansion transcripts and whether it could affect the release of mutant repeat expansion, I utilized the *BpmI* polymorphism assay.

The RNA was extracted from both nuclear and cytosolic fractions after siRNA-mediated down regulation for MBNL1 and MBNL2 in KB-Telo MyoD cells. RNA was then reverse transcribed which was followed by PCR using oligonucleotides for DMPK at 28 cycles. 154bp amplicon was generated by PCR amplification. The BpmI polymorphic site is present only in one of the alleles (the mutant allele in DM cells) and is absent from the normal allele in DM cells. Overnight digestion of the 154bp PCR-product with the restriction enzyme *BpmI* gave two bands on 3% ethidium stained agarose gel, one at 154bp and other at 138 bp which represented the normal and mutant expanded allele respectively.

Analysis of RNA from the DM cell line KB-Telo Myod showed that the DMPK mutant transcript was still present in the nuclear fraction and there was no sign of liberation of the mutant transcript in the cytoplasm following MBNL1 and MBNl2 knockdown (Fig 4.27). However, the MBNL1 and MBNL2 down-regulation resulted in a reduction in the relative proportion of the mutant transcript in the nucleus of KB-Telo MyoD cells compared to scrambled (SCR) or untreated cells. Analysis showed that the % proportion of the mutant allele in the nucleus was 27.09, 47.74 and 48.06 for MBNL 1/2

knockdown, scrambled (SCR) and untreated respectively as seen on agarose gel.

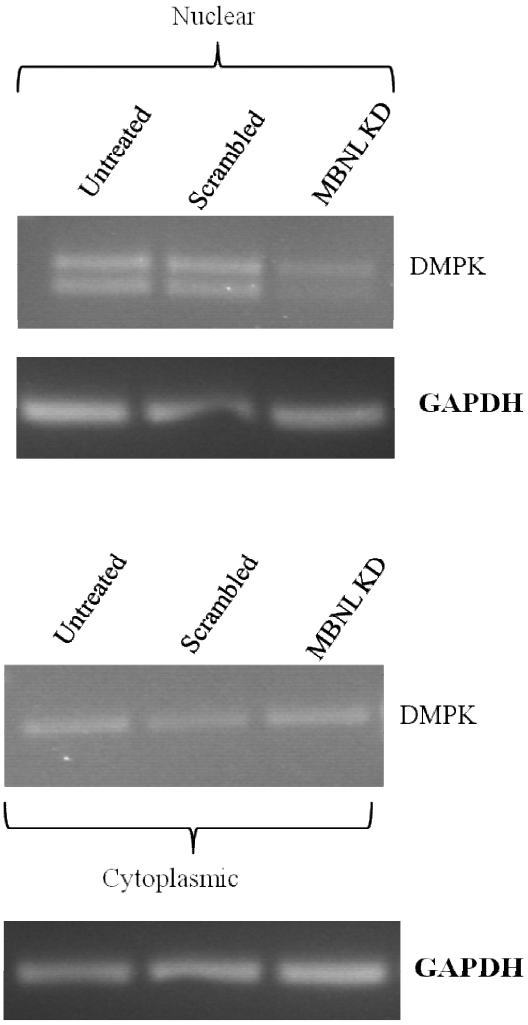

Figure 4.27 The effect of MBNL double knockdown on repeat expansion transcripts. Ethidium stained gel shows no sign of release of mutant DMPK transcript into cytoplasm fraction but shows a marked reduction in the relative proportion of the mutant DMPK transcript following double knockdown compared to scrambled or untreated controls in the nuclear fractions. GAPDH is used as the loading control.

4.9 Effect of Antisense oligonucleotides (AONs) on MBNL1 protein distribution in DM myoblasts

In past studies, Antisense oligonucleotides (AONs) have been widely used for gene-specific knockdown in disorders that involve RNA or protein gain-of-function effects. Various strategies like RNA interference (RNAi), antisense oligonucleotides and steric-blocking oligonucleotides have been employed to degrade or eliminate expanded $(C/CUG)_n$ transcripts.

It has already been shown that the hairpin structure formed by the expanded $(CUG)_n$ repeats (Broda et al., 2005; Napierala and Krzyzosiak, 1997) can be targeted by the RNA interference (RNAi) pathway (Malinina, 2005; Mooers et al., 2005). Langlois *et al*. (2005) showed that normal DMPK transcripts in cytoplasm and mutant transcript in nucleus in DM1 cells got reduced after treatment with short hairpin RNA that targeted sequences in the 5` end of the RNA. Also there has been evidence of silencing of expanded DMPK transcript levels and reduction in number of ribonuclear aggregates by a 2′-O-methyl phosphorothioate modified $(CAG)_7$ AON (Mulders et al., 2009). In 2012, Wheeler *et al*. published a paper in which they described a gapmer with 2'-O-methoxyethyl modification at both ends with a central gap of 10 unmodified nucleotides which was able to reduce CUG^{exp} RNA level by inducing RNase H activity. It also resulted in release of sequestered MBNL1 protein and an improvement in MBNL1 dependent splicing abnormalities (Wheeler et al., 2012) There is some published data on splice switching which lead to the correction of ClC-1 splicing in mouse models of myotonic dystrophy by steric-blocking AON (Wheeler et al., 2007)

We initially found that two types of chemically modified oligonucleotides (CMOs) : PNA and 2'OMe, were readily taken up by DM cells, via gymnotic delivery, and removed nuclear RNA foci at nanomolar concentrations, in a cell based assay, which uses high content imaging to visualise the number, size and intensity of foci (data not included). So I decided to assess the effect of one of the antisense oligonucleotides (AONs), PNA, on MBNL1 protein distribution in DM myoblasts. I conducted western blots to quantify results of experiments with 21-mer PNA.

DM15 cells were treated with 21-mer CAG_7 PNA to look at its effect on MBNL1 distribution before and after the treatment. Treatment with PNA at two different concentrations caused a significant reduction in nuclear MBNL1 protein compared to nuclear protein level in the untreated DM15 cells (Fig. 4.29 and 4.30). It was observed that the treatment shifted the pattern to the one observed in wild type myoblast cells (Me16 cells, Non-DM) (Fig. 4.28).

Me16 (non-DM)

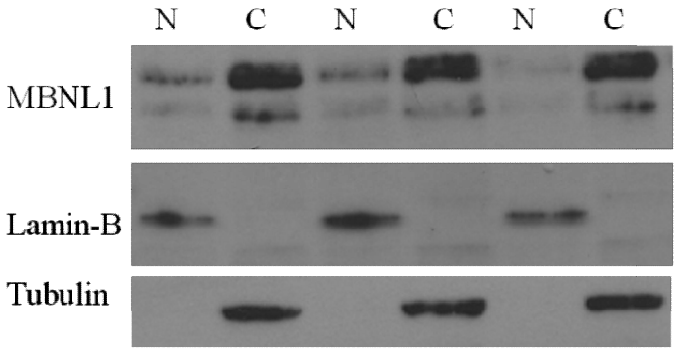

Figure 4.28 The sub-cellular distribution of MBNL1 in Me16 (non-DM, control) myoblast cells (A) Western blots showing the distribution of MBNL1 in nuclear (N) and cytosolic (C) compartments in Me16 (control myoblast) cell line.

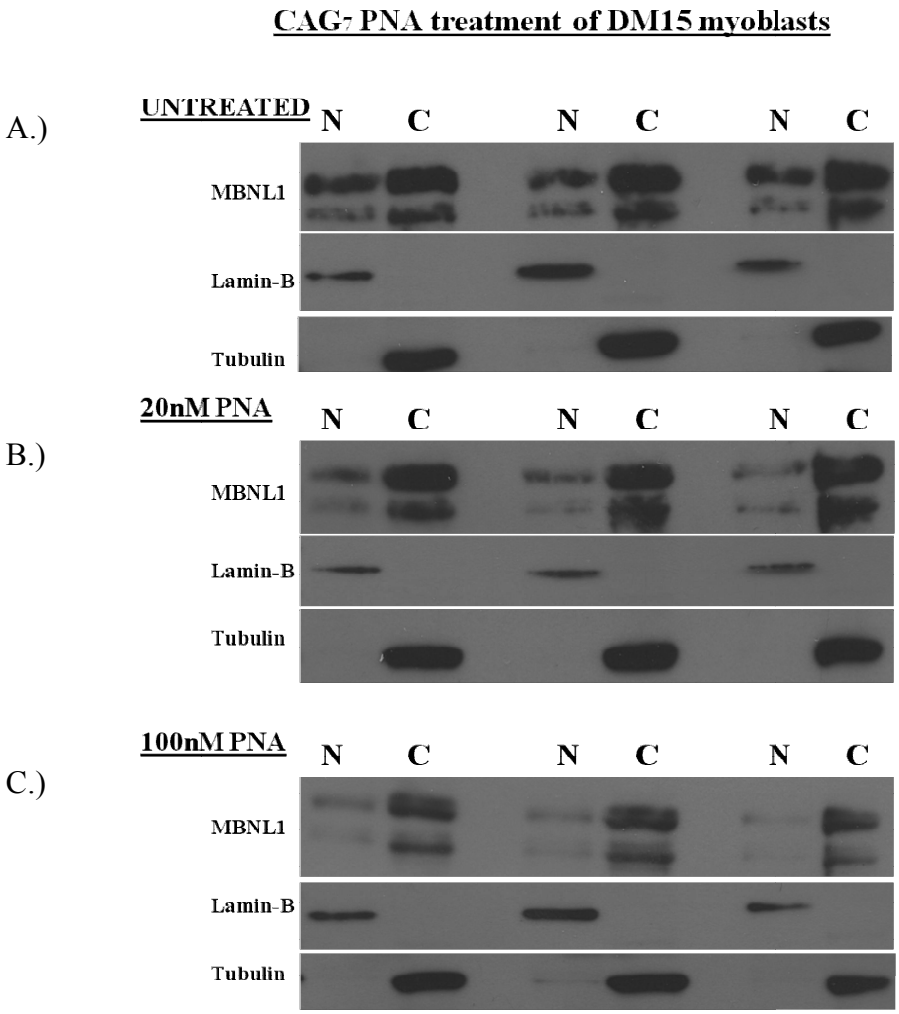

Figure 4.29 The sub-cellular distribution of MBNL1 before and after compound treatment with PNA. **(A)** Western blots showing the distribution of MBNL1 in nuclear (N) and cytosolic (C) compartments in DM15 (myoblast) cells **(B-C)** and after 21-mer PNA treatment at two different concentrations. Treatment showed significant reduction in nuclear MBNL1 protein when compared to untreated cells.

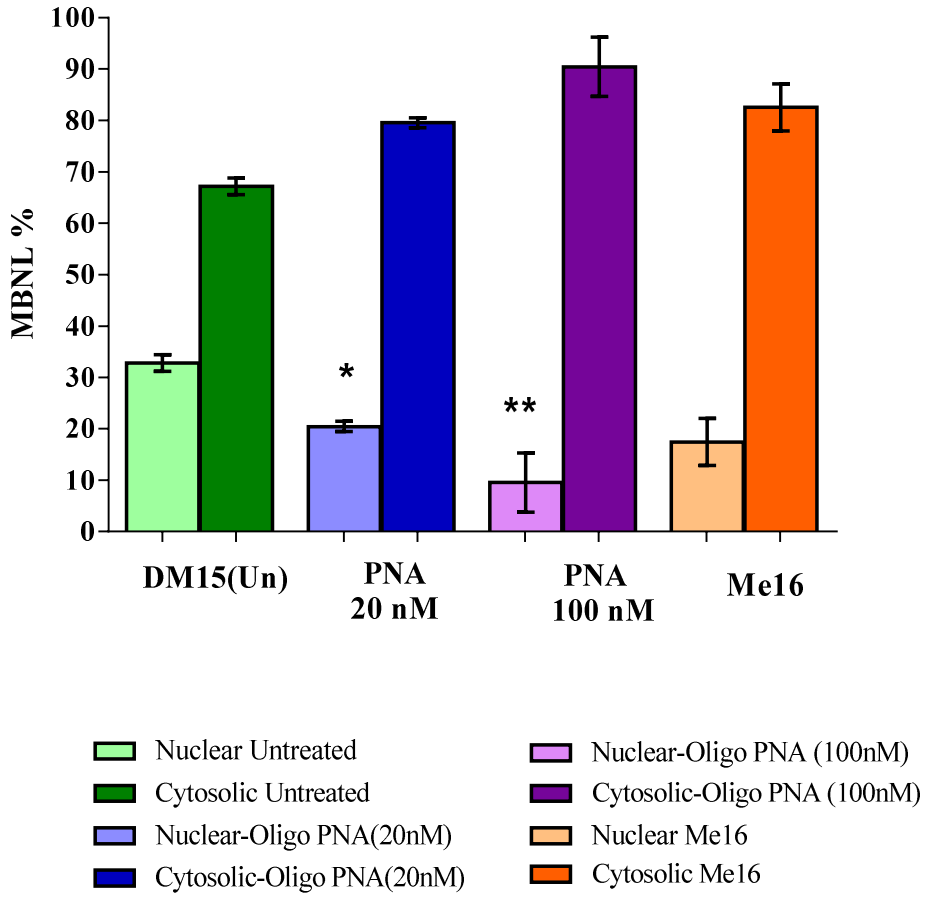

Figure 4.30 Histograms showing the sub-cellular distribution of MBNL1 before and after treatment with PNA Histograms show data compiled from intensity scans of triplicate blots for myoblast cell line DM15, normalized against values for lamin-B and tubulin following treatment with PNA. Me16 is the Non-DM cell line, which served as control cell line. All the statistical comparisons are done to the DM15 untreated sample. * represents a significant difference from the control DMSO (Student's two tailed *t* test; *P<0.05)

4.10 Summary

Tertiary assays were developed and applied in this chapter to validate the positive hits compounds that were highlighted in primary screens. Compounds were subjected to further analysis involving western blotting, to examine the effect of treatment on sub-cellular distribution. The data from the western blot suggests that the compounds chromomycin A3, hypericin, RO 31-8220, gemcitabine, IMOX significantly altered the ratio of nuclear to cytoplasmic MBNL1 compared to that observed in DMSO treated cells with ratios being more similar to those observed in non-DM cells.

Consistent with their effect on RNA foci and the depletion of MBNL1 from the nuclear compartment of DM cells, all the compounds (apart from gemcitabine) also significantly reduced the MBNL (protein) foci from DM1 cells after treatment compared to DMSO treated controls.

Studies were also conducted to down regulate the MBNL1 and MBNL2 in DM cells to test whether MBNL1/2 depletion would result in reduction of the nuclear foci. MBNL1 and MBNL2 double knockdown resulted in a 40% increase of nuclear RNA foci than observed in scrambled siRNA treated cells or untreated cells, though a significant reduction in size was observed in case of MBNL (protein) foci as shown by immunocytochemistry images.

MBNL 1 and MBNL2 down regulation did not result in the release of mutant transcript from the nucleus to the cytoplasm in KB-Telo Myod (DM) cells. However, it had a degradative effect on the mutant DMPK transcript.

Chapter -5: The role of Protein Kinases in DM

5.1 Introduction

Our lab has developed a cell based screening assay that allows us to determine the effect of compounds on RNA nuclear foci. A series of small molecule libraries were screened as part of this primary assay. The kinase inhibitor library used in the primary screening assay gave two compounds (Ro 31-8220 and Hypericin) that were capable of reducing nuclear foci. Both of these compounds are PKC inhibitors. But screening of other PKC inhibitors showed no effect on nuclear RNA foci. An extended screen of kinase inhibitors identified a compound IMOX which could also remove nuclear foci, an inhibitor of PKR, a double stranded RNA-activated kinase. The data provides strong support for the involvement of a kinase in DM pathophysiology, however the target of these compounds still remains elusive.

5.2 Protein kinases in Myotonic Dystrophy

Kinase involvement in the DM has been described previously, with particular interest in PKC. Published data suggests that PKC is activated in the presence of expanded CUG repeat containing RNA (Wang et al., 2009) . PKC activation leads to phosphorylation of CUGBP protein, which extends the half life of the protein leading to its increased levels, which in turns leads to CUGBP dependant splicing misregulation (Kuyumcu-Martinez et al., 2007). Compound R0 31-8220 has also been tested on an inducible DM1 mouse model where it

inhibited PKC α and βII. Inhibition of these isoforms leads to reduction of CUGBP1 hyperphosphorylation and reduced protein levels as reported by Wang and colleagues (2009).

Identification of R0 31-8220 and hypericin as 'positive hits' in the primary screening was encouraging as role of RO 31-8220 has already been described in context of CUGBP protein. Unlike MBNL1, CUGBP1 does not colocalize with RNA nuclear foci (Jiang et al., 2004; Mankodi et al., 2005) so therefore the reduction of nuclear foci in DM patients cells following RO 31-8220 treatment suggests there may be other mechanisms involved like phosphorylation of MBNL1 protein?

The hypothesis that MBNL may be a target of a kinase pathway also predicts that phosphorylation of the protein may play an important role. MBNL1 is a shuttling protein and shuttles between the nucleus and cytoplasm in unaffected cells. MBNL is sequestered in the nuclei of DM cells after binding to the repeat expanded RNA. It could be hypothesised that following inhibition of the kinase via RO 31-8220, the protein becomes unphosphorylated which prevents it from shuttling back to the nucleus and therefore prevents its sequestration by repeat expanded RNA in the nuclear foci. To test this, I decided to perform phosphorylation experiments using phospho-specific antibodies to test whether MBNL1 exists in phosphorylated state and what happens to its phosphorylated state following treatment with the protein kinase inhibitors.

Protein phosphorylation plays a important role in signal transduction in many cells (Hunter, 1995). Many proteins are activated upon phosphorylation, and the phosphorylation state of a protein has frequently been taken as a measure of

its activation state. Protein phosphorylation is a post-translational modification (PTM) of a protein in which a serine, a threonine or a tyrosine residue is phosphorylated by a protein kinase by addition of a phosphate (PO_4^{3-} group). Within a protein, the most common phosphorylation that can occur is on serine residue, followed by threonine. Tyrosine phosphorylation is relatively rare. Several antibodies can be used to detect whether a protein is phosphorylated or unphosphorylated at a particular site. Antibodies that bind to and detect phosphorylation-induced conformational changes in the protein are called phospho-specific antibodies. I have used western blotting and phospho-specific antibodies in immunoprecipitation assays to investigate if MBNL1 protein is phosphorylated and at which residue.

Figure 5.1 shows western blots probed with phospho-serine antibody after performing immunoprecipitation using anti-MBNL1 antibody (MBLa Ab.). The band marked with white star represents MBNL1 phosphorylated band at serine residue.

Figure 5.2 shows western blots probed with phospho-threonine and phospho tyrosine antibodies after performing immunoprecipitation pull down experiment with anti-MBNL1 antibody. There was no evidence for phosphorylation of MBNL1 protein at threonine or tyrosine residues.

These pull down experiments showed that MBNL1 protein is indeed phosphorylated at serine residue but there was no evidence of phosphorylation at threonine or tyrosine residues from these experiments.

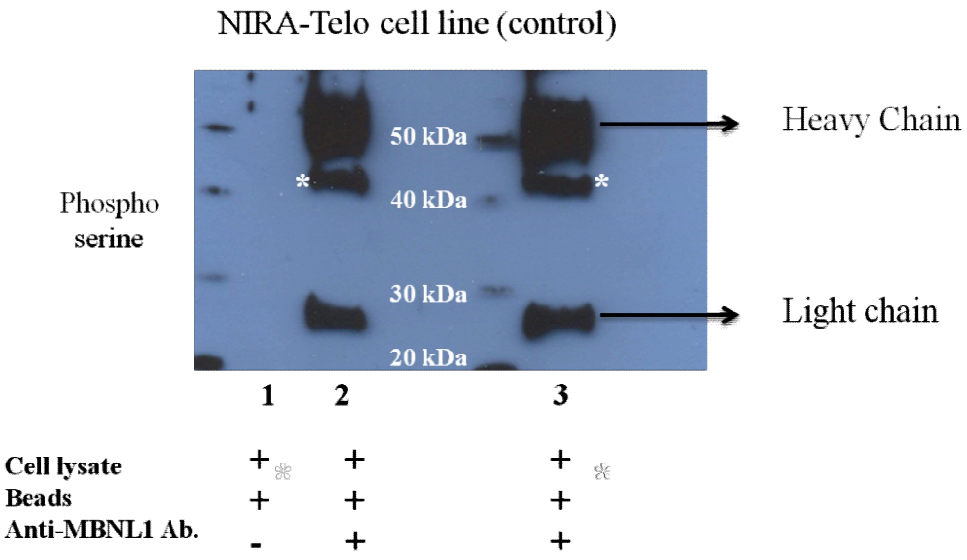

Figure 5.1 Immunoprecipitation experiment using serine phospho-specific antibody. **Lane 1** served as control lane .In **Lane (2, 3)** cell extracts were subjected to pull down using an anti-MBNL1 antibody plus A/G agarose beads and then probed with phospho-serine antibody. MBNL1 phosphorylated band can be seen at 42 kDa (Marked with white stars).

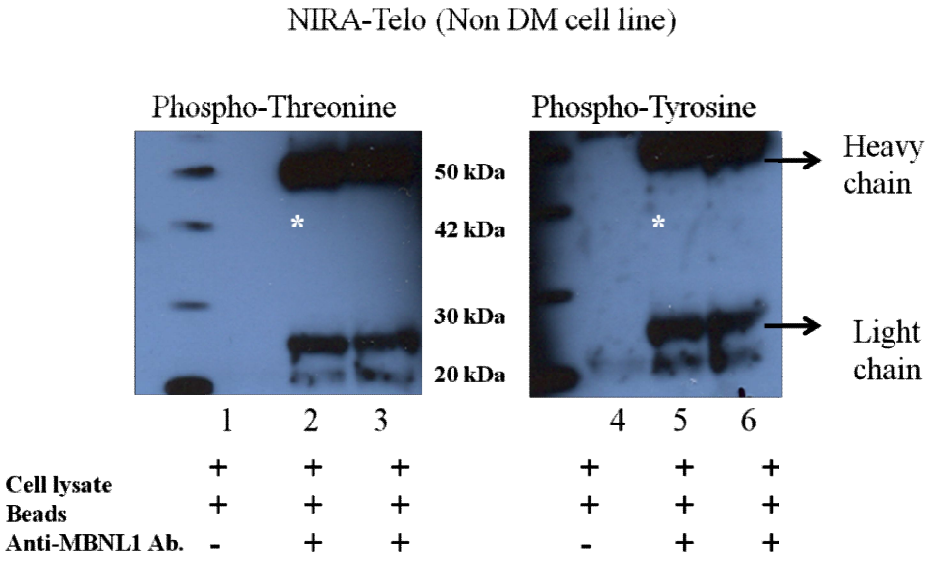

Figure 5.2 Immunoprecipitation experiments using threonine and tyrosine phospho-specific antibodies. **Lane** (**1, 4)** served as controls lane .In **Lane (2, 3)** cell extracts were subjected to pull down using an anti-MBNL1 antibody plus A/G agarose beads and then probed with phospho-threonine antibody. In **Lane (5, 6)** cell extracts were subjected to pull down before probing it with phospho-tyrosine antibody. No evidence of MBNL1 protein phosphorylation at these residues was observed (Marked with white stars).

5.3 MBNL1 phosphorylation studies

A variety of techniques can be used for detecting (or mapping) phosphorylated sites. In the view of findings in section 5.2, I have attempted to map the phosphorylated site (s) in MBNL1 protein using MS (Mass spectrometry) in combination with immuno-precipitation (IP).

5.3. 1 Immunoprecipitation of MBNL1 and Interacting proteins

The protocol for identification of MBNL1 is summarized in Fig 6.7. Proteins were extracted from NIRA-Telo (non-DM fibroblast) cells. Proteins were then quantified using the Bradford method (Bio-Rad). MBNL1 was immunoprecipitated from 5 mg of total proteins, using antibodies bound on magnetic beads according to the Dynal beads protocol (as described in section 2.5.3). Immunoprecipitated proteins were rinsed three times with washing buffer, before boiling for 5mins in LDS buffer. Immunoprecipitated proteins were loaded and resolved on 10% polyacrylamide gel and finally stained with colloidal Coomassie. Band of interest (marked red in Fig.5.3B) was excised and sent for protein identification by Mass spectrometry. The protein bands of interest were trypsin-digested and analysed on MALDI-TOF and MS-MS. The mass spectrometry analysis was carried out by BSRC Mass Spectrometry and Proteomics Facility in University of St Andrews.

Before sending the excised sample for mass spectrometry analysis, I decided to do a validation study on the excised band from the Coomassie stained gel. One of the excised bands (marked yellow in Fig.5.3B) was resolved on 10%

polyacrylamide gel again and probed with anti-MBNL1 antibody to validate the presence of MBNL1 protein in excised samples.

The proteins identified by Mass Spec were ACTB (Actin, cytoplasmic 1, (Beta-Actin)), Actin 11, Synembryn (protein Ric-8), Serine/threonine- protein kinase TEL1 and Actin 1 (Fig.5.4). Muscleblind-like protein 1 (MBNL1) was not identified by mass spectrometry studies and result showed that ACTB (Actin cytoplasmic 1, Beta-Actin) was the major contaminant in the excised band.

The majority of proteins identified in IP-experiment were non-specific binders. Several additional steps were employed like pre-clearing the lysate before IP, adjusting the washing buffer stringency to reduce background or non-specific binding. But none of these steps were able to reduce the non-specific binding or Actin contaminants. So the data described here was inconclusive and additional experiments must be conducted to map the phosphorylated site (s) of MBNL1 protein.

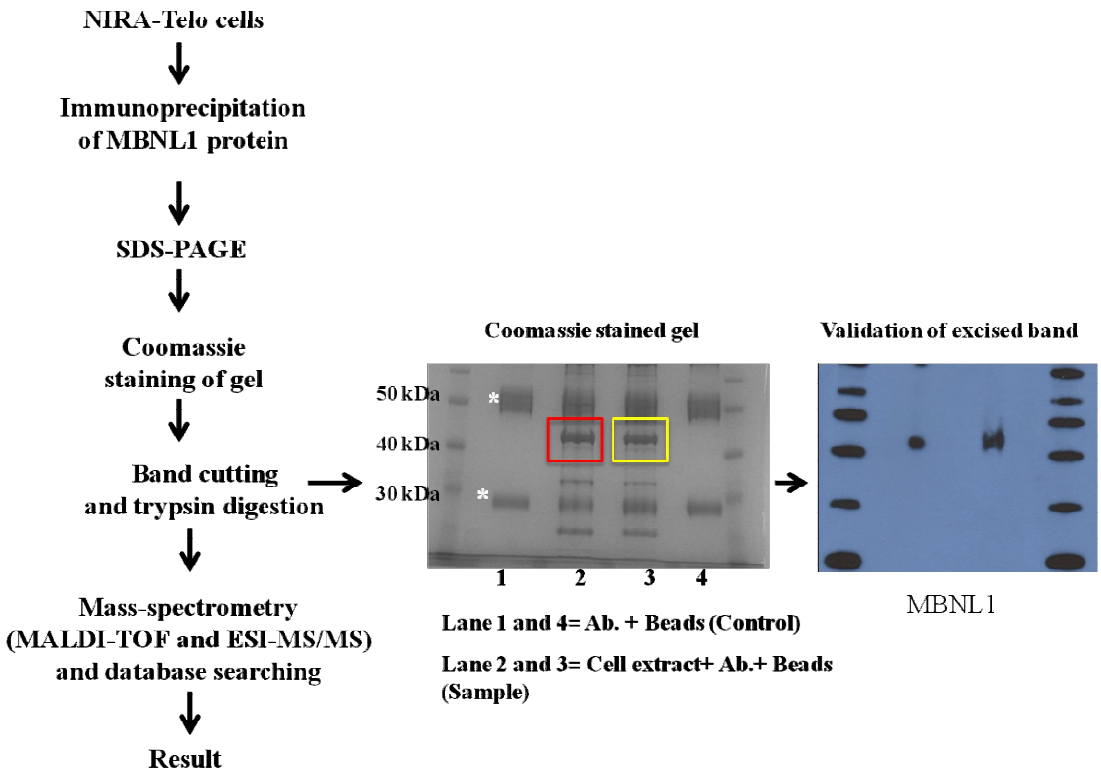

Figure 5.3 Separation of MBNL1 immunoprecipitated protein. (A) Immunoprecipitation-based approach to identify phosphorylated site (s) **(B)** SDS-PAGE gel obtained for MBNL1 immunoprecipitate. Immunoprecipitated protein were separated by 10% polyacrylamide gel and stained with colloidal Coomassie Blue. Band in red box was cut and trypsin-digested for analysis by mass spectrometry and the band in yellow box was cut and validated for MBNL1 protein presence. The positions where IgG (heavy and light chains) were detected are indicated (white *)

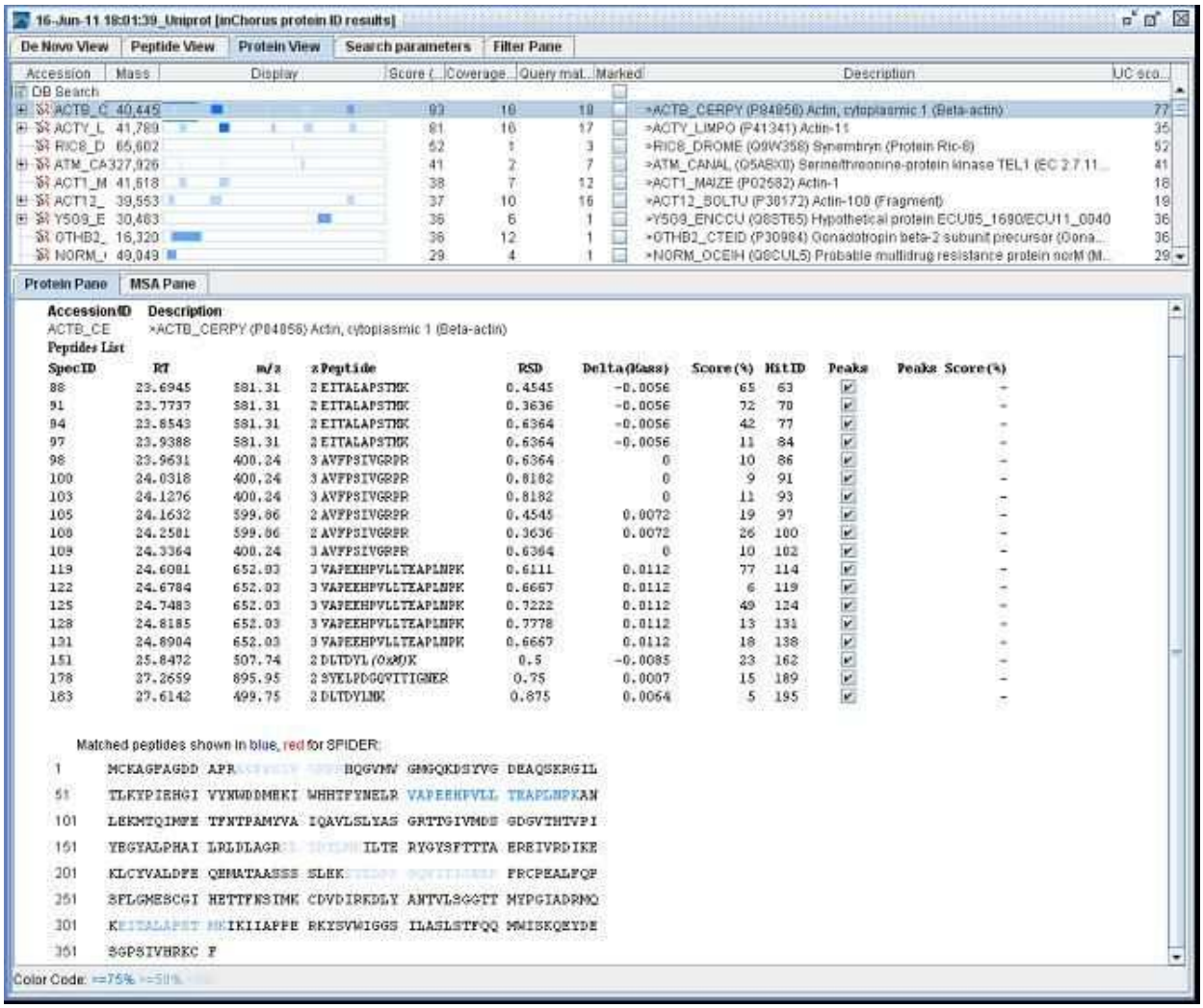

Figure 5.4 Proteins identified by mass spectrometry after the MBNL1 IP. Beta-Actin was identified as the major contaminant in IP because it came up with the highest score (93%) in the result window.

5.4 siRNA knockdown of isoforms of Protein Kinase C (PKC)

5.4.1 Introduction

Although the initial analysis suggested that Ro 31-8220 may not be acting via PKC, this was verified by performing knockdown of the PKC isoforms to ascertain the link between the presence of foci and PKC activity. It would be hypothesised that knockdown of a kinase target by siRNA should also remove or reduce nuclear foci if the kinase is the true target of the inhibitor compounds. SiRNA's targeting the kinase of interest was tested in the nuclear foci assay in DM cell lines (KB-Telo MyoD). Western blotting was also performed to confirm the level of knockdown for various PKC isoforms.

PKC also known as Protein kinase C, is a family of protein kinase enzymes that are involved in controlling the function of various other proteins through the phosphorylation of hydroxyl groups of serine and threonine amino acid residues on these proteins. PKC enzymes are activated by increase in concentration of of diacylglycerol (DAG) or calcium ions (Ca^{2+}). Different isoforms of PKC have been discovered which can be divided into three subfamilies or groups (Mellor and Parker, 1998), based on signals they require for activation: (1) the classical or conventional isoforms α, βI, β II, γ; (2) the novel PKC isoforms ε, θ, δ, μ, η; (3) and the atypical PKC isoforms ζ and λ (Nishizuka, 1995). The conventional isoforms requires Ca2+, DAG, and a phospholipid such as phosphatidylserine for activation. The novel PKC isoforms requires require DAG, but do not require Ca2+ for activation. Thus, classical and novel PKCs isoforms are activated through the same signal

transduction pathway as phospholipase C. But atypical isoforms requires neither DAG nor Ca^{2+} for their activation.

5.4.2 siRNA knockdown of PKC isoforms.

In order to validate PKC as potential therapeutic target for myotonic dystrophy I conducted knockdown screens using siRNA's in KB-Telo MyoD cells corresponding to each of the isoforms of PKC. The isoforms included were PKCα (alpha), PKCβ (beta), PKCγ (gamma), PKCδ (delta) and PKCε (epsilon).

Western blots showed clear reduction in protein levels in case of PKCα, PKCδ and PKCε. There was no evidence of knockdown in case of PKCβ and PKCγ (data not included) which might be due to different expression levels in different organs or cell types. Expression of most of the PKC isoforms is ubiquitous and only some of them are localized to specific tissues. For example, PKC γ has been shown to be specifically expressed in CNS and spinal cord (neuronal tissues), whereas PKCβ is present in pancreatic islet cells, brain and monocytes (Way et al., 2000).

Figure 5.5 and 5.6 shows siRNA mediated down-regulation of PKC alpha, PKC epsilon and PKC delta isoforms. There was a significant reduction in protein level after each knockdown.

Figure 5.7 shows the *In situ* merged images (DAPI+ Cy5) images for all PKC isoforms after siRNA knockdown in KB-Telo MyoD cells. There was no obvious reduction in foci number for any of the PKC isoforms compared to untreated cells.

A.) **B.)**

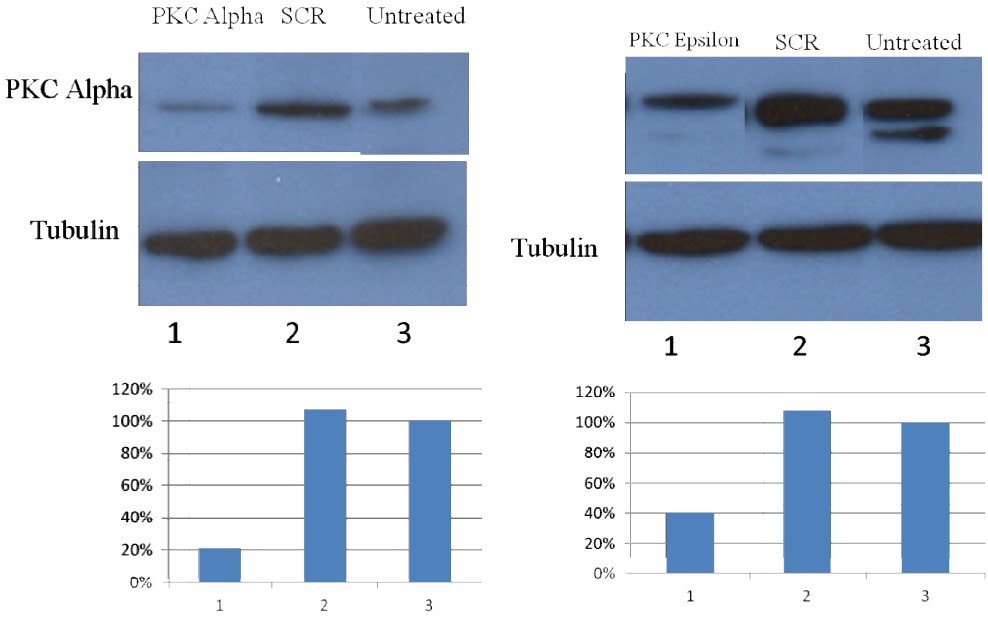

Figure 5.5 siRNA mediated down-regulation of PKC alpha and PKC epsilon isoforms. (A) Western blots showing the knockdown for PKC α **(B)** and PKC ε. Histograms show data compiled from intensity scans of blots normalized against tubulin.

A.)

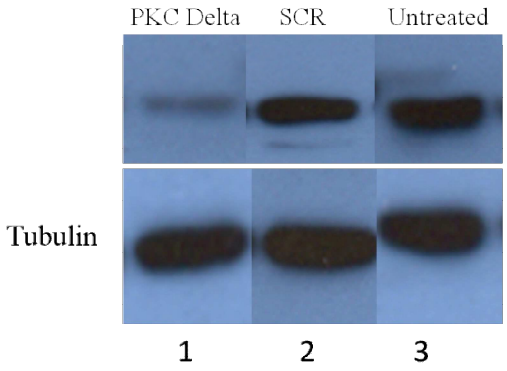

B.)

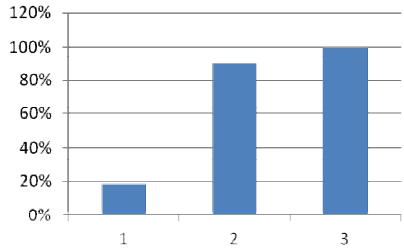

C.)

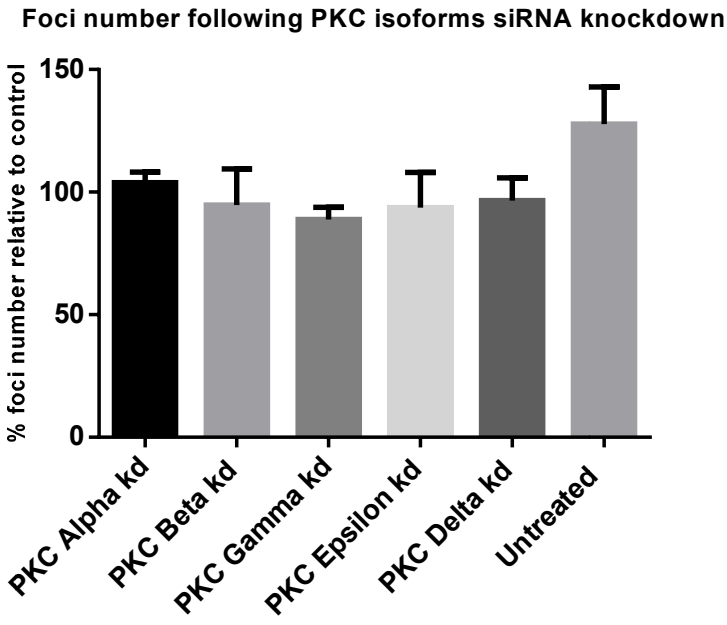

Figure 5.6 (A-B) Western blots showing the knockdown for PKC δ and histogram data compiled from intensity scan of blots **(C)** Histograms data from *In situ* hybridisation images for all PKC isoforms showing there was no obvious effect of knockdown on RNA foci number reduction when compared to control (untreated) cells.

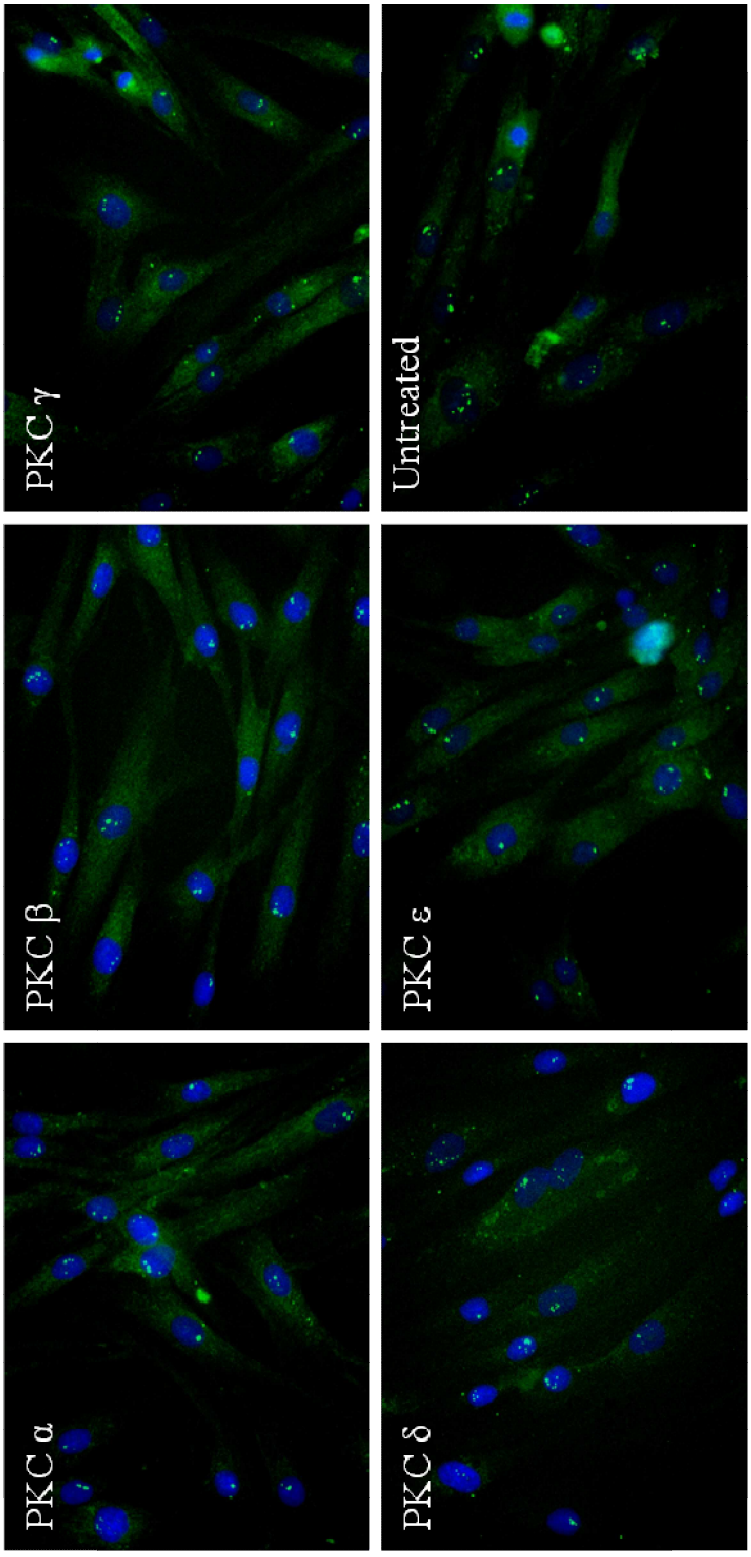

Figure 5.7 *In situ* images for all PKC isoforms after siRNA knockdown in KB-Telo MyoD cells. There was no obvious reduction in foci number for any of the PKC isoforms compared to untreated cells.

5.5 IMOX

The other compound that was screened as part of primary screen was IMOX (imidazolo-oxindole), which is an inhibitor of PKR (EIF2AK2, eukaryotic translation initiation factor 2-alpha kinase 2) a double stranded RNA-activated kinase. IMOX was able to eliminate foci and also resulted in redistribution of MBNL1 protein after treatment in western blots. PKR is activated in response to double-stranded RNA (dsRNA), the synthesis of which is caused virally. It been shown that PKR can also be activated in presence of expanded CUG repeat RNA's which form hairpins in DM (Tian et al., 2000). Once activated PKR autophosphorylates, which then leads to the phosphorylation of the α-subunit of eukaryotic inhibition factor 2 (eIF2α). This further inhibits cellular mRNA translation and protein synthesis.

So to establish PKR as a target for DM therapy, I conducted knockdown screen using siRNA corresponding to PKR to validate if it is the true target. The siRNA knockdown for PKR did not produce a significant reduction in nuclear foci in DM cells (Fig. 5.8C) suggesting that PKR cannot be used as a potential drug for DM treatment.

A.)

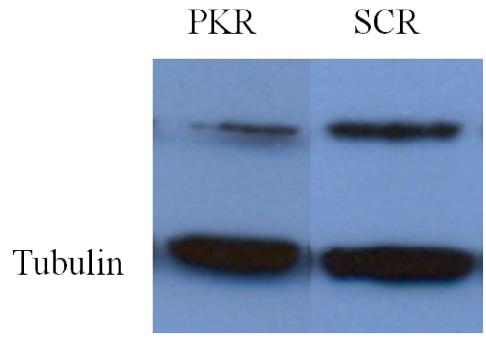

B.)

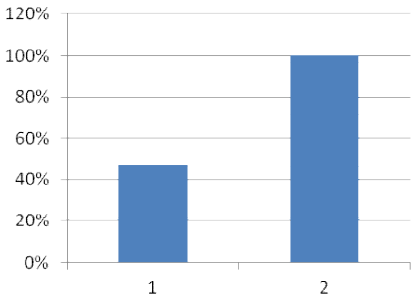

C.)

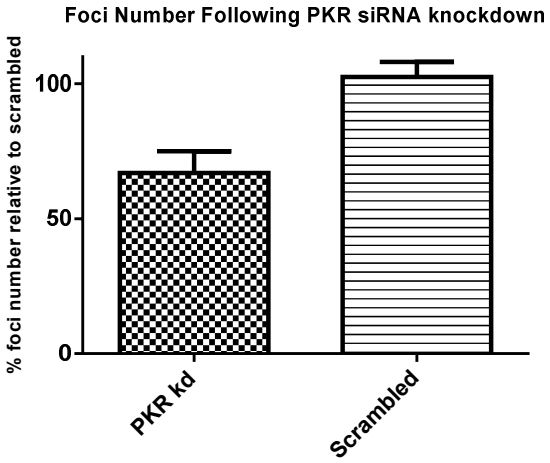

Figure 5.8 siRNA mediated down-regulation of PKR. (A) Western blots showing the knockdown for PKR **(B)**. Histograms show data compiled from intensity scans of knockdown blots normalized against tubulin **(C)** Histograms data for PKR isoforms showing there was no obvious effect of knockdown on RNA foci number reduction when compared to control (untreated) cells.

5.6 Summary

MBNL1 protein was found to be phosphorylated on serine residues following western blotting with phospho-specific antibodies in combination with immunoprecipitation assays. No phosphorylation of MBNL1 threonine or tyrosine residues were found after probing with phospho-specific threonine or tyrosine antibodies.

In a parallel line of investigation, mass spectrometry in combination with immunoprecipitation assays was used to map the phosphorylated sites of MBNL1 protein which resulted in the identification of actin as the major contaminant in mass spectrometry analysis.

Finally, the knockdown of all PKC isoforms and PKR isoform showed no obvious effect on RNA foci number reduction which suggested that they might not be the true target and cannot be used as potential drug targets for DM treatment.

Chapter 6: Discussion and Conclusions

One of the earliest events in DM pathophysiology occurs when mutant expanded RNAs are transcribed and accumulate in the nuclei of DM cells, where they sequester MBNL proteins, forming spots or foci. Our own lab has developed a cell based assay using an *in situ* hybridisation protocol to screen libraries of potentially useful compounds or small molecules which could eliminate nuclear foci. Four libraries were screened as part of the primary screen (Ketley et al., 2013).

Compounds chromomycin A3, RO 31-8220, gemcitabine, IMOX and hypericin reduced RNA nuclear foci in the primary and secondary assays. In order to assess whether these compounds affected other aspects of DM pathophysiology, I subjected them to additional assays like MBNL1 sub cellular distribution and immunocytochemistry. Western blots were used to examine the sub cellular distribution of MBNL1 protein in nuclear and cytosolic fractions of DM cells before and after treatment with compounds, identified during the screen.

Treatment with all the compounds produced a significant reduction in the proportion of nuclear MBNL1 compared to DMSO treated cells in DM fibroblast and myoblasts. The MBNL1 protein distribution in treated KB-Telo MyoD cells (DM1 fibroblasts) resembled that of non-DM cells with a much higher percentage in the cytoplasm (~80%) and only ~20% in the nuclear fraction. Treatment of DM15 myoblast cells (~3000 CTG repeats) with these

compounds also produced a redistribution of MBNL protein, with a significant increase in the cytoplasm and a striking reduction in the nucleus compartment.

Nuclear foci consist of mutant repeat expansion RNA and muscleblind-like proteins and most likely other proteins that are yet to be identified. It was hypothesized that if compounds can restore the MBNL1 protein distribution (as suggested by western blot data), they might be able to reduce or remove the MBNL foci (MBNL1 protein in foci). Consistent with the observed reduction of MBNL1 protein from nuclear compartment of DM cells after treatment. The number of MBNL foci was also reduced significantly as observed in immunocytochemistry images.

One possible explanation is that these compounds are either able to disrupt the MBNL1 and repeat expansion RNA interaction in the nuclear foci via a physical interaction (compounds outcompeting MBNL1 to bind to the repeat expansion RNA) or by a functional response in which MBNL1 protein is modified by a kinase targeted by the inhibitors (as might be in case of Ro 31-8220, IMOX or Hypericin). It is possible that the nuclear/cytoplasmic localization of MBNL1 protein is determined by a phosphorylation event which is modified after the treatment with RO 31-8220. To assess this possibility, phosphorylation studies were conducted to see whether MBNL1 exists in a phosphorylated state. IP Experiments were performed in combination with phospho-specific antibodies. The data pointed towards a phosphorylation event taking place. The MBNL1 protein was phosphorylated at serine residue as observed in the blots probed with serine phospho-specific antibodies. There was no evidence of phosphorylation at threonine or tyrosine

residues from these experiments. In view of these findings, further experiments were conducted to map the phosphorylated site (s) in MBNL1 protein using MS (Mass spectrometry) in combination with immuno-precipitation (IP). Actin came up with the highest score in the result window after mass spectrometry analysis. It appeared to mask the levels of Muscleblind-like protein 1 such that it was either difficult to identify low levels of MBNL1 or the sample somehow got contaminated with actin proteins. Despite several attempts it was not possible to overcome technical problems. Further enrichment experiments need to be done to resolve this contamination issue. Thus it was difficult to map the phosphorylated site and the data described here is difficult to interpret.

The underlying mechanism by which these compounds act on foci is not known and requires further investigation. Two of the compounds identified in the primary screens; gemcitabine and hypericin showed toxic profiles that matched the disappearance of RNA foci, whereas Ro 31-8220, IMOX and chromomycin A3 reduced foci numbers at concentrations that did not fully match the toxicity effect (Figure 1.9). Thus, Ro 31-8220, IMOX and chromomycin A3 were further studied.

Chromomycin A3 is a glycosidic antineoplastic antibiotic isolated from the bacterium *Streptomyces griseus* that inhibits the DNA-dependant RNA polymerase reaction by reversibly binding to guanine-cytosine (G-C) base pairs in the minor groove of DNA to inhibit RNA synthesis (Kaziro and Kamiyama, 1965). It has been shown that chromomycin A3 interacts with GC rich regions of duplex DNA (Berman et al., 1985; Chakrabarti et al., 2000), thus it is possible that it also interacts with stem-loop structures present in expanded repeat RNAs. This binding interaction could result in overall disruption of the

hairpin structure, thus releasing the MBNL protein from the foci and restoring the MBNL1 protein distribution (western blots data).

The other compound that was screened as part of a phosphatase and kinase library was Ro- 318220, which is a known PKC inhibitor. Although it was clear that Ro 31-8220 affected several aspects of DM pathophysiology, the actual mechanism of its activity on foci is less clear. The preliminary structural evidence suggests that Ro 31-8220 may not be acting via PKC. The phosphatase and kinase library used in the primary screening contained many other kinase inhibitors, some of them were also PKC inhibitors. But there was an obvious difference in terms of effect on the nuclear foci, despite being equally potent PKC inhibitors as Ro 31-8220 (Ketley et al., 2013). GF 109203X, a highly potent PKC inhibitor had very limited effect on the nuclear foci (RNA foci) and several other downstream assays like MBNL1 protein distribution and on MBNL1 protein foci essay. Structurally GF 109203X and Ro 31-8220 are very similar to each other, so a similar effect would be expected. But kinase inhibitors like Ro 31-8220 are notoriously promiscuous and are capable of inhibiting multiple other kinases with the same potency as PKC (Alessi, 1997). This suggests that another kinase may be involved and specifically may be acting on MBNL in the foci. Indeed there has been evidence of additional kinase involvement in response to repeat expansion RNA in literature (Hernandez-Hernandez et al., 2006; Jin et al., 2009; Timchenko et al., 2001) .

Nuclear foci comprise of repeat expansion RNA bound to muscleblind-like proteins and possibly other proteins which are still not known. To test the effect of the MBNL double knockdown on the RNA foci and MBNL (protein)

foci, *in situ* hybridization and immunocytochemistry studies were performed. In a parallel line of investigation to determine the effect of MBNL double knockdown on the mutant allele, a *BpmI* polymorphism assay was also employed, which allowed me to distinguish between the mutant and wild-type transcripts. MBNL1 and MBNL2 down-regulation resulted in an increase in the RNA nuclear foci number which would suggest that MBNL might play an important role in maintaining the DM1 focus integrity. Thus, depletion of MBNL from the cell causes the repeat expansions transcripts to disperse, leading to an increase in number of (smaller) RNA nuclear foci. This was further validated from histogram data compiled from the average intensity and average area of RNA foci after MBNL double knockdown. The data showed that the RNA foci were smaller in size and were of lesser intensity as compared to RNA foci seen in untreated cells. However, the result obtained from my study deviates from that reported by Dansithong and colleagues (2005) who suggested that depletion of MBNL1 alone was sufficient to reduce the number of RNA foci by ~70 %. The difference in results may be due to differences in cell lines used in our experiment compared with those reported by Dansithong *et al (*2005) in which DM myoblasts were used instead of DM fibroblasts.

Several RNA binding proteins and transcription factors like Sp1, STAT3, STAT1, and RARγ have been reported in past to interact with expanded CTG repeat sequences in vivo (Ebralidze et al., 2004). Thus, one possible explanation for the presence of smaller RNA foci after MBNL double knockdown may be due to some other proteins which are still bound to the mutant transcripts and therefore keeping it trapped in the nucleus.

The data from the chapter 4 shows that following MBNL double knockdown, the DMPK mutant transcript are still present in the nuclear fraction and there was no sign of liberation of the mutant transcript to the cytoplasm. This may be due to some intrinsic structural properties of the repeats. However, the MBNL1 and MBNL2 down-regulation resulted in a reduction in the relative proportion of the mutant transcript in the nucleus of KB-Telo MyoD cells compared to scrambled (SCR) or untreated cells. It may be possible that depletion of MBNL from the cell renders the mutant RNA transcripts more prone to degradation.

Thus, in summary, I have reported that the compounds chromomycin A3, gemcitabine, IMOX, RO 31-8220 and hypericin which were highlighted as part of primary screening resulted in a very significant shift of the ratio of nuclear to cytoplasmic MBNL1 in DM fibroblast and myoblast cells after treatment, consistent with the observed reduction of MBNL protein in foci as seen in immunocytochemistry studies. These compounds may provide the starting point for future drug development studies for DM therapy. Also the identification of RO 31-8220 in primary screen begs the question if there is a link between the roles of MBNL1 and CUGBP in DM.

6.1 Future work and recommendations

At the time of writing this report, it was not possible to map the phosphorylated site (s) of MBNL1 protein. Additional experiments such as 2-D gels need to be incorporated after conducting IP pull down experiments (using MBNL1 antibody) to separate the MBNL1 protein and contaminants (mainly Actin)

according to their iso-electric point (pH). This would allow us to excise spot/band containing only MBNL1 protein and then analyse it on MALDI-TOF and MS-MS for further mapping of the phosphorylated residue.

Also, we have reported a medium throughput assay using in situ hybridisation and high content imaging to identify compounds that may provide the starting point for future drug development studies for DM therapy. Target identification represents an early stage in the drug development pathway but is critical to establish a pharmaceutical collaboration to be able to conduct structure activity relationship analysis against *in vitro* target selectivity. These compounds are fairly toxic in our cell based assays. Thus, it is probably not suitable for human administration. Further work is required to conduct a medicinal chemistry programme to develop a suitable drug treatment for DM. In addition to the medicinal chemistry, ADME and in vivo PK of lead compounds will be outsourced via a pharmaceutical company. Continued medicinal chemistry-driven optimization of lead series compounds and *in vivo* testing in a mouse model of DM will be conducted in collaboration with colleagues in Paris. Following compound treatment in the DM mouse model we will measure specific strength measures like grip-test, treadmill, ankle dorsiflexion extension. Restoring these measures will be important if a drug is to offer potential therapeutic benefit to patients

7. References

Alessi, D.R. (1997). The protein kinase C inhibitors Ro 318220 and GF 109203X are equally potent inhibitors of MAPKAP kinase-1beta (Rsk-2) and p70 S6 kinase. FEBS letters *402*, 121-123.

Alwazzan, M., Hamshere, M.G., Lennon, G.G., and Brook, J.D. (1998). Six transcripts map within 200 kilobases of the myotonic dystrophy expanded repeat. Mammalian genome : official journal of the International Mammalian Genome Society *9*, 485-487.

Alwazzan, M., Newman, E., Hamshere, M.G., and Brook, J.D. (1999). Myotonic dystrophy is associated with a reduced level of RNA from the DMWD allele adjacent to the expanded repeat. Hum Mol Genet *8*, 1491-1497.

Amack, J.D., Paguio, A.P., and Mahadevan, M.S. (1999). Cis and trans effects of the myotonic dystrophy (DM) mutation in a cell culture model. Hum Mol Genet *8*, 1975-1984.

Arambula, J.F., Ramisetty, S.R., Baranger, A.M., and Zimmerman, S.C. (2009). A simple ligand that selectively targets CUG trinucleotide repeats and inhibits MBNL protein binding. Proc Natl Acad Sci U S A *106*, 16068-16073.

Begemann, G., Paricio, N., Artero, R., Kiss, I., Perez-Alonso, M., and Mlodzik, M. (1997). muscleblind, a gene required for photoreceptor differentiation in Drosophila, encodes novel nuclear Cys3His-type zinc-finger-containing proteins. Development *124*, 4321-4331.

Berman, E., Brown, S.C., James, T.L., and Shafer, R.H. (1985). NMR studies of chromomycin A3 interaction with DNA. Biochemistry *24*, 6887-6893.

Boucher, C.A., King, S.K., Carey, N., Krahe, R., Winchester, C.L., Rahman, S., Creavin, T., Meghji, P., Bailey, M.E., Chartier, F.L*., et al.* (1995). A novel homeodomain-encoding gene is associated with a large CpG island interrupted by the myotonic dystrophy unstable (CTG)n repeat. Hum Mol Genet *4*, 1919-1925.

Broda, M., Kierzek, E., Gdaniec, Z., Kulinski, T., and Kierzek, R. (2005). Thermodynamic stability of RNA structures formed by CNG trinucleotide repeats. Implication for prediction of RNA structure. Biochemistry *44*, 10873-10882.

Brook, J.D., McCurrach, M.E., Harley, H.G., Buckler, A.J., Church, D., Aburatani, H., Hunter, K., Stanton, V.P., Thirion, J.P., Hudson, T*., et al.* (1992). Molecular basis of myotonic dystrophy: expansion of a trinucleotide (CTG) repeat at the 3' end of a transcript encoding a protein kinase family member. Cell *69*, 385.

Buj-Bello, A., Furling, D., Tronchere, H., Laporte, J., Lerouge, T., Butler-Browne, G.S., and Mandel, J.L. (2002). Muscle-specific alternative splicing of myotubularin-related 1 gene is impaired in DM1 muscle cells. Hum Mol Genet *11*, 2297-2307.

Carango, P., Noble, J.E., Marks, H.G., and Funanage, V.L. (1993). Absence of myotonic dystrophy protein kinase (DMPK) mRNA as a result of a triplet repeat expansion in myotonic dystrophy. Genomics *18*, 340-348.

Chakrabarti, S., Bhattacharyya, D., and Dasgupta, D. (2000). Structural basis of DNA recognition by anticancer antibiotics, chromomycin A(3), and

mithramycin: roles of minor groove width and ligand flexibility. Biopolymers *56*, 85-95.
Chamberlain, C.M., and Ranum, L.P. (2012). Mouse model of muscleblind-like 1 overexpression: skeletal muscle effects and therapeutic promise. Hum Mol Genet *21*, 4645-4654.
Charlet, B.N., Savkur, R.S., Singh, G., Philips, A.V., Grice, E.A., and Cooper, T.A. (2002). Loss of the muscle-specific chloride channel in type 1 myotonic dystrophy due to misregulated alternative splicing. Mol Cell *10*, 45-53.
Colleran, J.A., Hawley, R.J., Pinnow, E.E., Kokkinos, P.F., and Fletcher, R.D. (1997). Value of the electrocardiogram in determining cardiac events and mortality in myotonic dystrophy. Am J Cardiol *80*, 1494-1497.
Cooper, T.A., Wan, L., and Dreyfuss, G. (2009). RNA and disease. Cell *136*, 777-793.
Dansithong, W., Paul, S., Comai, L., and Reddy, S. (2005). MBNL1 is the primary determinant of focus formation and aberrant insulin receptor splicing in DM1. J Biol Chem *280*, 5773-5780.
Davis, B.M., McCurrach, M.E., Taneja, K.L., Singer, R.H., and Housman, D.E. (1997). Expansion of a CUG trinucleotide repeat in the 3' untranslated region of myotonic dystrophy protein kinase transcripts results in nuclear retention of transcripts. Proc Natl Acad Sci U S A *94*, 7388-7393.
Day, J.W., Ricker, K., Jacobsen, J.F., Rasmussen, L.J., Dick, K.A., Kress, W., Schneider, C., Koch, M.C., Beilman, G.J., Harrison, A.R*., et al.* (2003). Myotonic dystrophy type 2: molecular, diagnostic and clinical spectrum. Neurology *60*, 657-664.
Day, J.W., Roelofs, R., Leroy, B., Pech, I., Benzow, K., and Ranum, L.P. (1999). Clinical and genetic characteristics of a five-generation family with a novel form of myotonic dystrophy (DM2). Neuromuscul Disord *9*, 19-27.
de Die-Smulders, C.E., Howeler, C.J., Thijs, C., Mirandolle, J.F., Anten, H.B., Smeets, H.J., Chandler, K.E., and Geraedts, J.P. (1998). Age and causes of death in adult-onset myotonic dystrophy. Brain : a journal of neurology *121 (Pt 8)*, 1557-1563.
Dutzler, R., Campbell, E.B., Cadene, M., Chait, B.T., and MacKinnon, R. (2002). X-ray structure of a ClC chloride channel at 3.0 A reveals the molecular basis of anion selectivity. Nature *415*, 287-294.
Ebralidze, A., Wang, Y., Petkova, V., Ebralidse, K., and Junghans, R.P. (2004). RNA leaching of transcription factors disrupts transcription in myotonic dystrophy. Science *303*, 383-387.
Fardaei, M., Larkin, K., Brook, J.D., and Hamshere, M.G. (2001). In vivo co-localisation of MBNL protein with DMPK expanded-repeat transcripts. Nucleic Acids Res *29*, 2766-2771.
Fardaei, M., Rogers, M.T., Thorpe, H.M., Larkin, K., Hamshere, M.G., Harper, P.S., and Brook, J.D. (2002). Three proteins, MBNL, MBLL and MBXL, co-localize in vivo with nuclear foci of expanded-repeat transcripts in DM1 and DM2 cells. Hum Mol Genet *11*, 805-814.
Fu, Y.H., Pizzuti, A., Fenwick, R.G., Jr., King, J., Rajnarayan, S., Dunne, P.W., Dubel, J., Nasser, G.A., Ashizawa, T., de Jong, P*., et al.* (1992). An unstable triplet repeat in a gene related to myotonic muscular dystrophy. Science *255*, 1256-1258.

Futatsugi, A., Kuwajima, G., and Mikoshiba, K. (1995). Tissue-specific and developmentally regulated alternative splicing in mouse skeletal muscle ryanodine receptor mRNA. The Biochemical journal *305 (Pt 2)*, 373-378.
Gareiss, P.C., Sobczak, K., McNaughton, B.R., Palde, P.B., Thornton, C.A., and Miller, B.L. (2008). Dynamic combinatorial selection of molecules capable of inhibiting the (CUG) repeat RNA-MBNL1 interaction in vitro: discovery of lead compounds targeting myotonic dystrophy (DM1). Journal of the American Chemical Society *130*, 16254-16261.
Grunnet, M., Jespersen, T., Colding-Jorgensen, E., Schwartz, M., Klaerke, D.A., Vissing, J., Olesen, S.P., and Duno, M. (2003). Characterization of two new dominant ClC-1 channel mutations associated with myotonia. Muscle & nerve *28*, 722-732.
Gutmann, L., and Phillips, L.H., 2nd (1991). Myotonia congenita. Seminars in neurology *11*, 244-248.
Hamshere, M.G., Newman, E.E., Alwazzan, M., Athwal, B.S., and Brook, J.D. (1997). Transcriptional abnormality in myotonic dystrophy affects DMPK but not neighboring genes. Proc Natl Acad Sci U S A *94*, 7394-7399.
Harper, P.S., Rivas, M.L., Bias, W.B., Hutchinson, J.R., Dyken, P.R., and McKusick, V.A. (1972). Genetic linkage confirmed between the locus for myotonic dystrophy and the ABH-secretion and Lutheran blood group loci. Am J Hum Genet *24*, 310-316.
Hernandez-Hernandez, O., Bermudez-de-Leon, M., Gomez, P., Velazquez-Bernardino, P., Garcia-Sierra, F., and Cisneros, B. (2006). Myotonic dystrophy expanded CUG repeats disturb the expression and phosphorylation of tau in PC12 cells. Journal of neuroscience research *84*, 841-851.
Ho, T.H., Bundman, D., Armstrong, D.L., and Cooper, T.A. (2005a). Transgenic mice expressing CUG-BP1 reproduce splicing mis-regulation observed in myotonic dystrophy. Hum Mol Genet *14*, 1539-1547.
Ho, T.H., Charlet, B.N., Poulos, M.G., Singh, G., Swanson, M.S., and Cooper, T.A. (2004). Muscleblind proteins regulate alternative splicing. EMBO J *23*, 3103-3112.
Ho, T.H., Savkur, R.S., Poulos, M.G., Mancini, M.A., Swanson, M.S., and Cooper, T.A. (2005b). Colocalization of muscleblind with RNA foci is separable from mis-regulation of alternative splicing in myotonic dystrophy. Journal of cell science *118*, 2923-2933.
Hofmann-Radvanyi, H., Lavedan, C., Rabes, J.P., Savoy, D., Duros, C., Johnson, K., and Junien, C. (1993). Myotonic dystrophy: absence of CTG enlarged transcript in congenital forms, and low expression of the normal allele. Hum Mol Genet *2*, 1263-1266.
Holt, I., Jacquemin, V., Fardaei, M., Sewry, C.A., Butler-Browne, G.S., Furling, D., Brook, J.D., and Morris, G.E. (2009). Muscleblind-like proteins: similarities and differences in normal and myotonic dystrophy muscle. Am J Pathol *174*, 216-227.
Hund, E., Jansen, O., Koch, M.C., Ricker, K., Fogel, W., Niedermaier, N., Otto, M., Kuhn, E., and Meinck, H.M. (1997). Proximal myotonic myopathy with MRI white matter abnormalities of the brain. Neurology *48*, 33-37.
Hunter, T. (1995). Protein kinases and phosphatases: the yin and yang of protein phosphorylation and signaling. Cell *80*, 225-236.
Jiang, H., Mankodi, A., Swanson, M.S., Moxley, R.T., and Thornton, C.A. (2004). Myotonic dystrophy type 1 is associated with nuclear foci of mutant

RNA, sequestration of muscleblind proteins and deregulated alternative splicing in neurons. Hum Mol Genet *13*, 3079-3088.
Jin, J., Wang, G.L., Salisbury, E., Timchenko, L., and Timchenko, N.A. (2009). GSK3beta-cyclin D3-CUGBP1-eIF2 pathway in aging and in myotonic dystrophy. Cell cycle *8*, 2356-2359.
Kamisago, M., Sharma, S.D., DePalma, S.R., Solomon, S., Sharma, P., McDonough, B., Smoot, L., Mullen, M.P., Woolf, P.K., Wigle, E.D*., et al.* (2000). Mutations in sarcomere protein genes as a cause of dilated cardiomyopathy. The New England journal of medicine *343*, 1688-1696.
Kanadia, R.N., Johnstone, K.A., Mankodi, A., Lungu, C., Thornton, C.A., Esson, D., Timmers, A.M., Hauswirth, W.W., and Swanson, M.S. (2003). A muscleblind knockout model for myotonic dystrophy. Science *302*, 1978-1980.
Kanadia, R.N., Shin, J., Yuan, Y., Beattie, S.G., Wheeler, T.M., Thornton, C.A., and Swanson, M.S. (2006). Reversal of RNA missplicing and myotonia after muscleblind overexpression in a mouse poly(CUG) model for myotonic dystrophy. Proc Natl Acad Sci U S A *103*, 11748-11753.
Kaziro, Y., and Kamiyama, M. (1965). Inhibition of Rna Polymerase Reaction by Chromomycin A3. Biochemical and biophysical research communications *19*, 433-437.
Ketley, A., Chen, C.Z., Li, X., Arya, S., Robinson, T.E., Granados-Riveron, J., Udosen, I., Morris, G.E., Holt, I., Furling, D*., et al.* (2013). High content screening identifies small molecules that remove nuclear foci, affect MBNL distribution and CELF1 protein levels via a PKC independent pathway in Myotonic Dystrophy cell lines. Hum Mol Genet.
Kimura, T., Nakamori, M., Lueck, J.D., Pouliquin, P., Aoike, F., Fujimura, H., Dirksen, R.T., Takahashi, M.P., Dulhunty, A.F., and Sakoda, S. (2005). Altered mRNA splicing of the skeletal muscle ryanodine receptor and sarcoplasmic/endoplasmic reticulum Ca2+-ATPase in myotonic dystrophy type 1. Hum Mol Genet *14*, 2189-2200.
Kiuchi, A., Otsuka, N., Namba, Y., Nakano, I., and Tomonaga, M. (1991). Presenile appearance of abundant Alzheimer's neurofibrillary tangles without senile plaques in the brain in myotonic dystrophy. Acta neuropathologica *82*, 1-5.
Klesert, T.R., Cho, D.H., Clark, J.I., Maylie, J., Adelman, J., Snider, L., Yuen, E.C., Soriano, P., and Tapscott, S.J. (2000). Mice deficient in Six5 develop cataracts: implications for myotonic dystrophy. Nat Genet *25*, 105-109.
Klesert, T.R., Otten, A.D., Bird, T.D., and Tapscott, S.J. (1997). Trinucleotide repeat expansion at the myotonic dystrophy locus reduces expression of DMAHP. Nat Genet *16*, 402-406.
Kuyumcu-Martinez, N.M., Wang, G.S., and Cooper, T.A. (2007). Increased steady-state levels of CUGBP1 in myotonic dystrophy 1 are due to PKC-mediated hyperphosphorylation. Mol Cell *28*, 68-78.
Ladd, A.L., and Pliam, N.B. (2001). The role of bone graft and alternatives in unstable distal radius fracture treatment. The Orthopedic clinics of North America *32*, 337-351, ix.
Ladd, A.N., Charlet, N., and Cooper, T.A. (2001). The CELF family of RNA binding proteins is implicated in cell-specific and developmentally regulated alternative splicing. Mol Cell Biol *21*, 1285-1296.
Ladd, A.N., Nguyen, N.H., Malhotra, K., and Cooper, T.A. (2004). CELF6, a member of the CELF family of RNA-binding proteins, regulates muscle-

specific splicing enhancer-dependent alternative splicing. J Biol Chem *279*, 17756-17764.
Lazarus, A., Varin, J., Ounnoughene, Z., Radvanyi, H., Junien, C., Coste, J., Laforet, P., Eymard, B., Becane, H.M., Weber, S.*, et al.* (1999). Relationships among electrophysiological findings and clinical status, heart function, and extent of DNA mutation in myotonic dystrophy. Circulation *99*, 1041-1046.
Leroy, O., Wang, J., Maurage, C.A., Parent, M., Cooper, T., Buee, L., Sergeant, N., Andreadis, A., and Caillet-Boudin, M.L. (2006). Brain-specific change in alternative splicing of Tau exon 6 in myotonic dystrophy type 1. Biochim Biophys Acta *1762*, 460-467.
Lin, X., Miller, J.W., Mankodi, A., Kanadia, R.N., Yuan, Y., Moxley, R.T., Swanson, M.S., and Thornton, C.A. (2006). Failure of MBNL1-dependent post-natal splicing transitions in myotonic dystrophy. Hum Mol Genet *15*, 2087-2097.
Liquori, C.L., Ikeda, Y., Weatherspoon, M., Ricker, K., Schoser, B.G., Dalton, J.C., Day, J.W., and Ranum, L.P. (2003). Myotonic dystrophy type 2: human founder haplotype and evolutionary conservation of the repeat tract. Am J Hum Genet *73*, 849-862.
Liquori, C.L., Ricker, K., Moseley, M.L., Jacobsen, J.F., Kress, W., Naylor, S.L., Day, J.W., and Ranum, L.P. (2001). Myotonic dystrophy type 2 caused by a CCTG expansion in intron 1 of ZNF9. Science *293*, 864-867.
Lu, X., Timchenko, N.A., and Timchenko, L.T. (1999). Cardiac elav-type RNA-binding protein (ETR-3) binds to RNA CUG repeats expanded in myotonic dystrophy. Hum Mol Genet *8*, 53-60.
Lytton, J., Westlin, M., Burk, S.E., Shull, G.E., and MacLennan, D.H. (1992). Functional comparisons between isoforms of the sarcoplasmic or endoplasmic reticulum family of calcium pumps. J Biol Chem *267*, 14483-14489.
Machuca-Tzili, L., Brook, D., and Hilton-Jones, D. (2005). Clinical and molecular aspects of the myotonic dystrophies: a review. Muscle & nerve *32*, 1-18.
MacLennan, D.H., Rice, W.J., and Green, N.M. (1997). The mechanism of Ca2+ transport by sarco(endo)plasmic reticulum Ca2+-ATPases. J Biol Chem *272*, 28815-28818.
Mahadevan, M., Tsilfidis, C., Sabourin, L., Shutler, G., Amemiya, C., Jansen, G., Neville, C., Narang, M., Barcelo, J., O'Hoy, K.*, et al.* (1992). Myotonic dystrophy mutation: an unstable CTG repeat in the 3' untranslated region of the gene. Science *255*, 1253-1255.
Mahadevan, M.S., Amemiya, C., Jansen, G., Sabourin, L., Baird, S., Neville, C.E., Wormskamp, N., Segers, B., Batzer, M., Lamerdin, J.*, et al.* (1993). Structure and genomic sequence of the myotonic dystrophy (DM kinase) gene. Hum Mol Genet *2*, 299-304.
Mahadevan, M.S., Yadava, R.S., Yu, Q., Balijepalli, S., Frenzel-McCardell, C.D., Bourne, T.D., and Phillips, L.H. (2006). Reversible model of RNA toxicity and cardiac conduction defects in myotonic dystrophy. Nat Genet *38*, 1066-1070.
Malinina, L. (2005). Possible involvement of the RNAi pathway in trinucleotide repeat expansion diseases. Journal of biomolecular structure & dynamics *23*, 233-235.

Mankodi, A., Lin, X., Blaxall, B.C., Swanson, M.S., and Thornton, C.A. (2005). Nuclear RNA foci in the heart in myotonic dystrophy. Circulation research *97*, 1152-1155.
Mankodi, A., Logigian, E., Callahan, L., McClain, C., White, R., Henderson, D., Krym, M., and Thornton, C.A. (2000). Myotonic dystrophy in transgenic mice expressing an expanded CUG repeat. Science *289*, 1769-1773.
Mankodi, A., Takahashi, M.P., Jiang, H., Beck, C.L., Bowers, W.J., Moxley, R.T., Cannon, S.C., and Thornton, C.A. (2002). Expanded CUG repeats trigger aberrant splicing of ClC-1 chloride channel pre-mRNA and hyperexcitability of skeletal muscle in myotonic dystrophy. Mol Cell *10*, 35-44.
Mankodi, A., Urbinati, C.R., Yuan, Q.P., Moxley, R.T., Sansone, V., Krym, M., Henderson, D., Schalling, M., Swanson, M.S., and Thornton, C.A. (2001). Muscleblind localizes to nuclear foci of aberrant RNA in myotonic dystrophy types 1 and 2. Hum Mol Genet *10*, 2165-2170.
Martorell, L., Monckton, D.G., Gamez, J., Johnson, K.J., Gich, I., Lopez de Munain, A., and Baiget, M. (1998). Progression of somatic CTG repeat length heterogeneity in the blood cells of myotonic dystrophy patients. Hum Mol Genet *7*, 307-312.
Mathieu, J., Allard, P., Potvin, L., Prevost, C., and Begin, P. (1999). A 10-year study of mortality in a cohort of patients with myotonic dystrophy. Neurology *52*, 1658-1662.
Matsuura, T., Yamagata, T., Burgess, D.L., Rasmussen, A., Grewal, R.P., Watase, K., Khajavi, M., McCall, A.E., Davis, C.F., Zu, L.*, et al.* (2000). Large expansion of the ATTCT pentanucleotide repeat in spinocerebellar ataxia type 10. Nat Genet *26*, 191-194.
Mellor, H., and Parker, P.J. (1998). The extended protein kinase C superfamily. The Biochemical journal *332 (Pt 2)*, 281-292.
Meola, G., Sansone, V., Marinou, K., Cotelli, M., Moxley, R.T., 3rd, Thornton, C.A., and De Ambroggi, L. (2002). Proximal myotonic myopathy: a syndrome with a favourable prognosis? Journal of the neurological sciences *193*, 89-96.
Meola, G., Sansone, V., Perani, D., Colleluori, A., Cappa, S., Cotelli, M., Fazio, F., Thornton, C.A., and Moxley, R.T. (1999). Reduced cerebral blood flow and impaired visual-spatial function in proximal myotonic myopathy. Neurology *53*, 1042-1050.
Michalowski, S., Miller, J.W., Urbinati, C.R., Paliouras, M., Swanson, M.S., and Griffith, J. (1999). Visualization of double-stranded RNAs from the myotonic dystrophy protein kinase gene and interactions with CUG-binding protein. Nucleic Acids Res *27*, 3534-3542.
Miller, J.W., Urbinati, C.R., Teng-Umnuay, P., Stenberg, M.G., Byrne, B.J., Thornton, C.A., and Swanson, M.S. (2000). Recruitment of human muscleblind proteins to (CUG)(n) expansions associated with myotonic dystrophy. EMBO J *19*, 4439-4448.
Mitake, S., Inagaki, T., Niimi, T., Shirai, T., and Yamamoto, M. (1989). [Development of Alzheimer neurofibrillary changes in two autopsy cases of myotonic dystrophy]. Rinsho shinkeigaku = Clinical neurology *29*, 488-492.
Moller, D.E., Yokota, A., Caro, J.F., and Flier, J.S. (1989). Tissue-specific expression of two alternatively spliced insulin receptor mRNAs in man. Molecular endocrinology *3*, 1263-1269.

Mooers, B.H., Logue, J.S., and Berglund, J.A. (2005). The structural basis of myotonic dystrophy from the crystal structure of CUG repeats. Proc Natl Acad Sci U S A *102*, 16626-16631.
Mosthaf, L., Grako, K., Dull, T.J., Coussens, L., Ullrich, A., and McClain, D.A. (1990). Functionally distinct insulin receptors generated by tissue-specific alternative splicing. EMBO J *9*, 2409-2413.
Moxley, R.T., 3rd (1996). The myotonias: their diagnosis and treatment. Compr Ther *22*, 8-21.
Mulders, S.A., van den Broek, W.J., Wheeler, T.M., Croes, H.J., van Kuik-Romeijn, P., de Kimpe, S.J., Furling, D., Platenburg, G.J., Gourdon, G., Thornton, C.A.*, et al.* (2009). Triplet-repeat oligonucleotide-mediated reversal of RNA toxicity in myotonic dystrophy. Proc Natl Acad Sci U S A *106*, 13915-13920.
Napierala, M., and Krzyzosiak, W.J. (1997). CUG repeats present in myotonin kinase RNA form metastable "slippery" hairpins. J Biol Chem *272*, 31079-31085.
Nguyen, H.H., Wolfe, J.T., 3rd, Holmes, D.R., Jr., and Edwards, W.D. (1988). Pathology of the cardiac conduction system in myotonic dystrophy: a study of 12 cases. J Am Coll Cardiol *11*, 662-671.
Nishizuka, Y. (1995). Protein kinase C and lipid signaling for sustained cellular responses. FASEB journal : official publication of the Federation of American Societies for Experimental Biology *9*, 484-496.
O'Leary, D.A., Sharif, O., Anderson, P., Tu, B., Welch, G., Zhou, Y., Caldwell, J.S., Engels, I.H., and Brinker, A. (2009). Identification of small molecule and genetic modulators of AON-induced dystrophin exon skipping by high-throughput screening. PloS one *4*, e8348.
O'Rourke, J.R., and Swanson, M.S. (2009). Mechanisms of RNA-mediated disease. J Biol Chem *284*, 7419-7423.
Orengo, J.P., Bundman, D., and Cooper, T.A. (2006). A bichromatic fluorescent reporter for cell-based screens of alternative splicing. Nucleic Acids Res *34*, e148.
Orengo, J.P., Chambon, P., Metzger, D., Mosier, D.R., Snipes, G.J., and Cooper, T.A. (2008). Expanded CTG repeats within the DMPK 3' UTR causes severe skeletal muscle wasting in an inducible mouse model for myotonic dystrophy. Proc Natl Acad Sci U S A *105*, 2646-2651.
Otten, A.D., and Tapscott, S.J. (1995). Triplet repeat expansion in myotonic dystrophy alters the adjacent chromatin structure. Proc Natl Acad Sci U S A *92*, 5465-5469.
Oyamada, R., Hayashi, M., Katoh, Y., Tsuchiya, K., Mizutani, T., Tominaga, I., and Kashima, H. (2006). Neurofibrillary tangles and deposition of oxidative products in the brain in cases of myotonic dystrophy. Neuropathology : official journal of the Japanese Society of Neuropathology *26*, 107-114.
Parniewski, P., and Staczek, P. (2002). Molecular mechanisms of TRS instability. Advances in experimental medicine and biology *516*, 1-25.
Pascual, M., Vicente, M., Monferrer, L., and Artero, R. (2006). The Muscleblind family of proteins: an emerging class of regulators of developmentally programmed alternative splicing. Differentiation *74*, 65-80.
Philips, A.V., Timchenko, L.T., and Cooper, T.A. (1998). Disruption of splicing regulated by a CUG-binding protein in myotonic dystrophy. Science *280*, 737-741.

Pushechnikov, A., Lee, M.M., Childs-Disney, J.L., Sobczak, K., French, J.M., Thornton, C.A., and Disney, M.D. (2009). Rational design of ligands targeting triplet repeating transcripts that cause RNA dominant disease: application to myotonic muscular dystrophy type 1 and spinocerebellar ataxia type 3. Journal of the American Chemical Society *131*, 9767-9779.
Reddy, S., Smith, D.B., Rich, M.M., Leferovich, J.M., Reilly, P., Davis, B.M., Tran, K., Rayburn, H., Bronson, R., Cros, D.*, et al.* (1996). Mice lacking the myotonic dystrophy protein kinase develop a late onset progressive myopathy. Nat Genet *13*, 325-335.
Renwick, J.H., Bundey, S.E., Ferguson-Smith, M.A., and Izatt, M.M. (1971). Confirmation of linkage of the loci for myotonic dystrophy and ABH secretion. J Med Genet *8*, 407-416.
Ricker, K. (1999). Myotonic dystrophy and proximal myotonic myophathy. J Neurol *246*, 334-338.
Ricker, K., Koch, M.C., Lehmann-Horn, F., Pongratz, D., Otto, M., Heine, R., and Moxley, R.T., 3rd (1994). Proximal myotonic myopathy: a new dominant disorder with myotonia, muscle weakness, and cataracts. Neurology *44*, 1448-1452.
Roberts, R., Timchenko, N.A., Miller, J.W., Reddy, S., Caskey, C.T., Swanson, M.S., and Timchenko, L.T. (1997). Altered phosphorylation and intracellular distribution of a (CUG)n triplet repeat RNA-binding protein in patients with myotonic dystrophy and in myotonin protein kinase knockout mice. Proc Natl Acad Sci U S A *94*, 13221-13226.
Sarkar, P.S., Appukuttan, B., Han, J., Ito, Y., Ai, C., Tsai, W., Chai, Y., Stout, J.T., and Reddy, S. (2000). Heterozygous loss of Six5 in mice is sufficient to cause ocular cataracts. Nat Genet *25*, 110-114.
Sasaki, R., Ichiyasu, H., Ito, N., Ikeda, T., Takano, H., Ikeuchi, T., Kuzuhara, S., Uchino, M., Tsuji, S., and Uyama, E. (1999). Novel chloride channel gene mutations in two unrelated Japanese families with Becker's autosomal recessive generalized myotonia. Neuromuscul Disord *9*, 587-592.
Sasaki, R., Ito, N., Shimamura, M., Murakami, T., Kuzuhara, S., Uchino, M., and Uyama, E. (2001). A novel CLCN1 mutation: P480T in a Japanese family with Thomsen's myotonia congenita. Muscle & nerve *24*, 357-363.
Savkur, R.S., Philips, A.V., and Cooper, T.A. (2001). Aberrant regulation of insulin receptor alternative splicing is associated with insulin resistance in myotonic dystrophy. Nat Genet *29*, 40-47.
Savkur, R.S., Philips, A.V., Cooper, T.A., Dalton, J.C., Moseley, M.L., Ranum, L.P., and Day, J.W. (2004). Insulin receptor splicing alteration in myotonic dystrophy type 2. Am J Hum Genet *74*, 1309-1313.
Seidman, J.G., and Seidman, C. (2001). The genetic basis for cardiomyopathy: from mutation identification to mechanistic paradigms. Cell *104*, 557-567.
Seino, S., and Bell, G.I. (1989). Alternative splicing of human insulin receptor messenger RNA. Biochemical and biophysical research communications *159*, 312-316.
Sergeant, N., Sablonniere, B., Schraen-Maschke, S., Ghestem, A., Maurage, C.A., Wattez, A., Vermersch, P., and Delacourte, A. (2001). Dysregulation of human brain microtubule-associated tau mRNA maturation in myotonic dystrophy type 1. Hum Mol Genet *10*, 2143-2155.
Seznec, H., Agbulut, O., Sergeant, N., Savouret, C., Ghestem, A., Tabti, N., Willer, J.C., Ourth, L., Duros, C., Brisson, E.*, et al.* (2001). Mice transgenic for

the human myotonic dystrophy region with expanded CTG repeats display muscular and brain abnormalities. Hum Mol Genet *10*, 2717-2726.
Shaw, D.J., McCurrach, M., Rundle, S.A., Harley, H.G., Crow, S.R., Sohn, R., Thirion, J.P., Hamshere, M.G., Buckler, A.J., Harper, P.S.*, et al.* (1993). Genomic organization and transcriptional units at the myotonic dystrophy locus. Genomics *18*, 673-679.
Shin, R.W., Iwaki, T., Kitamoto, T., and Tateishi, J. (1991). Hydrated autoclave pretreatment enhances tau immunoreactivity in formalin-fixed normal and Alzheimer's disease brain tissues. Laboratory investigation; a journal of technical methods and pathology *64*, 693-702.
Taneja, K.L., McCurrach, M., Schalling, M., Housman, D., and Singer, R.H. (1995). Foci of trinucleotide repeat transcripts in nuclei of myotonic dystrophy cells and tissues. The Journal of cell biology *128*, 995-1002.
Tapscott, S.J. (2000). Deconstructing myotonic dystrophy. Science *289*, 1701-1702.
Thornton, C.A., Wymer, J.P., Simmons, Z., McClain, C., and Moxley, R.T., 3rd (1997). Expansion of the myotonic dystrophy CTG repeat reduces expression of the flanking DMAHP gene. Nat Genet *16*, 407-409.
Tian, B., White, R.J., Xia, T., Welle, S., Turner, D.H., Mathews, M.B., and Thornton, C.A. (2000). Expanded CUG repeat RNAs form hairpins that activate the double-stranded RNA-dependent protein kinase PKR. Rna *6*, 79-87.
Timchenko, L.T., Miller, J.W., Timchenko, N.A., DeVore, D.R., Datar, K.V., Lin, L., Roberts, R., Caskey, C.T., and Swanson, M.S. (1996). Identification of a (CUG)n triplet repeat RNA-binding protein and its expression in myotonic dystrophy. Nucleic Acids Res *24*, 4407-4414.
Timchenko, N.A., Iakova, P., Cai, Z.J., Smith, J.R., and Timchenko, L.T. (2001). Molecular basis for impaired muscle differentiation in myotonic dystrophy. Mol Cell Biol *21*, 6927-6938.
Timchenko, N.A., Patel, R., Iakova, P., Cai, Z.J., Quan, L., and Timchenko, L.T. (2004). Overexpression of CUG triplet repeat-binding protein, CUGBP1, in mice inhibits myogenesis. J Biol Chem *279*, 13129-13139.
Vanier, T.M. (1960). Dystrophia myotonica in childhood. British medical journal *2*, 1284-1288.
Vermersch, P., Sergeant, N., Ruchoux, M.M., Hofmann-Radvanyi, H., Wattez, A., Petit, H., Dwailly, P., and Delacourte, A. (1996). Specific tau variants in the brains of patients with myotonic dystrophy. Neurology *47*, 711-717.
Wang, G.S., and Cooper, T.A. (2007). Splicing in disease: disruption of the splicing code and the decoding machinery. Nature reviews Genetics *8*, 749-761.
Wang, G.S., Kearney, D.L., De Biasi, M., Taffet, G., and Cooper, T.A. (2007). Elevation of RNA-binding protein CUGBP1 is an early event in an inducible heart-specific mouse model of myotonic dystrophy. J Clin Invest *117*, 2802-2811.
Wang, G.S., Kuyumcu-Martinez, M.N., Sarma, S., Mathur, N., Wehrens, X.H., and Cooper, T.A. (2009). PKC inhibition ameliorates the cardiac phenotype in a mouse model of myotonic dystrophy type 1. J Clin Invest *119*, 3797-3806.
Wang, Y.H., Amirhaeri, S., Kang, S., Wells, R.D., and Griffith, J.D. (1994). Preferential nucleosome assembly at DNA triplet repeats from the myotonic dystrophy gene. Science *265*, 669-671.

Warf, M.B., Nakamori, M., Matthys, C.M., Thornton, C.A., and Berglund, J.A. (2009). Pentamidine reverses the splicing defects associated with myotonic dystrophy. Proc Natl Acad Sci U S A *106*, 18551-18556.
Way, K.J., Chou, E., and King, G.L. (2000). Identification of PKC-isoform-specific biological actions using pharmacological approaches. Trends in pharmacological sciences *21*, 181-187.
Wesstrom, G., Bensch, J., and Schollin, J. (1986). Congenital myotonic dystrophy. Incidence, clinical aspects and early prognosis. Acta paediatrica Scandinavica *75*, 849-854.
Wheeler, T.M., Leger, A.J., Pandey, S.K., MacLeod, A.R., Nakamori, M., Cheng, S.H., Wentworth, B.M., Bennett, C.F., and Thornton, C.A. (2012). Targeting nuclear RNA for in vivo correction of myotonic dystrophy. Nature *488*, 111-115.
Wheeler, T.M., Lueck, J.D., Swanson, M.S., Dirksen, R.T., and Thornton, C.A. (2007). Correction of ClC-1 splicing eliminates chloride channelopathy and myotonia in mouse models of myotonic dystrophy. J Clin Invest *117*, 3952-3957.
Wheeler, T.M., Sobczak, K., Lueck, J.D., Osborne, R.J., Lin, X., Dirksen, R.T., and Thornton, C.A. (2009). Reversal of RNA dominance by displacement of protein sequestered on triplet repeat RNA. Science *325*, 336-339.
Winchester, C.L., Ferrier, R.K., Sermoni, A., Clark, B.J., and Johnson, K.J. (1999). Characterization of the expression of DMPK and SIX5 in the human eye and implications for pathogenesis in myotonic dystrophy. Hum Mol Genet *8*, 481-492.
Wuytack, F., Raeymaekers, L., De Smedt, H., Eggermont, J.A., Missiaen, L., Van Den Bosch, L., De Jaegere, S., Verboomen, H., Plessers, L., and Casteels, R. (1992). Ca(2+)-transport ATPases and their regulation in muscle and brain. Annals of the New York Academy of Sciences *671*, 82-91.
Zeesman, S., Carson, N., and Whelan, D.T. (2002). Paternal transmission of the congenital form of myotonic dystrophy type 1: a new case and review of the literature. American journal of medical genetics *107*, 222-226.